Federal University of Ceará
Department of Teleinformatics Engineering
Postgraduate Program in Teleinformatics Engineering

MIMO Array Capacity Optimization using a Genetic Algorithm

Doctor of Science Thesis

Author
Manuel Osório Binelo

Advisor
Prof. Dr. Francisco Rodrigo Porto Cavalcanti

Co-advisor
Prof. Dr. André Lima Férrer de Almeida

Fortaleza – Ceará
January 2013

UNIVERSIDADE FEDERAL DO CEARÁ
DEPARTAMENTO DE ENGENHARIA DE TELEINFORMÁTICA
PROGRAMA DE PÓS-GRADUAÇÃO EM ENGENHARIA DE TELEINFORMÁTICA

Otimização da Capacidade de Arranjos MIMO usando Algoritmo Genético

Autor
Manuel Osório Binelo

Orientador
Prof. Dr. Francisco Rodrigo Porto Cavalcanti

Co-orientador
Prof. Dr. André Lima Férrer de Almeida

Tese apresentada à Coordenação do Programa de Pós-graduação em Engenharia de Teleinformática da Universidade Federal do Ceará como parte dos requisitos para obtenção do grau de ***Doutor em Engenharia de Teleinformática****.*

FORTALEZA – CEARÁ
JANEIRO 2013

Abstract

One challenging task in multiple input multiple output (MIMO) systems design is to accommodate the multiple antennas in the mobile device without compromising the system capacity, due to spatial and electrical constraints. In this work, an experimental MIMO wireless channel characterization in an outdoor environment is performed in order to study the different factors that affect MIMO capacity. The data acquired during wideband channel measurement campaigns made in Stockholm, Sweden, were used in order to predict the impact of direction of arrival (DOA) distribution and polarization diversity on the channel capacity, choosing specific measurement routes and locations as well as different MIMO antenna array configurations. This thesis proposes a genetic algorithm (GA) to obtain the position and orientation of each MIMO array antenna that maximizes the ergodic capacity for a given propagation scenario. The simulations of the GA use the characterized experimental channel model, as a case of study, in order to evaluate the impact of different characteristics of the propagation environment in the capacity. Based on an interface between the antenna model and the propagation channel model, the ergodic capacity is considered as the objective function of the MIMO array optimization.

Simulation results corroborate the importance of polarization and antenna pattern diversities for MIMO in small terminals. The results also show that the electromagnetic coupling effect can be exploited by the optimizer in order to decrease signal correlation and increase MIMO capacity. A comparison among uniform linear array (ULA), uniform circular array (UCA) and the GA-optimized array is also carried out, showing that the topology given by the optimizer is superior to that of the standard ULA and UCA arrays for the considered propagation channel. This work also presents a method for optimizing the capacity of MIMO antenna array systems with antenna selection, evolving the antenna array best suited for antenna selection in a given scenario. As a result of the proposed GA optimizer, different array configurations were obtained for cases with and without antenna selection, showing that true polarization diversity (TPD) schemes are particularly suited for antenna selection systems.

Key words: MIMO, array optimization, genetic algorithm, MIMO capacity, antenna selection..

Resumo

Um a questão bastante complicada no projeto de sistemas MIMO é acomodar as múltiplas antenas no dispositivo móvel sem comprometer a capacidade do sistema, devido a restrições elétricas e de espaço. Neste trabalho é desenvolvida a caracterização de um canal MIMO sem fio em ambiente externo para o estudo dos diferentes fatores que afetam a capacidade de comunicação. Os dados adquiridos em campanhas de medição feitas em Estocolmo foram utilizados para modelar o impacto da distribuição de DOA e da diversidade de polarização na capacidade do canal, escolhendo rotas específicas de medida e diferentes configurações de arranjos de antena. Essa tese propõe um algoritmo genético para obter a posição e orientação de cada antena do arranjo MIMO que maximizem a capacidade ergótica para um dado cenário de propagação. Baseando-se em uma interface entre o modelo de antena e o modelo de propagação do canal, a capacidade ergódica é usada como função objetivo da otimização do arranjo MIMO.

Os resultados das simulação indicam a importância das diversidades de polarização e de padrão de antena para sistemas MIMO em terminais de pequeno porte. Os resultados também mostram que o efeito do acoplamento eletromagnético pode ser explorado pelo otimizador para diminuir a correlação do sinal aumentando assim a capacidade MIMO. Também é feita uma comparação entre arranjo linear uniforme(ULA), arranjo circular uniforme(UCA) e um arranjo otimizado pelo algoritmo genético, mostrando que a topologia resultante do algoritmo genético é superior tanto a ao arranjo ULA quanto ao arranjo UCA, para o canal de propagação considerado. Este trabalho também apresenta um método para otimização da capacidade de sistemas MIMO com seleção de antena, evoluindo um arranjo de antenas melhor adaptado para a seleção de antenas em um dado cenário de propagação. Como resultado do método proposto, diferentes configurações de arranjos foram obtidas para o caso com e sem seleção de antenas, mostrando que sistemas de diversidade de polarização(TPD) são particularmente adequados para sistemas com seleção de antena.

Palavras-chave: MIMO, otimização de arranjos, algoritmos genéticos, capacidade MIMO, seleção de antena..

Dedicatories

"Remember this, my dear brothers: everyone should be quick to listen but slow to speak and slow to human anger; God's saving justice is never served by human anger."
- Saint James

Dedicated to my parents, Jose Henrique Guimaraes Binelo and Terezinha de Jesus Binelo, who have emphasized the importance of love, faith and hope in this author...

Acknowledgements

I was in south Brazil after finishing my graduation in Computing Science and my master's degree in Mathematical Modeling when I applied for the doctor's degree in Teleinformatics Engineering at UFC. When I started my master's degree, it was a stiff change in my career to leave Computing Science and to head to Mathematics. A change full of hard obstacles but that proved to be very valuable. And then again, for my doctor's degree, I was aiming at another change, with even harder obstacles ahead. But the obstacles were not grater than the sense of accomplishment I fill now. As the reader could suspect, this work carries the marks from my experience on computing and on numeric methods, and I hope this exercise in multi-disciplinarity will be found of some value by the reader.

This journey would not be possible without the support of my advisor Prof. Dr. Francisco Rodrigo Porto Cavalcanti and my co-advisor Prof. Dr. Adré Lima Férrer de Almeida, whom I want to give my most sincere thanks. I also want the thank all the professors and colleagues at the GTEL research laboratory for all the support and friendship during these years. An internship in Ericsson AB in Stockholm, at the beginning of my work, was of extreme importance for the development of this thesis. I want to thank the researchers at Ericsson AB, in special Jonas Medbo and Henrik Asplund.

Finally, I want to thank my family, that was always by my side, even when thousands of miles away. Lastly, and more important, thank God for the living of all those people mentioned above, and for all the love and for having so much patience with me.

List of Symbols

M_t	Number of transmit antennas
M_r	Number of receive antennas
$\mathbf{x}$	Transmitted symbol vector
$\mathbf{n}$	Noise vector
$\mathbf{H}$	Matrix of channel gains from transmit antenna j to receive antenna i
C	Hergodic capacity
α	Angle spread
$\mathbf{R}$	Correlation matrix
f_i	Fitness function
o_i	Objective function
σ	Standard deviation in the population
p_k	Selection probability
(ϕ_{Rx}, θ_{Rx})	DOA azimuth and elevation angles
(ϕ_{Tx}, θ_{Tx})	DOD azimuth and elevation angles
L	Number of arriving paths
A_l	Multipath contribution
$\mathbf{W}_l$	Polarimetric transmission matrix
γ	Polarization factor
$h_{m,n}$	The $(m,n)^{th}$ entry of the MIMO channel matrix
$\mathbf{g}_{Rx}$	Antenna pattern response to the direction $(\phi_{Rx,m,l}, \theta_{Rx,m,l})$ at the receiver
$\mathbf{g}_{Tx}$	Antenna pattern response to the direction $(\phi_{Tx,m,l}, \theta_{Tx,m,l})$ at the transmitter
$\mathbf{r}_{Rx,m}$	Antenna orientation
$\mathbf{x_{Rx}}$	Relative position of the m^{th} receive antenna
$\mathbf{x}_{Tx}$	Relative position of the n^{th} transmit antenna
N_q	Number of realizations to compute the expectation statistics
$\mathbf{H}_q$	The q^{th} channel realization
$\mathbf{k}$	Wave vector
L_t	Number of RF chains available at the transmitter
N_t	Available antenna elements at the transmitter
L_t	Number of RF chains available at the receiver
N_t	Available antenna elements at the receiver
$\tilde{\mathbf{H}}$	Modified channel matrix of size $L_t L_r$
$S(\tilde{\mathbf{H}})$	Set of all possible sub-matrices $\tilde{\mathbf{H}}$
N_s	Number of snapshots in the route
$\mathbf{H}^a{}_{qs}$	Sub-matrix of the channel matrix $\mathbf{H}$ for the channel realization q of snapshot s
$\mathbf{H}_{qsu}$	Valid subset u of columns for a selection of antennas in the realization q of snapshot s

Contents

List of Figures

Chapter 1

Introduction

The use of multiple input multiple output (MIMO) communication systems has become extremely important for mobile communications. As the electromagnetic spectrum becomes an increasingly expensive resource, and as the mobile consumer requires more bandwidth for data applications, the fact that MIMO systems can increase the system capacity linearly with number of transmit or receive antennas [1] gains importance [1], [2].

The advantage of using multiple antennas comes from use of a new dimension, the space. The spatial dimension comes as complement to time, the first dimension in digital communication, the reason why MIMO systems are also called space-time systems. With the emergence of MIMO systems, multipaths were converted into a benefit for the communication system [3]. With multiple antennas at both ends of the link, it is possible to exploit the diversity gain for signal robustness or to use spatial multiplexing. However, it is not possible to do both at the same time, there is a tradeoff involved [3].

In order to maximize the capacity gain of MIMO systems it is very important to have uncorrelated signals at antenna elements. This is easily achievable when it is possible to spatially separate the antennas by several wavelengths. That is not a problem for base stations, but is potentially problematic for mobile terminals which have constraints on physical size. In order to have uncorrelated signals in a MIMO array within a mobile terminal it is important to consider a combination of factors: the position and orientation of the antennas, the electromagnetic coupling effect among antennas, propagation channel characteristics and its interaction with the antenna system.

Another important aspect to consider is the possibility to use antenna selection in MIMO systems. In this case more physical antennas than actual signal receivers are employed. Based on channel state information, an algorithm selects the antennas which maximizes MIMO channel capacity. This work proposes an optimization process aimed at antenna array design and antenna selection for MIMO systems under physical space constraints, such as the ones within typical mobile terminals.

The main objective of this thesis is to develop an optimization method for MIMO antenna array design, considering small terminals and antenna selection. First, an experimental characterization of an outdoor MIMO wireless channel is performed, and then the impact of different direction of arrival (DOA) distributions and polarization diversity configurations on MIMO capacity is analyzed. A method for MIMO array optimization based on GA that can be interfaced with an environment channel propagation model is presented, using simple cluster

[1] The linear growth is predicted by information theory, but in practice, the growth might be less expressive.

examples. The work is then expanded creating a cluster based model of the propagation environment validated by the measurements. Finally, the validated propagation model is interfaced with GA method presented. The main question this thesis tries to answer is whether or not it is possible to automate the design of MIMO antenna arrays. Other questions are about the possible sources of signal diversity in MIMO mobile terminals which have constraints on physical size, the impact of mutual coupling of antennas in the optimized array configurations, and whether or not antenna selection requires different array configurations for optimal performance.

1.1 Review of related work

One important factor for MIMO systems is the polarization diversity, especially considering the spatial constraints of mobile terminals. The work [4] does an experimental characterization of the outdoor MIMO wireless channel temporal variation. One of the conclusions is that dual polarized antennas produce channels with lower temporal variation. A comparison between dual-polarization and single polarization MIMO channels is made by [5], the work concludes that higher capacity can be achieved with dual-polarization antenna configurations, when compared to the single-polarization antenna configurations. The evaluation of polarization rotation for macrocell MIMO channels is made in [6]. According to them, polarization diversity outperforms the spatial diversity in LOS scenario and shows a small gain in rich scattering scenarios. Another important factor to be considered is antenna separation as shown in [7]. The characteristics of the propagation environment are also important such as multipath cluster distribution as discussed in [8] and [9]. The work [10] also investigates the impact of propagation environment as the relationship between different MIMO arrays and different propagation scenarios. The conclusion in [10] is that for a small angular spread of 8^o it is necessary to have a 4 wavelength antenna separation in order to achieve an uncorrelated channel.

Implementing MIMO transceivers in small mobile terminals is a challenging task and is discussed in [11]. The large amount of variables makes it difficult to find the best configuration based solely on the empirical inference of the designer. One example is the work [12], where small arrays (based on Planar Inverted F Antennas or PIFAs) are compared to dipole arrays. The work concludes that PIFA arrays are ideal for compact array designs and attributes this result to the nearly omnidirectional pattern of PIFA, but it does not justify the position and orientation of the PIFA antennas and does not investigate the influence of the orientation.

Since the small size of mobile terminals prevents the designer from using sufficient separation among antennas, other techniques must be employed. One of these techniques is true polarization diversity (TPD) where different angles can be used in order to obtain signal diversity [13]. According to [13], TPD is shown to improve MIMO capacity. The work [14] investigates uniform circular arrays (UCA) and uniform linear arrays (ULA). The conclusion is that ULAs are better for some directions of arrival, and UCAs have a more stable behavior. A similar analysis is made in [15]. Another important factor is the electromagnetic mutual coupling among antennas. This effect can affect the MIMO performance [16], [17] but also be exploited in order to gain capacity [18].

From these previous works, we can see that several variables can affect MIMO capacity, such as antenna position, individual antenna orientation, array orientation, mutual electromagnetic coupling, among others. Thus, in order to find the best characteristics for small MIMO arrays, one can resort to at least two options. First an engineer can search by

trial and error for a good design among an endless amount of reference cases. Or instead we can shift to a computer-based design approach based on an optimization method. In fact, such approach has become more common in engineering as seen in [19] and is the one adopted in this thesis.

Genetic algorithm based optimization has been used with success in various engineering problems. The work [20] uses a GA optimization method in order to fifind the best antenna array configuration for channel sounding. Channel sounding is used to find the directions of arrival for a given propagation scenario. In [20] the system starts with big regular bi-dimensional or three-dimensional array of antennas (more than 20 antennas), and then the algorithm changes individual antennas position and orientation trying to fi?nd the array that minimizes the parameter estimation error. In [21], GA was used to find channel parameters such as multipath attenuations and delays. For blind channel estimation, [22] shows that a GA method can offer better estimation accuracy than traditional methods. A GA method was used in blind equalization for joint MIMO channel and data estimation in [23]. In [24], GA was used for array optimization of MIMO radar. GA was applied to the array optimization in order to reduce the peaks of side lobes (PSL) by acting on the elements positions. The work [25] uses GA in order to find the optimal distribution of a 3×3-antenna MIMO system for an indoor propagation channel. An interesting aspect of that work is the inclusion of electromagnetic coupling in the model. However, the work does not show either which array layouts were found or how the layouts change according to different multipath channel parameters.

Nature inspired methods for MIMO antenna design are defended by [26], but the works mentioned therein deal with the problem of antenna geometry definition and not antenna array topology for different propagation environments. In [27] a method of moments is proposed to optimize MIMO antenna position and orientation. The optimization is based on minimizing the antenna cross correlation, by considering an i.i.d MIMO channel. Although antenna cross correlation can degrade capacity, we cannot say that the confifiguration that minimizes antenna correlation is necessarily the same that maximizes MIMO capacity in non i.i.d. propagation scenarios [28]. A similar approach is used in [29]. The work [30] solves the problem of MIMO PIFA placement for an i.i.d. channel also minimizing antenna cross correlation, but using infinitesimal dipoles method and invasive weeds optimization.

As we can see in the literature review, most works on MIMO systems only take into account one specific aspect of the problem (e.g. antenna model or propagation environment model), and oversimplify the remaining aspects of the problem (e. g. ignoring electromagnetic interactions among antennas in the array or using an i.i.d MIMO channel instead of taking into consideration a realistic propagation scenario). In this work, instead, we propose a holistic process. In this work, a more a comprehensive process is proposed, starting with channel characterization and channel model definition based on channel measurements of a typical outdoor urban scenario, and then interfacing this model with a genetic algorithm-based optimization tool, which searches for best position and orientation of antennas taking into account the electromagnetic mutual coupling among antennas.

Another question that is not frequently treated is the array optimization taking into account antenna selection. Works such [31], [32], [33] and [34] have investigated various aspects of antenna selection in MIMO systems, but no work has investigated what characteristics make a MIMO array configuration well suited for antenna selection in comparison to regular MIMO array systems. The GA method presented is then further modified in order to obtain an array suited for antenna selection.

1.2 Summary of contributions

This work offers four main contributions:

- **MIMO Array Capacity Optimization Using a Genetic Algorithm** - The configuration of antenna arrays int terms of antennas position and orientation is very important for the MIMO channel capacity, specially considering small sized terminals. The engineer frequently has to rely on intuition and trial-and-error to design the antenna array. This work proposes a genetic algorithm capable of automating this task, evolving the best array configuration for a given propagation scenario.
- **Genetic Algorithm to Consider Antenna Selection** - The GA method is extended in order to consider a realistic propagation model and the use of antenna selection. The results show that characteristics renders good performance for a regular MIMO system are different from those when antenna selection is considered.
- **MIMO Channel Model Validation** - Some works concentrate into the propagation environment and simplify the effects of the antenna array model. Other works concentrate in the antenna array model and use a simplified channel model, frequently i.i.d. This work proposes a more comprehensive approach. The channel model used in the genetic algorithm is validated according to measurements. This validation permits the integration with the propagation model with the antenna model which considers effects such as electromagnetic mutual coupling and far field response.
- **Capacity Study of Measured Outdoor MIMO Wireless Channels** - As previously mentioned, the characteristics of the propagation environment have a strong impact on the performance of a MIMO system. Differently from SISO systems, where LOS is the perfect scenario, in MIMO the multipath components are essential for multiplexing gain. Different characteristics such as polarization and clusters of scatterers distribution have different impact in the resulting MIMO channel capacity. This work uses measurement data in order to make an analysis of MIMO channel capacity.

1.3 Organization

The structure of this thesis is divided into the following chapters:

Chapter 2 - This chapter provides a quick overview of the trinity of theoretical fundamentals discussed in this thesis: MIMO channels and genetic algorithms. The information shown here, albeit basic, will serve as a motivating starting point for the deductions shown throughout this material.

Chapter 3 - This chapter deals with the analysis of measurement data of MIMO channel acquired in an urban scenario in Stockholm.

Chapter 4 - This chapter proposes a genetic algorithm as a tool to the optimization of MIMO antenna arrays. It optimizes antennas position and orientation considering a propagation model with clusters of scatterers and affects such as electromagnetic mutual coupling of antennas and farfield response.

Chapter 5 - The channel model used in chapter 4 is validated according to the measurements canalized in chapter 3. The genetic algorithms presented in chapter 4 is extended in order to consider antenna selection in the array. The simulations presented here consider a realistic channel model based in measurements along with antenna selection.

Chapter 6 - A general conclusion about this thesis is presented, highlighting new research perspectives.

1.4 Publications

The list of publications originated so far from the work in this thesis includes conference and journal papers as follows:

- M. Binelo, A.L.F. de Almeida, J. Medbo, H. Asplund and F.R.P. Cavalcanti, "MIMO Channel Characterization and Capacity Evaluation in an Outdoor Environment", Vehicular Technology Conference Fall (VTC 2010-Fall), 2010 IEEE 72nd , Ottowa, Canada, September 2010.
- M. Binelo, A.L.F. de Almeida, and F.R.P. Cavalcanti, "A Heuristic Approach to Antenna Array Topology Optimization in MIMO Systems", 29th Brazilian Symposium on Communications (SBrT'11), Curitiba, Paraná, Brazil, October 2011.
- M. Binelo, A.L.F. de Almeida, and F.R.P. Cavalcanti, "MIMO Array Capacity Optimization Using a Genetic Algorithm ", IEEE Transactions on Vehicular Technology, 2011, volume: 60 , issue: 6 pages: 2471 - 2481.

To this date, a paper with title "Capacity Optimization of MIMO Arrays With Antenna Selection Using a Genetic Algorithm" was submitted and is in revision process waiting approval at the journal IEEE Transactions on Vehicular Technology.

Chapter 2

Capacity Study of Measured Outdoor MIMO Wireless Channels

2.1 Introduction

The advancements made in mobile telecommunication technology permitted the emergence of a variety of data applications, turning the mobile terminal into a personal computer. This fact has largely increased the demand for bandwidth in mobile telecommunications. Unfortunately, the electromagnetic spectrum is a very limited resource, what has justified numerous works on alternative technologies to increase data throughput.

It was shown that multiple input multiple output (MIMO) systems are capable of providing the raise in throughput without the need of more spectrum bandwidth [1], [2]. The multipath components of the channel, which are a problem for single input single output (SISO) systems, are the source of diversity in MIMO channels, generating independent parallel channels.

Consider a general system composed by M_t transmit antennas and M_r receive antennas. The narrowband MIMO channel can be represented by [35]:

$$\mathbf{y} = \mathbf{H}\mathbf{x} + \mathbf{n} \tag{2.1}$$

$$y \begin{pmatrix} y_1 \\ \vdots \\ y_{M_r} \end{pmatrix} = \begin{pmatrix} h_{11} & \cdots & h_{1M_t} \\ \vdots & \ddots & \vdots \\ h_{M_r1} & \cdots & h_{M_rM_t} \end{pmatrix} \begin{pmatrix} x_1 \\ \vdots \\ x_{M_t} \end{pmatrix} + \begin{pmatrix} n_1 \\ \vdots \\ n_{M_r} \end{pmatrix} \tag{2.2}$$

Where x is the transmitted symbol vector, n is the noise vector and H is the matrix of channel gains from transmit antenna j to receive antenna i. By processing H, we can obtain parallel independent communication channels. Applying the singular value decomposition (SVD) to H:

$$\mathbf{H} = \mathbf{U}\mathbf{\Sigma}\mathbf{V}^H, \tag{2.3}$$

we obtain the matrix $\mathbf{\Sigma}$ of singular values σ_i, and [35] shows how each of these single values are related to each independent SISO channel, achieving the so called multiplexing gain. In the model of the ideal propagation MIMO scenario, where there is a rich scattering channel, the entries in H are independent and identically distributed (i.i.d.). H will have a full rank and full multiplexing gain will be achieved [36].

The work [37] does an in-depth analysis of the impact of geometric characteristics in the

MIMO channel capacity. It starts with the analysis of LOS MIMO systems, then analyzes systems with no antenna separation, analyzes systems with clusters of scatterers and one of the conclusions that arises is the dependence on multipaths and antenna separation of at least half wavelength.

In practice most scenarios will not have enough scattering for full multiplexing gain. And the scenario specific characteristics will have a strong impact in the system capacity [38]. Also, the limited spatial diversity has to be fully exploited by the system. This aspects raise the importance of realistic channel models in MIMO studies. According to [39], MIMO channel models can be classified in physical models and analytical models. Analytical models characterize the impulse response. They capture the wave propagation and antenna configuration simultaneously [39]. These characteristics do not favor an analysis of the interaction of the propagation environment and the antenna system. Popular analytical models are the Kronecker model [40] and Weichselberger model [41].

Physical models, on the other hand, characterize an environment according to electromagnetic wave propagation, by describing the double directional multipath propagation and the location and orientation of the transmitter and receiver antennas [39]. The physical models can be further classified in deterministic models, geometry-based stochastic models, and non-geometric stochastic models [39]. While deterministic models, such as ray tracing, can be very accurate, they lack the capacity of easy generalization. This happens because they are defined for a specific scenario. Purely stochastic models, while providing good generalization capacity, lack the geometric spatial aspect of the environment and cannot be easily related to real scenarios. Geometric-stochastic models combine aspects of both previously cited approaches. They use geometric information such as scatterers location, size and kind, but generate the propagation waves using stochastic distributions of these parameters. So they can provide the geometric information needed for the antenna model interface but are also easily generalized.

The incorporation of realistic parameters into the used antennas and channel model is very important. In particular, it should be noted that the successful operation of MIMO technology in small wireless terminals is challenging from at least two points of view. First, the physical space available to embed the antenna elements in the terminal itself is generally restricted. Second, the electromagnetic properties of antenna arrays may be performance limiting factors. These two main issues must be jointly taken into account and interfaced with realistic MIMO propagation models if one decides to predict with reasonable accuracy the performance limits of MIMO communications in practical scenarios.

The MIMO system performance depends not just on the received SNR, but also on the other intrinsic propagation channel characteristics such as direction-of-arrival (DOA) and polarization. Recent works [4], [5] and [6] show the importance of exploiting polarization diversity in MIMO systems. The impact of antenna separation on MIMO capacity is discussed in [7]. Another important factor affecting system performance is multipath cluster distribution, as discussed in [8] and [9].

In this chapter an experimental characterization of an outdoor MIMO wireless channel is performed, and then the impact of different DOA distributions and polarization diversity on MIMO capacity is analyzed using the data acquired during measurement campaigns made in Kista neighborhood, in Stockholm, Sweden. The receiver uses double polarized patch antennas in order to study different cross-polarized MIMO configurations. Relying on a virtual array technique with high spatial sampling resolution, the DOA parameters are estimated by means of an iterative maximum likelihood based method [42]. This work resorted to wideband

measurements for a more complete channel characterization, similarly to the approach used in [43].

2.2 Measurement Setup

The measurements were carried out using a van equipped with antennas in various setups. The van was driven around the neighborhood of Kista, Stockholm. High-resolution data were obtained, post-processed and then exploited to characterize the MIMO channel, allowing us to obtain a model of an equivalent synthetic channel [44].

Figure 2.1 shows the region where the measurements were taken. The red dot marks the base-station location. The measurement equipment is able to take one snapshot at each half wavelength. The MIMO system analyzed here has a maximum of eight outputs ports (four double-polarized antennas) at the Base Station, and four inputs (two double-polarized receiving antennas) at the Mobile Station. Figure 2.2 shows the antenna array used at the Mobile Station (elements 4V, 4H, 5V, 5H). The measured frequencies range from 1.3638GHz to 2.6384GHz. The antenna array was transversely placed at the roof of the van with the antenna patches pointing upwards.

Figure 2.1: Kista map

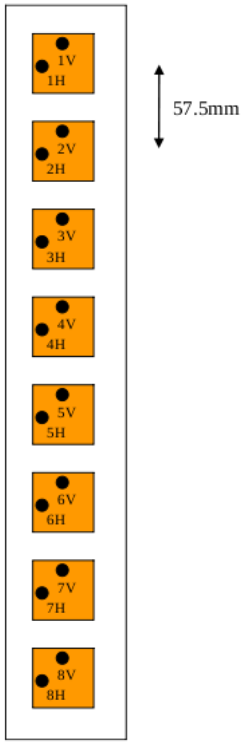

Figure 2.2: Array of patch antennas

2.3 Channel Modeling Issues

One of the goals in analyzing the measurements is to create a measurement-based realistic MIMO channel model, and then to interface this channel model with different antenna models for performance evaluation. A widely adopted model represented by a linear combination of a finite set of plane waves, each one with its own dominant direction of arrival, amplitude, phase and delay according to the following equation is considered:

$$x_{k,m} = n_{k,m} \sum_{l=1}^{N_{sou}} \frac{s_l[l,m]}{r_{k,l}} exp(-2y\pi \frac{r_{k,l}}{\lambda}_m). \tag{2.4}$$

For the estimation of the spatio-temporal channel parameters in (2.4), the Iterative Maximum Likelihood (IML) method [42] was used. This approach has also been applied to characterize indoor propagation scenarios in [45]. Note, however, that, since only two double polarized antennas were used by the channel sounder, the spatial resolution of the antenna array is expected to be too small to provide accurate estimations of the directions of arrival. In order to solve this problem, the so-called "virtual array" was employed. A virtual array was formed by means of successive measurements made during the motion of the van. For reducing the measurement complexity, only the first antenna of the physical array mounted over the van was used. Figure 2.3 illustrates this concept. It is worth mentioning that the absence of electromagnetic coupling between the antenna is an interesting aspect of the virtual array, which has also motivated its use.

When using the virtual array measurement technique, it is very important to know the accurate van speed in order to track the antenna position during the successive measurement points. Although GPS information could in principle be used, it was verified that it does not offer the required precision. The solution used here was to calculate the vehicle speed from the doppler spread. Specifically, the doppler spectrum is obtained by means of the time-domain

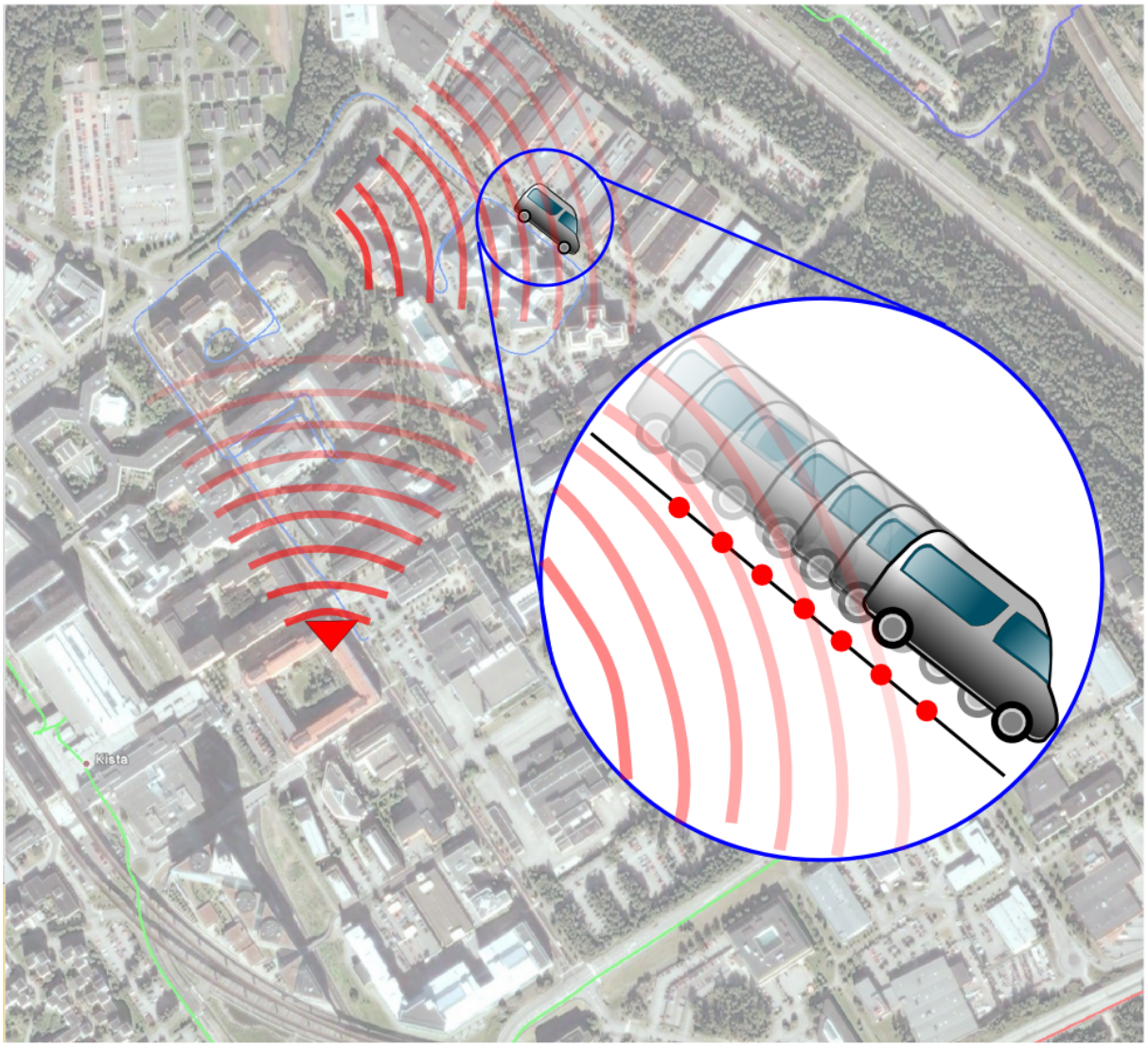

Figure 2.3: virtual array concept

Fourier transform of the collected data. Figure 2.4 shows the obtained Doppler spectrum while Figure 2.5 compares the speed registered by the GPS device wit that estimated from the Doppler spread. We can observe a significant difference between them.

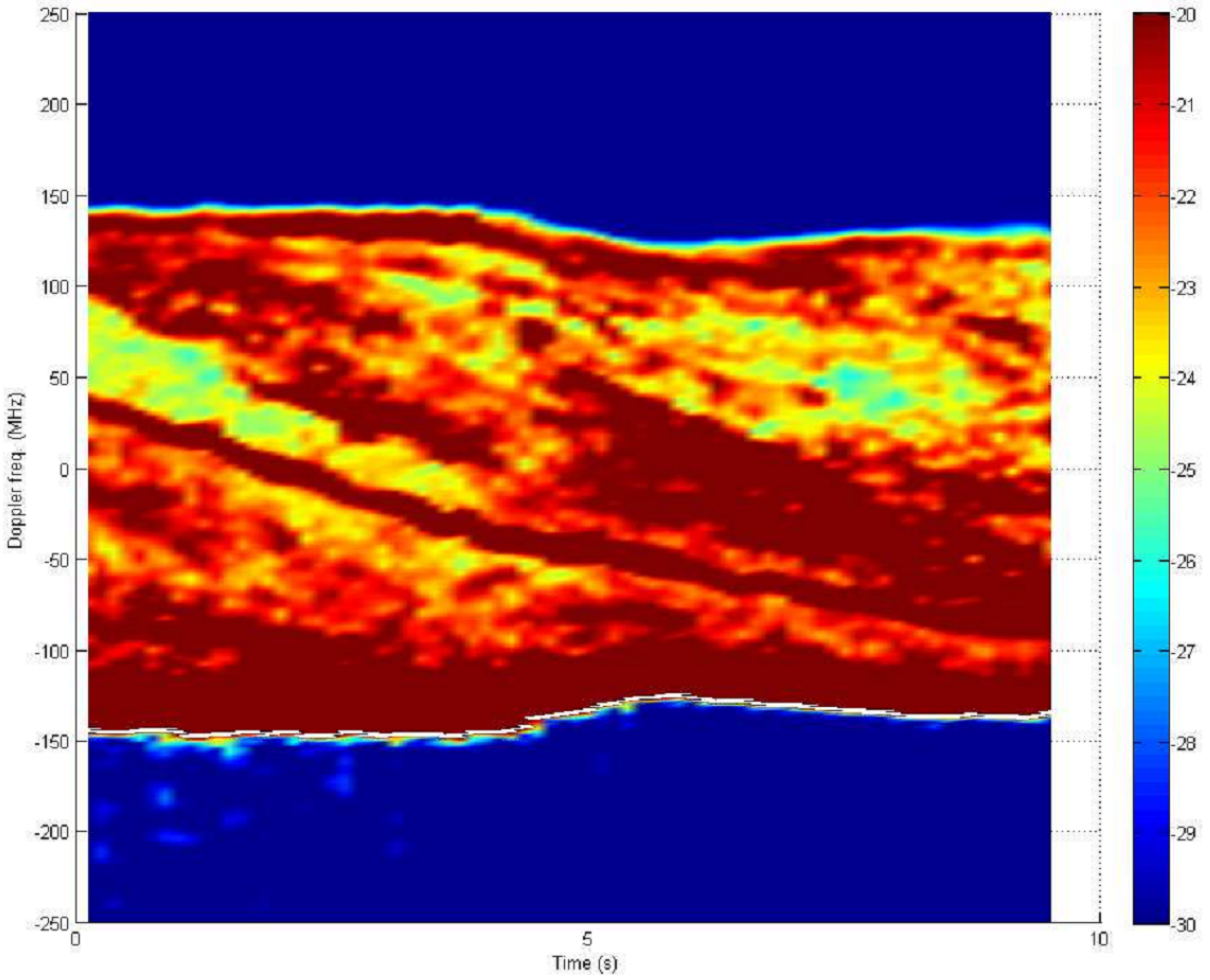

Figure 2.4: Doppler spectrum at segment 32

Each virtual array is approximated by a linear array of about 2 meters, comprising about sixty virtual antenna elements. Despite its simplicity, one limitation of the linear virtual array is that azimuth and elevation angles cannot be distinguished due to rotational ambiguity. This implies that each angle of arrival estimated by the IML method will lie on the surface of a cone, as illustrated in Figure 2.6.

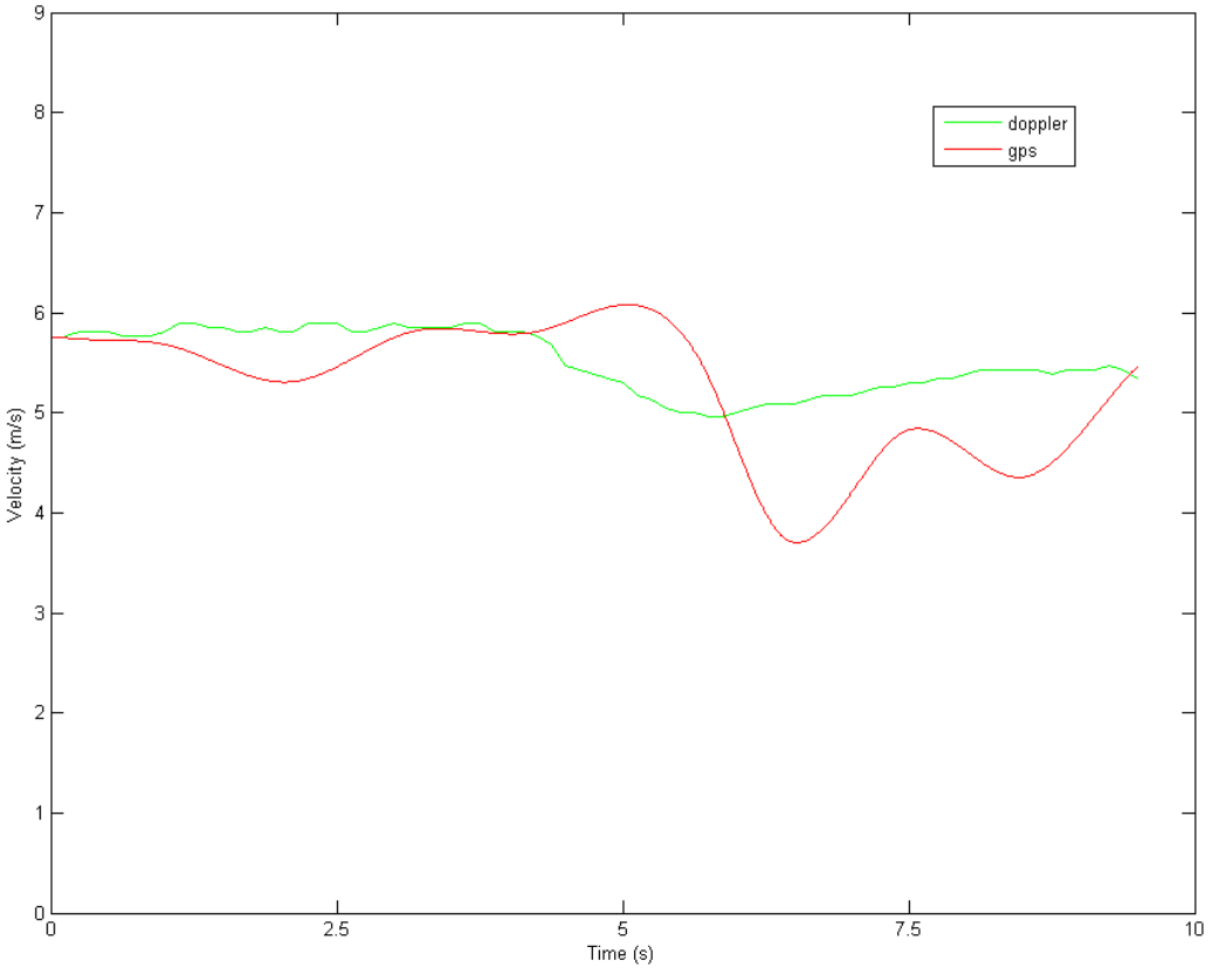

Figure 2.5: Speed at segment 32

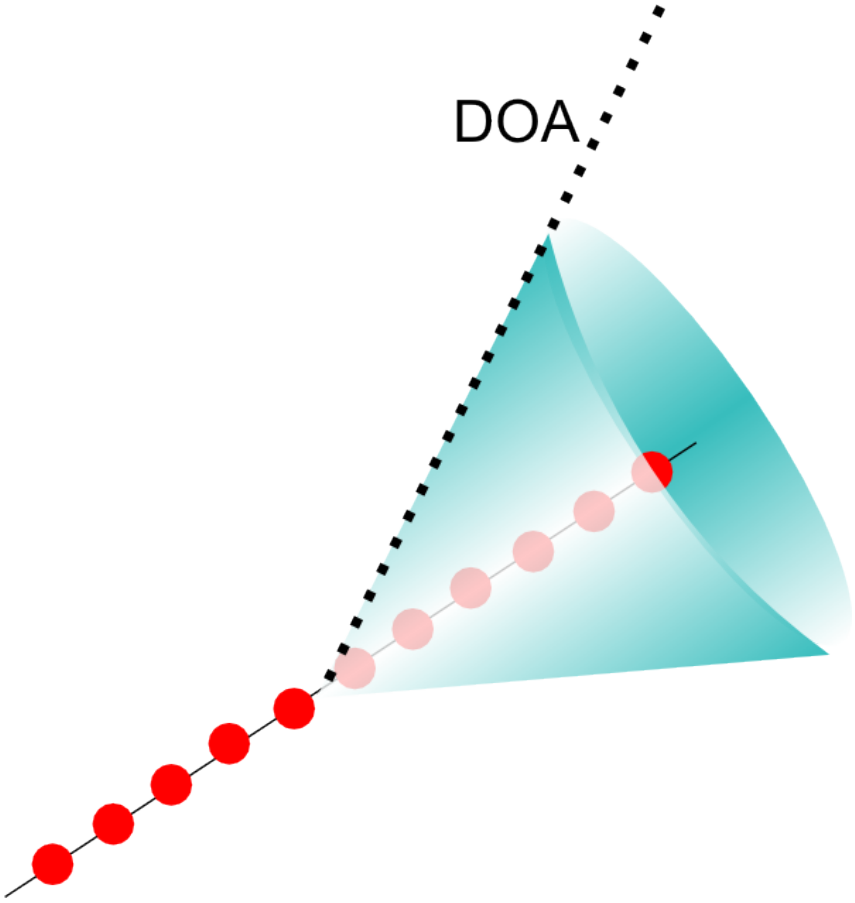

Figure 2.6: Virtual array and AOA cone

2.4 Simulation Results

This section presents the study the distribution of the received power, spatial correlation, and capacity along the measurement route. In a second part, it will focus on two specific segments of the route and discuss the relation between multipath spatial distribution and capacity. Finally, it will address the effects of spatial correlation and antenna polarization on the MIMO capacity for the two considered segments. These two segments have been selected because they present a strong change of signal behavior. Recall that the DOA and power distributions were obtained using the IML method. Figure 2.7 provides an illustration of the two segments of the measurement route considered in our analysis.

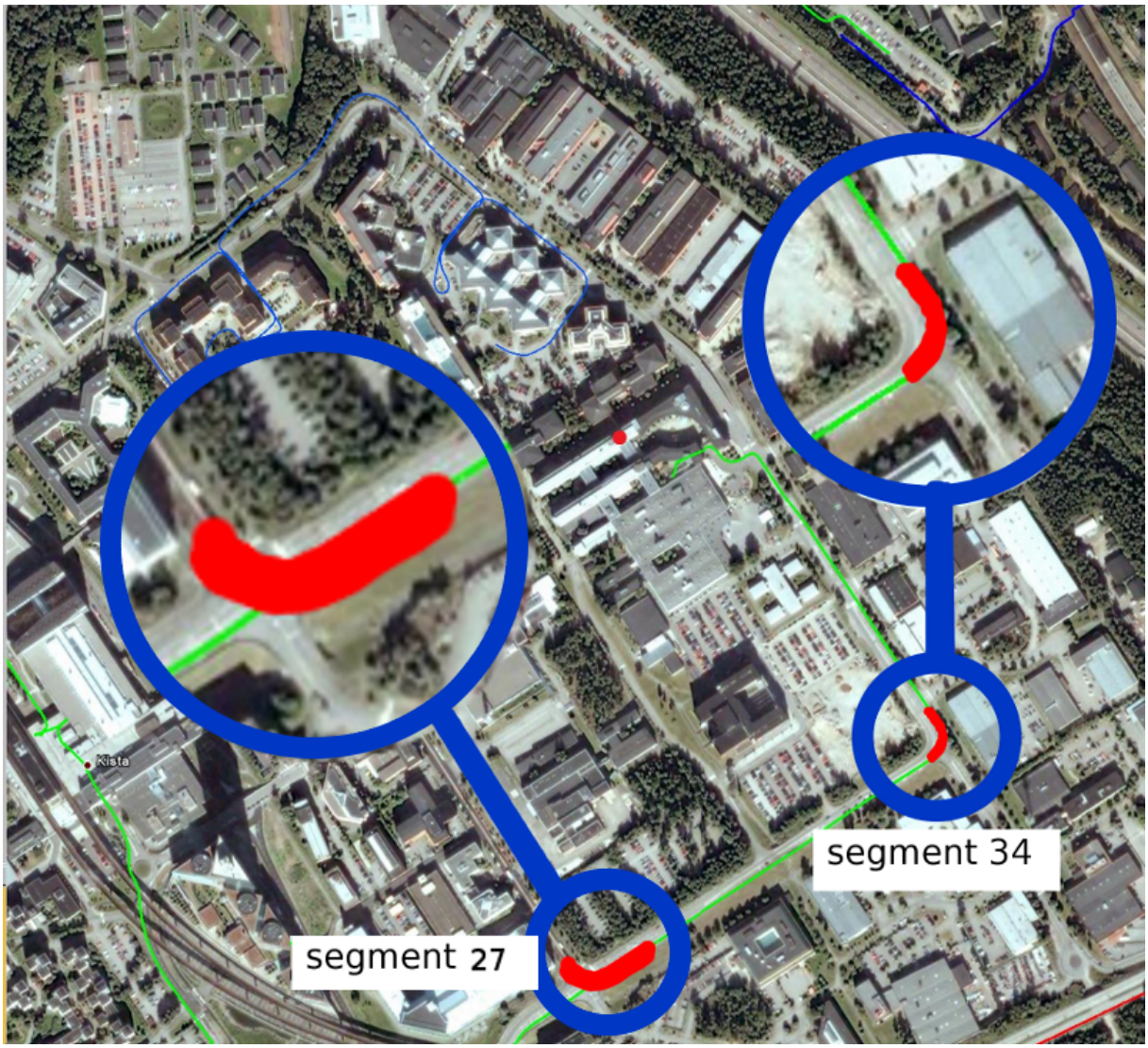

Figure 2.7: route segments 27 and 34

2.4.1 Capacity Fluctuations Along the Route

Figure 2.8 depicts the variation of the received signal power along the measurement route. As a reference for comparisons, Figure 2.9 shows the capacity of a 8 × 1 MISO system composed of four double polarized antennas at the transmitter and one vertically polarized antenna at the receiver (4V element in Fig. 2.2). The channel capacity at the k-th snapshot was calculated using the equation:

$$C_k = log_2 det \left[\mathbf{I}_{N_r} + SNR \left(\frac{\mathbf{H}_k}{\|\mathbf{H}_1\|_F} \right) \left(\frac{\mathbf{H}_k}{\|\mathbf{H}_1\|_F} \right)^H \right] \tag{2.5}$$

An SNR of 20dB is assumed for the first snapshot. In order to analyse the influence of the received signal power on the capacity fluctuations along the route, the channel matrix of each snapshot is normalized by that obtained at the first snapshot. So the capacity depends on power variation along the route. Note that this evaluation methodology represents a scenario where no specific power control is used.

Comparing Figures 2.8 and 2.9, it is possible to observe that the capacity fluctuations follow the variation of the received power, as expected. Now, lets look at the spatial correlation along the route. Figure 2.10 shows the correlation between the first and the fourth receiving elements of an 8 × 2 MIMO system, now using two cross-polarized antenna elements at the receiver (4V and 5H array elements in Fig. 2.2). It shows that locations exhibiting a higher received signal power also present higher correlations. This indicates that points with a higher receive signal power are probably receiving a strong LOS component and/or specular reflected multipath components, which are naturally more correlated at the receiver. On the other hand, regions with lower received signal powers are usually composed of diffuse reflection paths which are less correlated.

Studies like [1], [2] have shown that MIMO capacity depends on the signal uncorrelation. Figure 2.11 shows that the MIMO capacity is indeed proportional to the received power, like the SIMO system. The system (8x4) is composed by four double polarized transmitters and two double polarized receivers (elements 4V, 4H, 5V and 5H). But the MIMO/SIMO gain shown on Figure 2.12 express the importance of signal uncorrelation to the MIMO system.

The gain is at least over 1x and as high as almost 8x in some points. Why not a maximum of 4x gain? This can be explained by the fact that the maximum 4x gain is expected when the receiving antennas have the same characteristics. But as they have different polarization, the places where the gain is higher then 4x are places where the 4V element performance (the SIMO receiver element) is specially weak.

2.4.2 MIMO Capacity Gains

Now this work focus on two interesting route segments. Figure 2.13 shows the DOA along the route segment 27. We can see that a strong multipath cluster appears at 120^o and changes its position to 20^o at snapshot 50 while an additional multipath cluster appears at 60^o. Figure 2.14 shows the correlation of different receiving antenna pairs at segment 27. We can see that the antenna correlation is the same for all the antenna pairs until snapshot 25. After this point, the correlation between the vertically polarized elements (4V,5V) becomes higher then that for the other antenna pairs. After snapshot 25, we can identify only one dominant multipath cluster. It is also worth noting that the dual-polarized antenna element (4V,4H) presents the same correlation pattern as the cross-polarized antenna pair (4V,5H), which indicates that we can trade spatial diversity for polarization diversity in this case.

Figure 2.15 shows the capacity fluctuations along segment 27 for different MIMO and

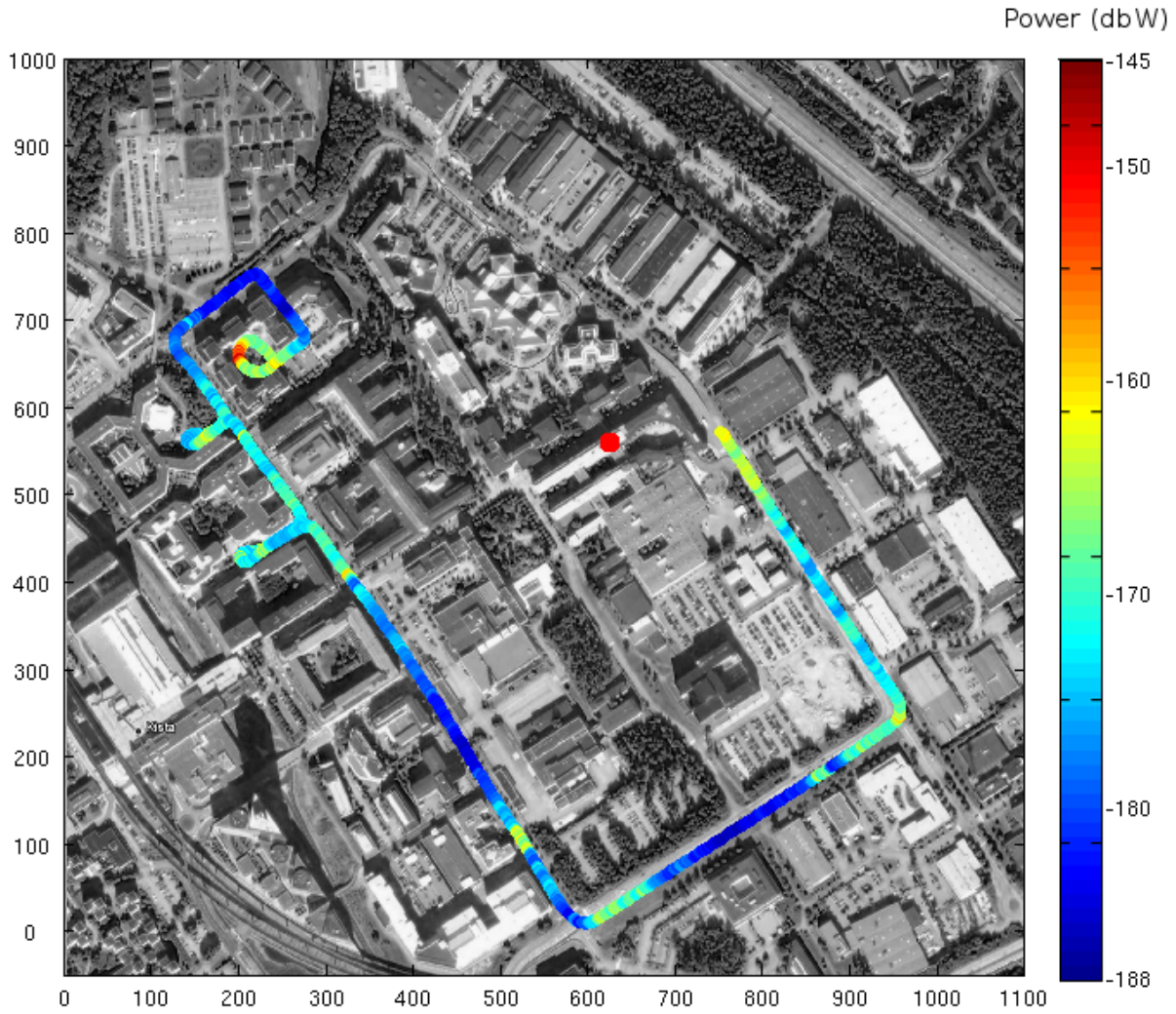

Figure 2.8: Received power variation along the route

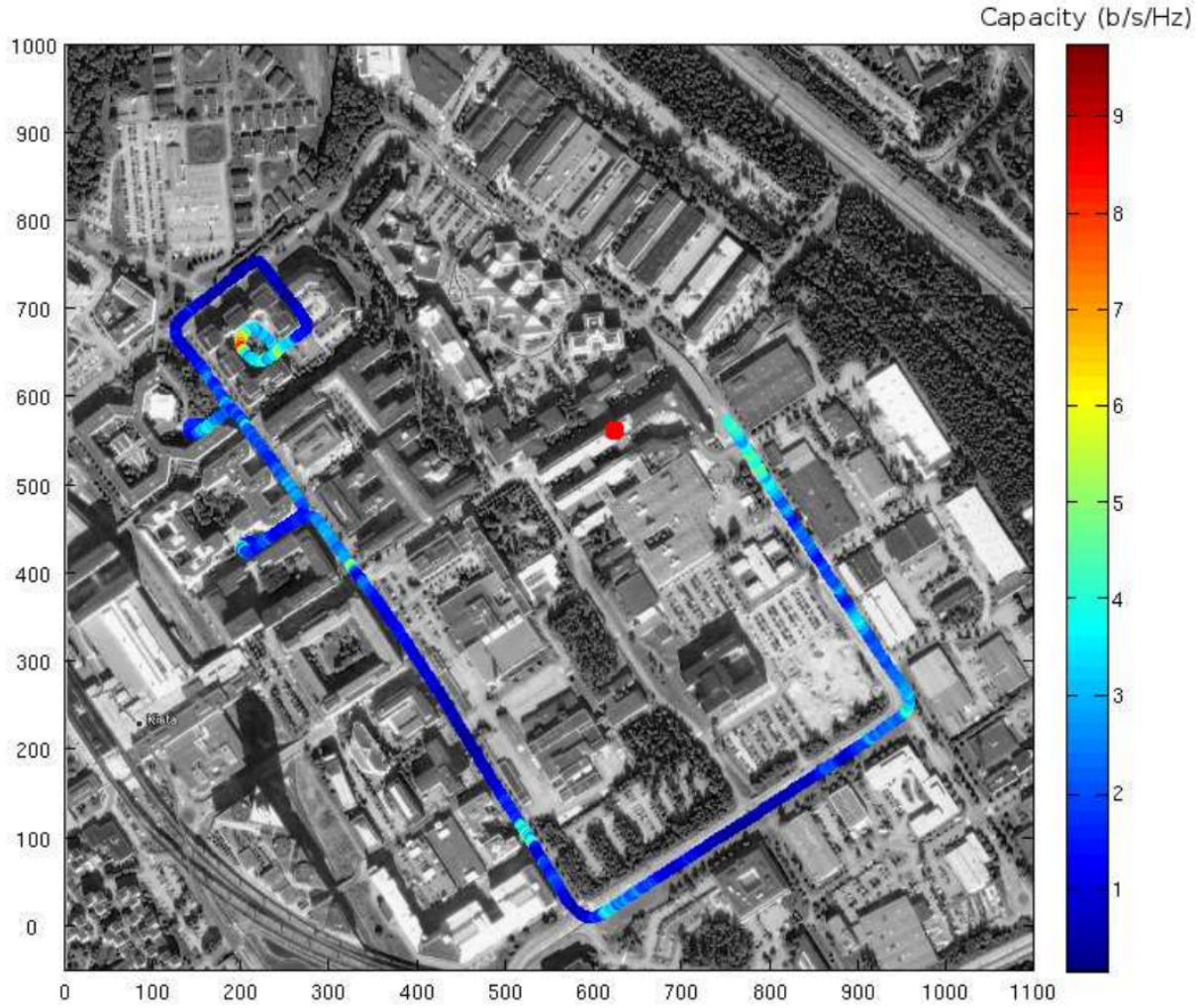

Figure 2.9: Capacity fluctuation along the route (SNR of 20dB)

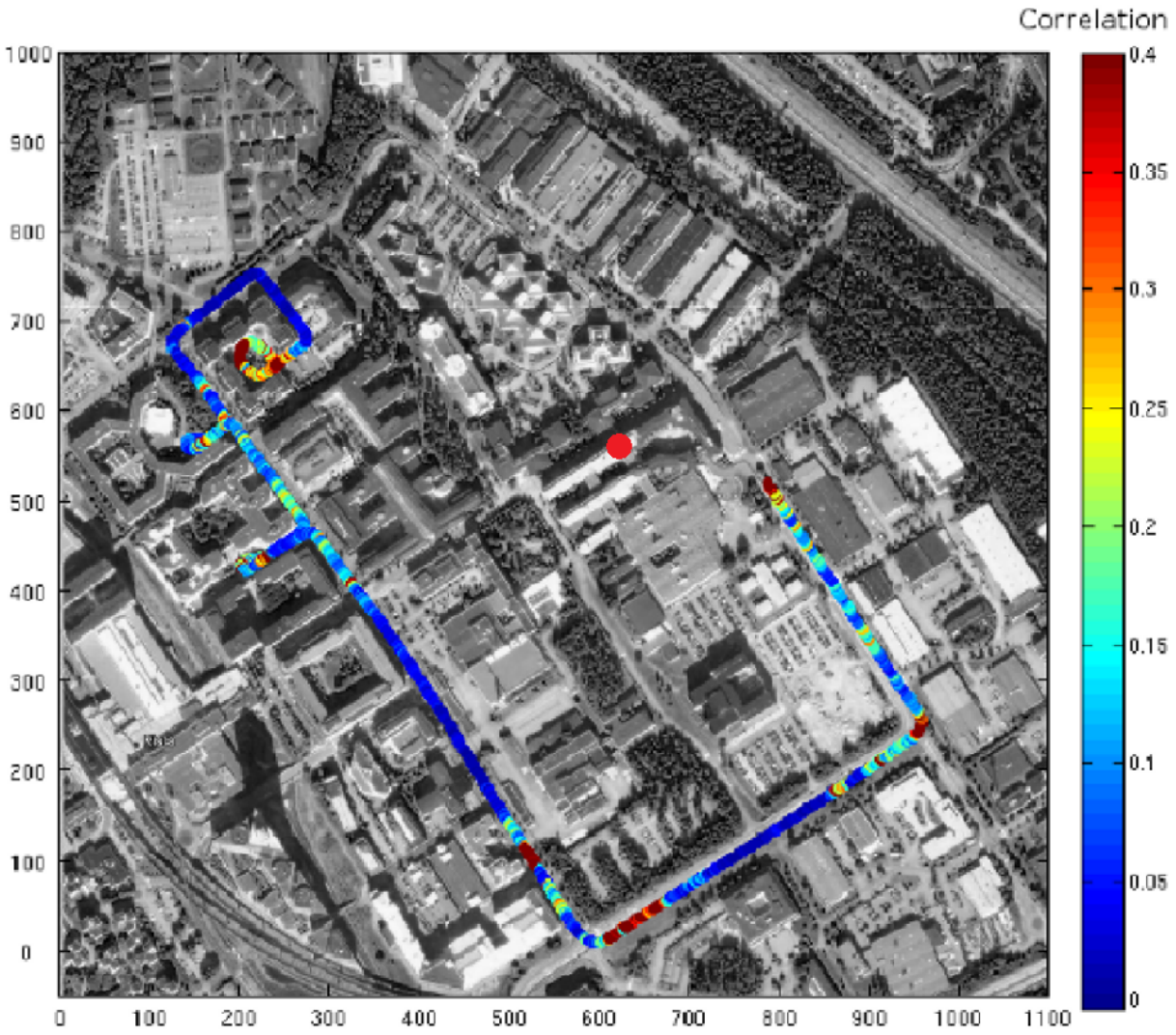

Figure 2.10: Signal correlation along the route

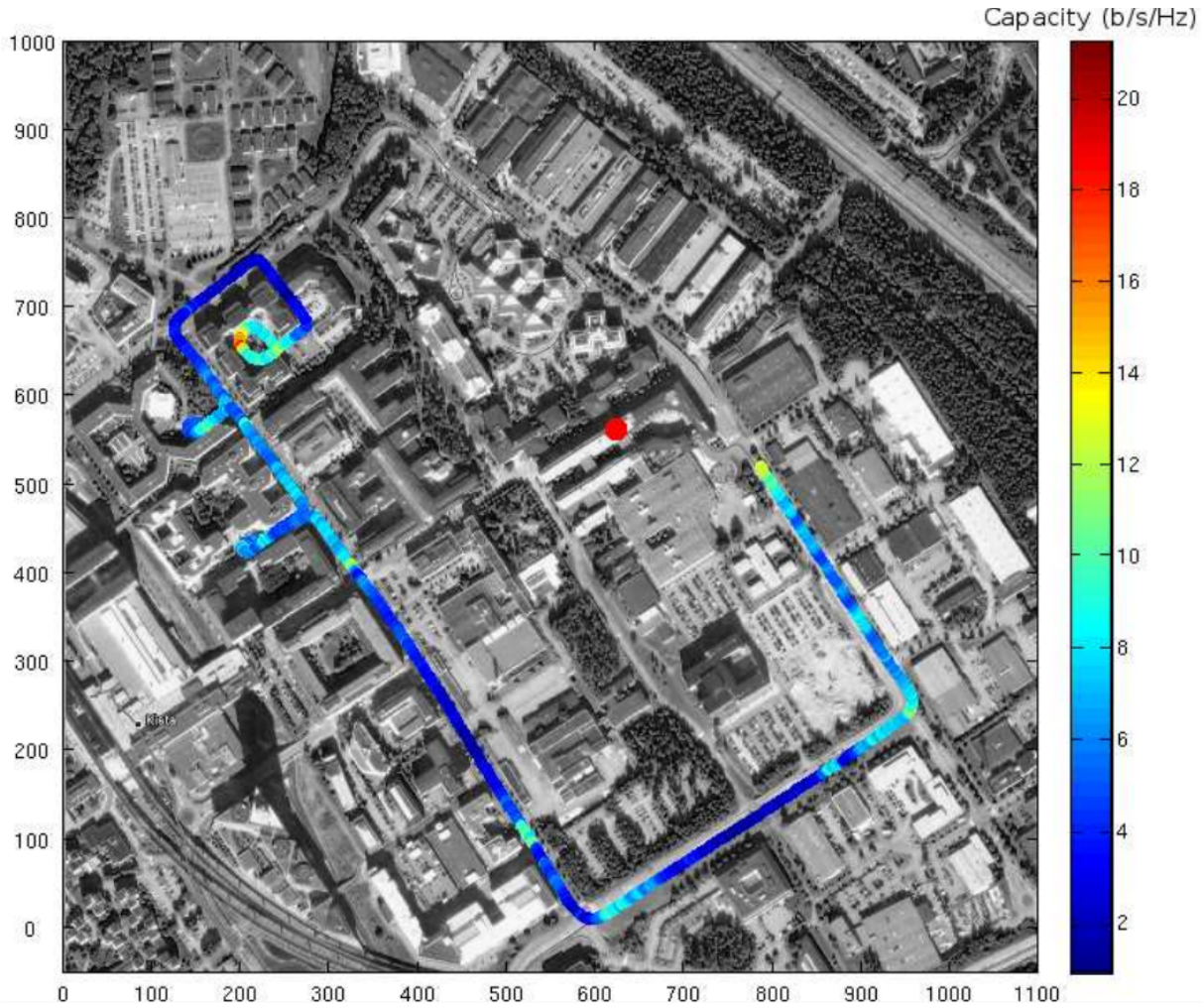

Figure 2.11: MIMO(8x4) capacity along the route (SNR of 20db)

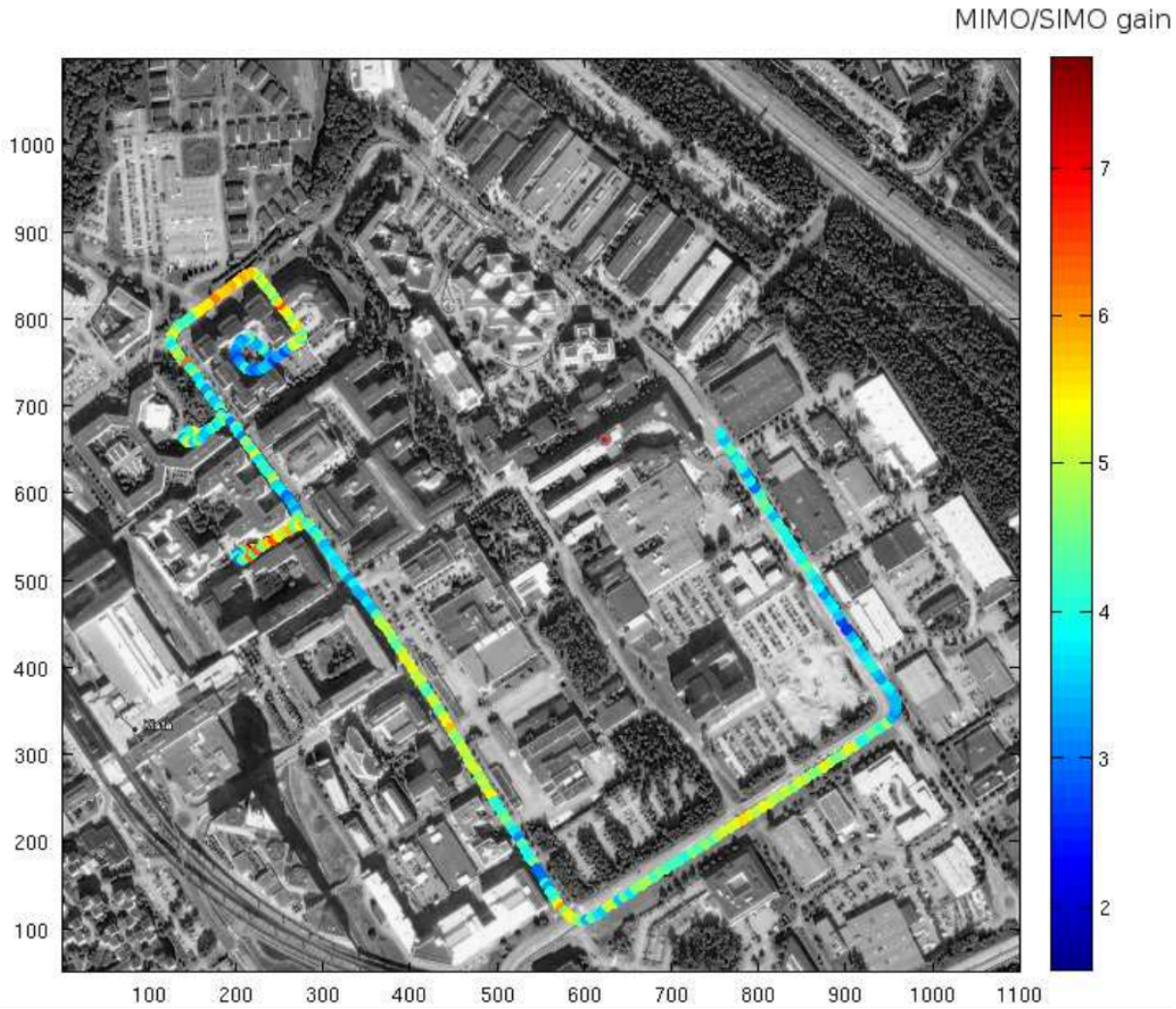

Figure 2.12: MIMO/SIMO capacity gain along the route

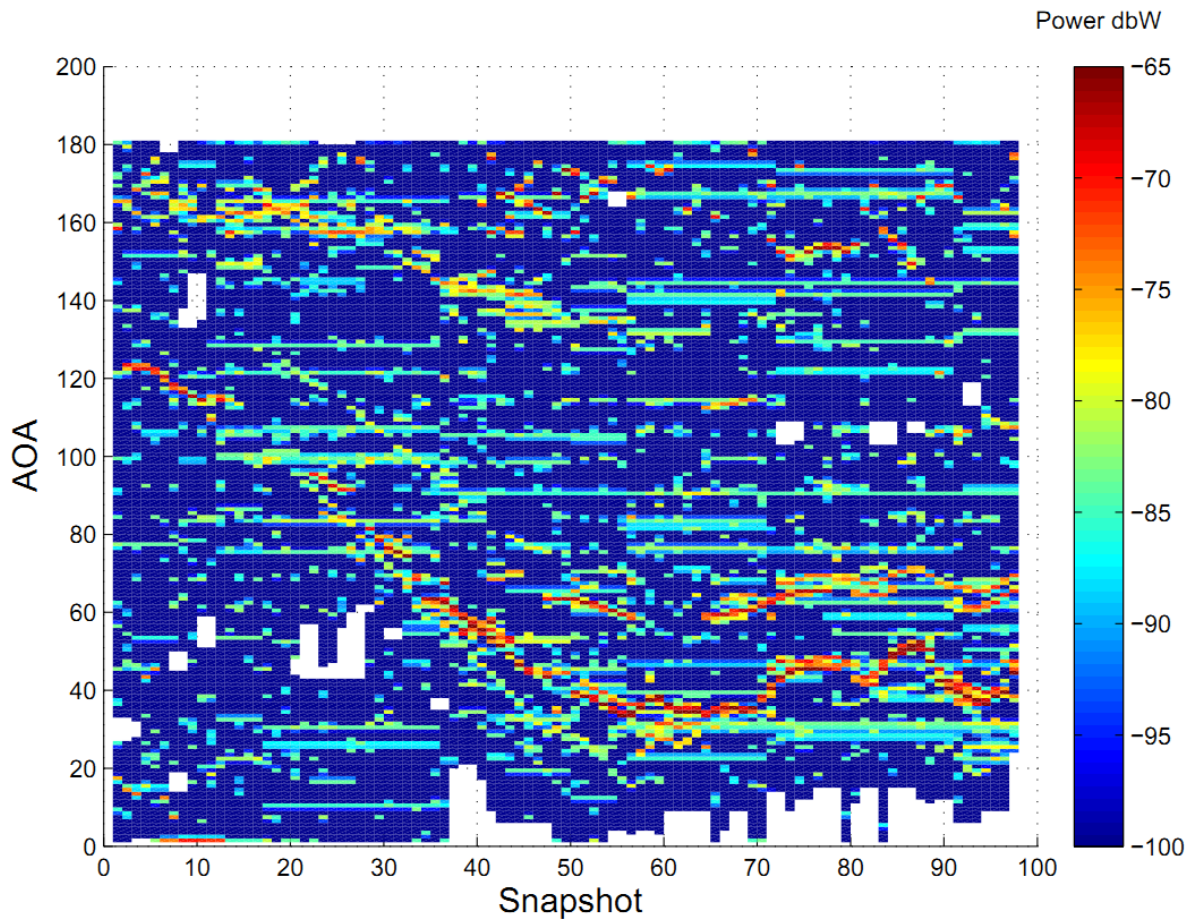

Figure 2.13: DOA distribution along segment 27.

MISO system configurations, for an SNR of 20dB. The 8×4 MIMO system uses all the available antennas, i.e. the 4 double-polarized transmitting antennas and the 2 double-polarized receiving antennas. The 8×1V MISO system uses only the antenna element 4V at the receiver while the 8×1H MISO system uses only the antenna element 4H at the receiver. The 8×2V MIMO system system uses elements 4V and 5V at the receiver. The 8×2H MISO system uses elements 4H and 5H. The 8×2VH1 MIMO system explores only the polarization diversity, because it uses a single double-polarized antenna element (4V,4H) at the receiver. Finally, the 8×2VH2 uses elements 4V and 5H at the receiver aiming at exploring both polarization and spatial diversities.

Note that system configurations that rely mostly on spatial antenna separation have a strong decrease on the capacity, while systems relying on polarization diversity are much more stable and are less affected by changes on DOA distribution. It is also important to note that both polarization diversity systems 8×2VH1 and 8×2VH2 have the same capacity performance. As expected, the capacity of the MISO systems are the same and remains constant because it only depends on the received SNR which is fixed at 20dB.

Now, looking at segment 34, Figure 2.16 shows two different behaviors. First of all, note that between snapshots 1 and 40, two important multipath clusters are changing their DOAs. For instance, the strongest cluster changes its DOA from 100^o to 40^o. After snapshot 50, there are less important clusters and the received power is more spatially spread. Figure 2.17 shows the correlation of antenna pairs at the receiver. It is possible to see that between snapshots 30 and 50, where stronger clusters are present, there are strong antenna correlations. After snapshot 50, there are no dominating clusters, antenna

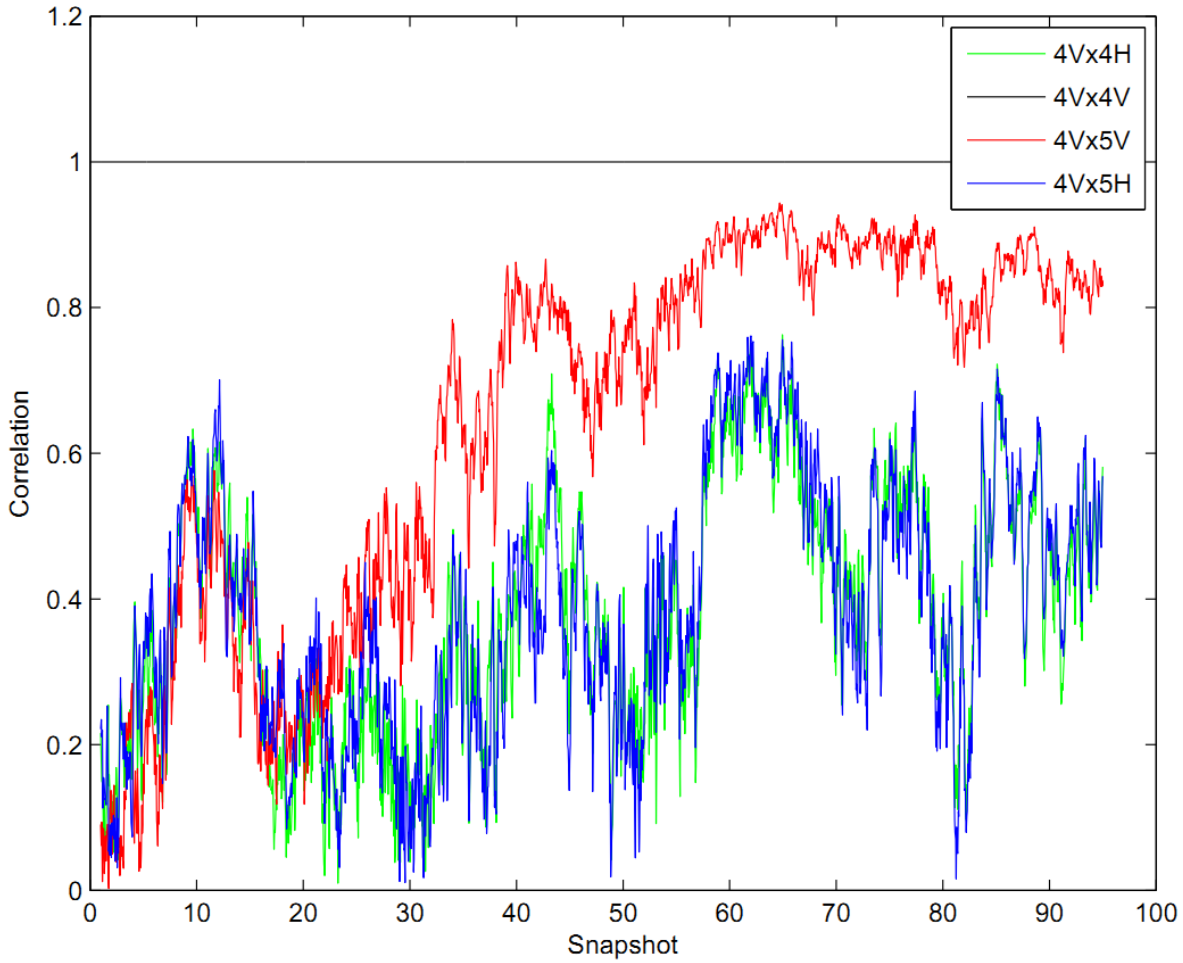

Figure 2.14: Correlation curves for segment 27.

correlation decreases for all the considered antenna pairs. In particular, the vertically polarized antenna pair presents a higher correlation than the other antenna pairs at the beginning of the segment.

Figure 2.18 shows the capacities for different MIMO and MISO system configurations. The configurations are the same as those used in the previous experiment. The 8×2VH1 system using polarization diversity is much more stable and offers better peak and average capacities. In the first half of the route, when we have the stronger clusters, systems relying only on spatial diversity present the worst results. In the last part of the route, where stronger multipath clusters are absent, all systems present a similar performance. Again it is possible to note that the antenna separation in system 8×2VH2 brought no additional capacity gain compared to the 8×2VH1 pure polarization diversity system. Figure 2.19 shows the capacity CDFs for all system configurations and an SNR fixed to 20dB. It can be seen that polarization diversity MIMO systems outperform pure spatial diversity systems, corroborating the importance of exploring polarization information at the receiver in an outdoor propagation scenario.

2.5 MIMO Channel Model Validation

The last section performed an experimental characterization of an outdoor MIMO wireless channel, and then analyzed the impact of different direction of arrival (DOA) distributions and polarization diversity configurations on MIMO capacity.

One important conclusion is the importance of polarization diversity for MIMO capacity,

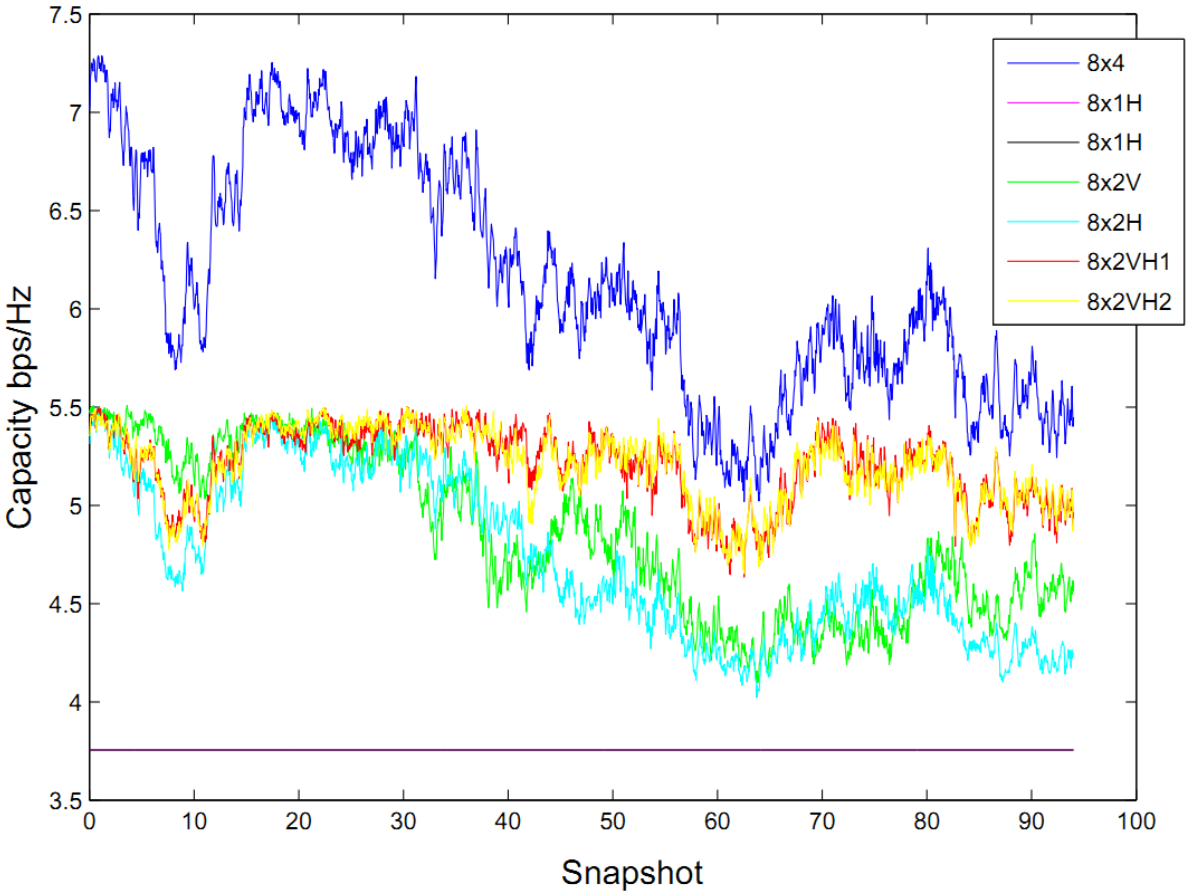

Figure 2.15: Capacity fluctuations for different system configurations along segment 27.

especially considering the spatial constraints of mobile terminals. The conclusions on polarization diversity agree with works such as [4], [5] and [6]. But there are other important factors to be considered, such as antenna separation as shown in [7]. The characteristics of the propagation environment are also important such as multipath cluster distribution as discussed in [8] and [9]. The work [10] also investigates the impact of propagation environment as the relationship between different MIMO arrays and different propagation scenarios. The conclusion in [10] is that for a small angular spread of 8^o it is necessary to have a 4 wavelength antenna separation in order to achieve an uncorrelated channel.

This section use the measurement data in order to create a cluster based model of the propagation environment validated by the measurements. The last section focused on the channel characterization and ergodic capacity study of MIMO channels measurements. The aim was to estimate the DOA parameters by means of an iterative maximum likelihood algorithm [42], resulting in the estimation of the DOAs of the dominant multipaths. Unfortunately, the precision of the DOA estimation is not sufficient to directly infer the cluster's angle spread. This statistical information is very important for the antenna optimization model that will be presented in the next chapters. Herein, we start from the inferred main directions of arrival, and then use an optimization procedure in order to find out the angle spreads. The model is evaluated by comparing the statistics of correlation and capacities of the synthetic channel with those of the measured channel.

2.5.1 Cluster Angle Spread Determination

The model used for the simulations in [18] is based on clusters of scatterers defined by a main direction, and its associated angle spread, as illustrated in Figure 3.3.

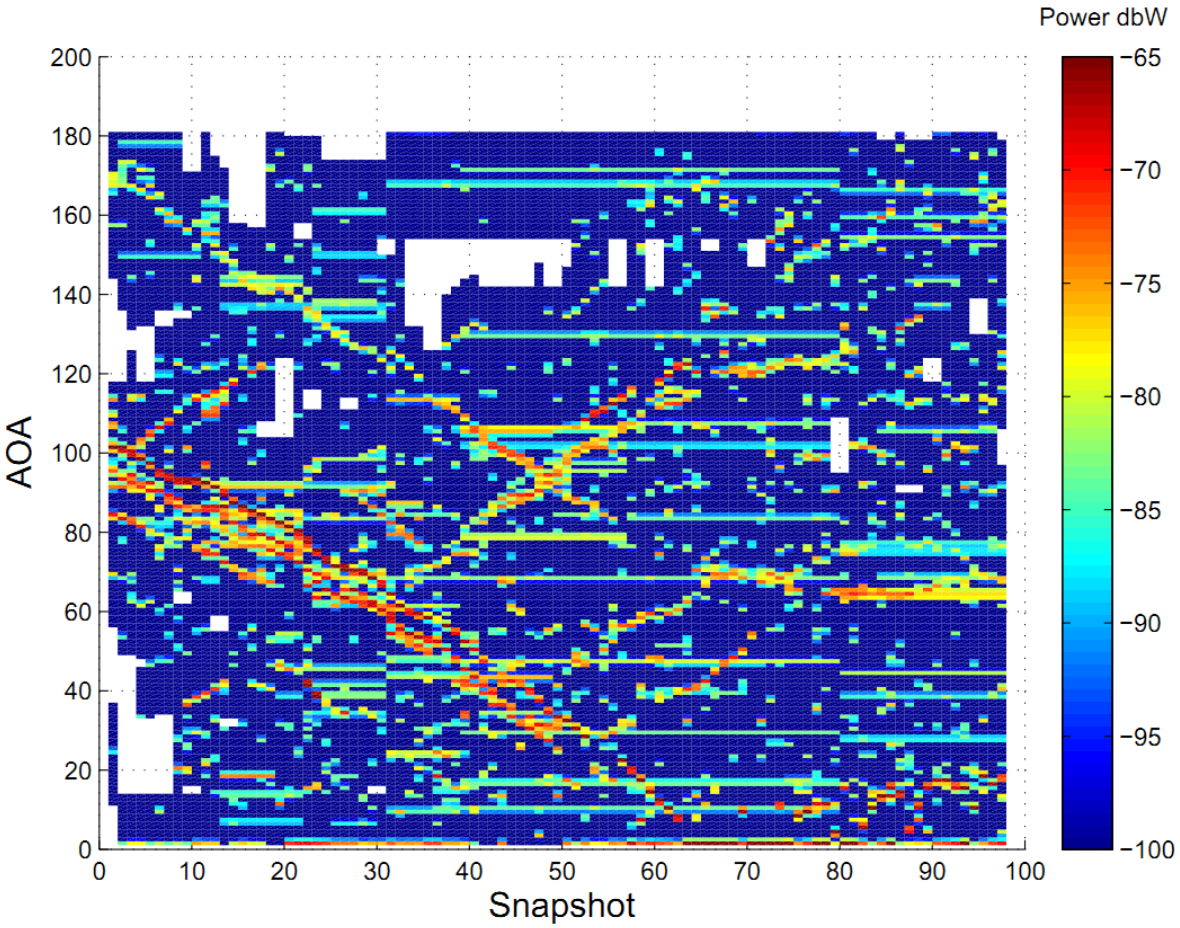

Figure 2.16: DOA distribution along segment 34.

Before making any assumption regarding the angle spread, it is important to see if the directions of arrival obtained are believable. The work of [46] shows that different directions of arrival over a linear array have a strong impact over signal correlation among antennas. If a fixed angle spread for the directions of arrival is arbitrarily choosen, and two antennas with the same separation distance of the measured ones, one can expect to see a similar behavior between the channel model correlations and measured data correlations. Of course, the curves will not coincide, but it should be expected, if the directions of arrival are correctly inferred, a similar tendency of the curves.

Figure 2.21 shows the signal correlation between two antennas for the measured data and the model using an arbitrary fixed angle spread. It is possible to see that,except for some deviations, especially after snapshot 70, the curves have the same behavior.

In order find the correct angle spreads for the clusters, one unfortunate but necessary simplification has to be made. It is not possible to recover different angle spreads for different clusters in the same data snapshot. So the best that is possible to do is to find a general angle spread for all clusters for a given snapshot. It can be done by comparing the correlation of the measured data in one snapshot to its respective correlation given by the model. This is done solving the following minimization problem:

$$\alpha^* = \arg\min_{\alpha} \|\mathbf{R}_{RX_{MODEL}}(\alpha) - \mathbf{R}_{RX_{DATA}}\|_F \tag{2.6}$$

where α is the angle spread for the snapshot and α^* denotes its optimum value according to the above criterion. $\mathbf{R}_{RX_{MODEL}}$ is the correlation for the two receive antennas obtained

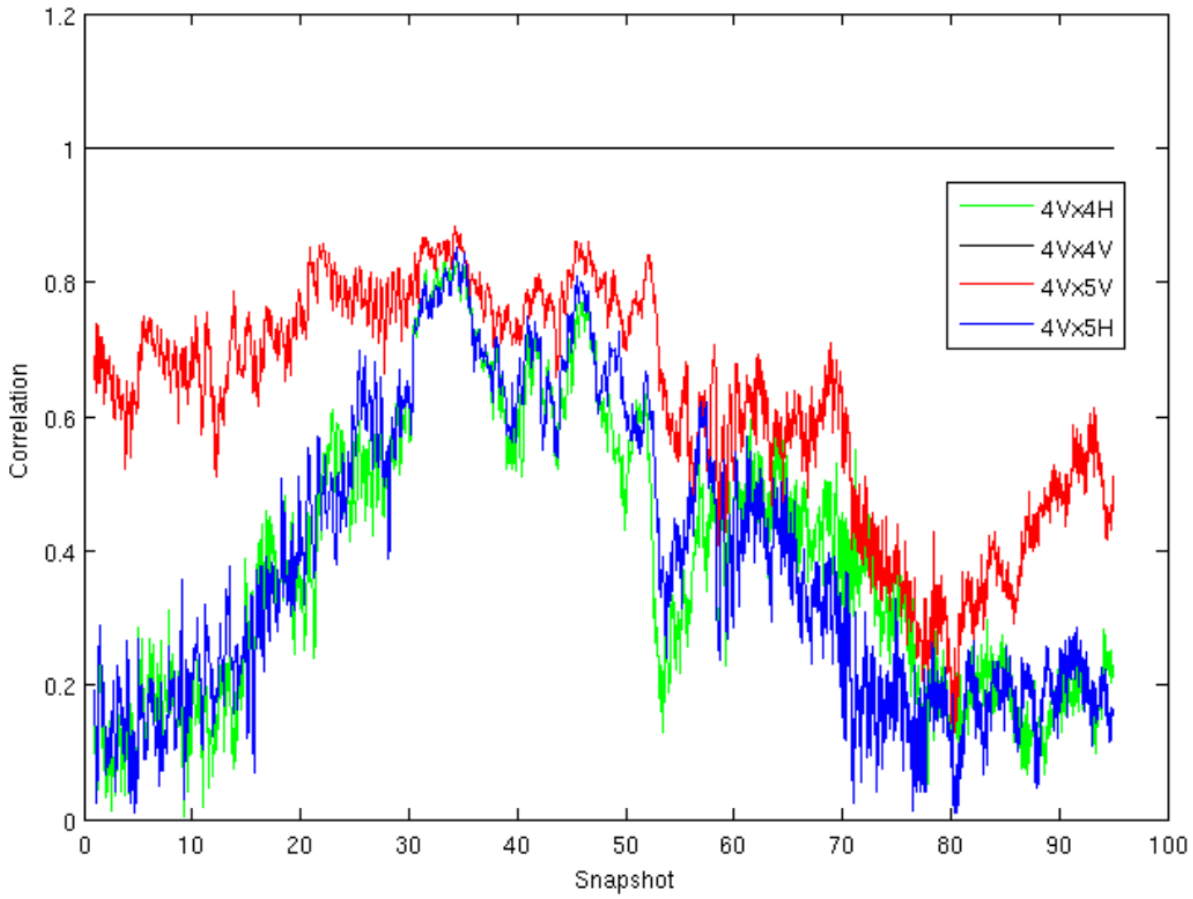

Figure 2.17: Antenna correlations along segment 34.

for the channel matrices generated by the model, and $\mathbf{R}_{RX_{DATA}}$ is the correlation for the two receive antennas obtained for the channel matrices of the measurement data.

The function $\mathbf{R}_{RX_{MODEL}}(\alpha)$ has two important characteristics. First, it is a monotonic function, since the correlation decreases as the angle spread is increased. This characteristic makes the proposed functional easy to minimize. But on the other hand, it is a non differentiable function, preventing the use of simple but efficient gradient based methods. The method chosen for the optimization was the bisection method [47]. It is a very simple method that has proven to be useful for minimizing (2.6).

Figure 2.22 shows the curve of the correlation between receive antennas for the measured data and for the model with angle spread found by the procedure explained above. The curve is for segment 34 of the route, and one can see that the corrected model curve fits much better. Figure 2.23 shows the cumulative distribution function (CDF) of the cluster angle spread obtained from the channel snapshots taken all over the route, recalling that the clusters use Laplacian multipath distributions [48], [49], [50].

2.5.2 Model Validation

To validate the model, two antennas in the same positions as the antennas used in the measurements were simulated, and the simulation model was run for all routes. Then, statistical data from the channel matrices of the measurement data was compared to the channel matrices obtained from the simulations. Figure 2.24 draws a comparison between the cumulative distribution function of the receive antennas correlation for the simulated model and the actual data. Considering the simplifications in the model, its behavior is very

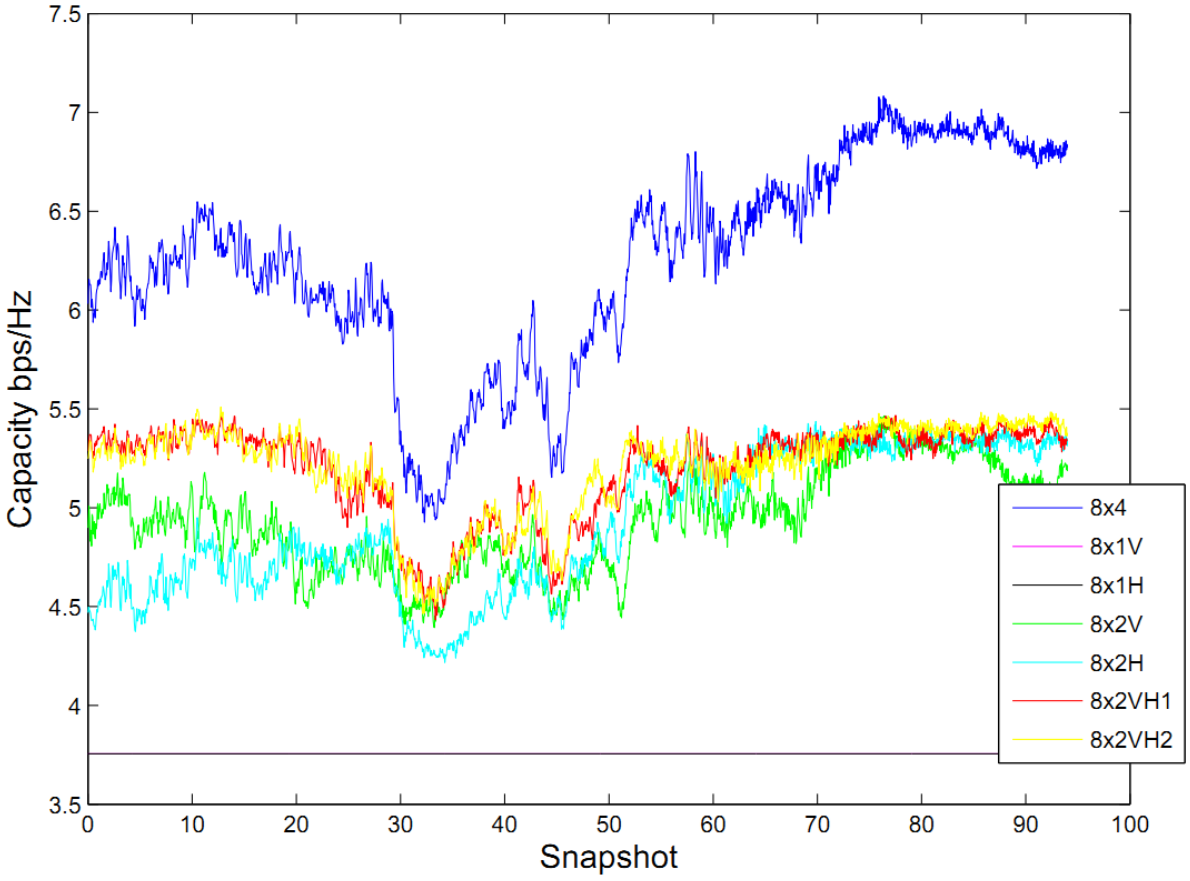

Figure 2.18: Capacity fluctuations for different system configurations along segment 34.

similar to that of the measurement data.

The figure 2.25 shows the cumulative distribution functions of the ergodic capacities for various MIMO systems, comparing the capacities of the measured data and the capacities obtained by the model simulations. The biggest difference is when we compare $8 \times 2V$ and $8 \times 2VH$. While the measurement data is very similar in the two cases, the model presents a difference between them. This might be attributed to the difficulty of capturing the effects of diffuse scattering and its effect in polarization into the model.

2.6 Conclusions

An experimental capacity evaluation based on measured wideband MIMO channels in an outdoor wireless environment was performed. This study allows us to evaluate the impact of different polarization diversity configurations and DOA distributions on the MIMO capacity. These results corroborate the peak and average capacity gains provided by polarization diversity MIMO systems compared to spatial diversity systems. These gains are attributed to the fact that the distance between receiving antennas is at the order of $\lambda/2$, which is a practical assumption in mobile receiver terminals.

Even using some simplifications, it was possible to create a cluster of scatterers propagation model based on real MIMO channel measurements. This updated channel model is important to produce more realistic simulations for antenna array optimization.

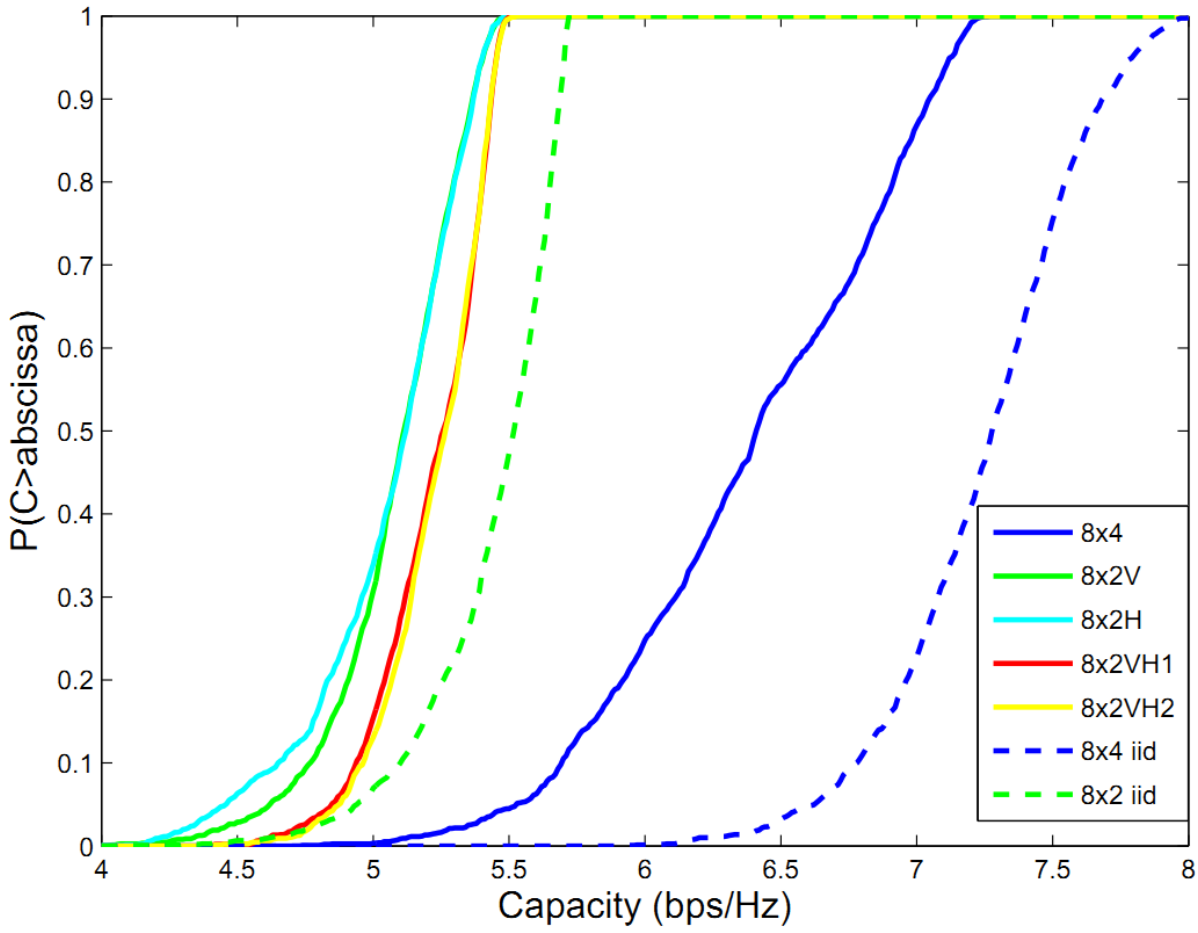

Figure 2.19: Capacity CDFs for different system configurations and SNR=20dB.

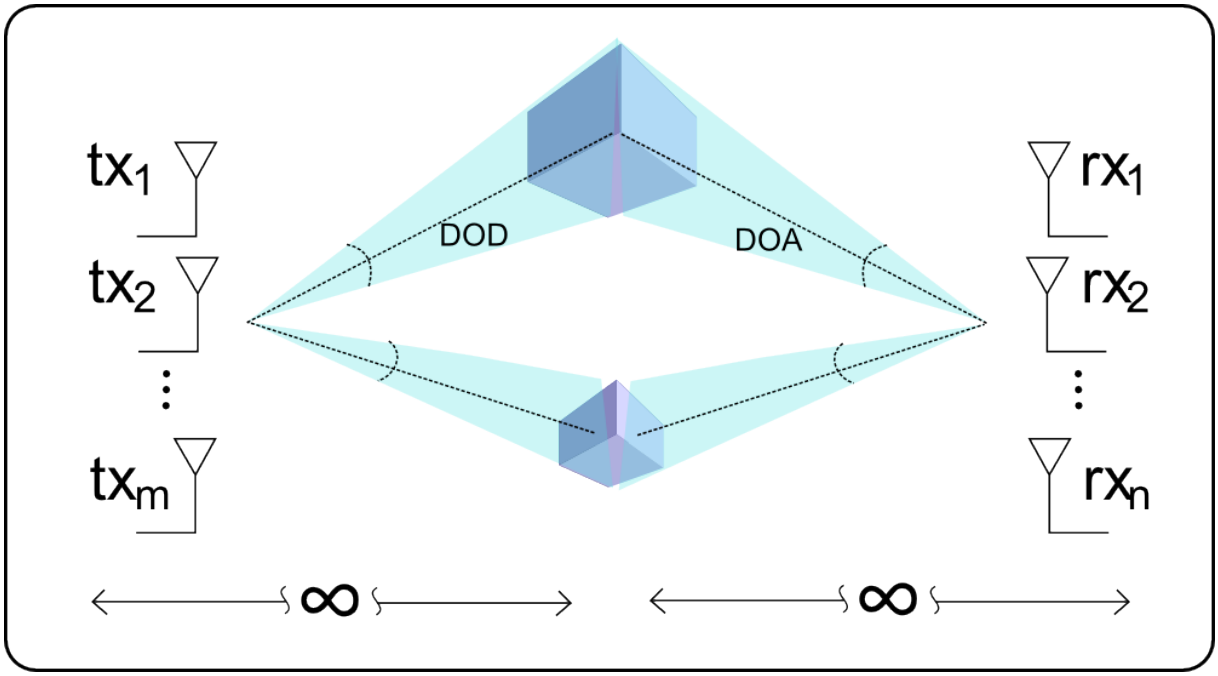

Figure 2.20: Geometric channel model.

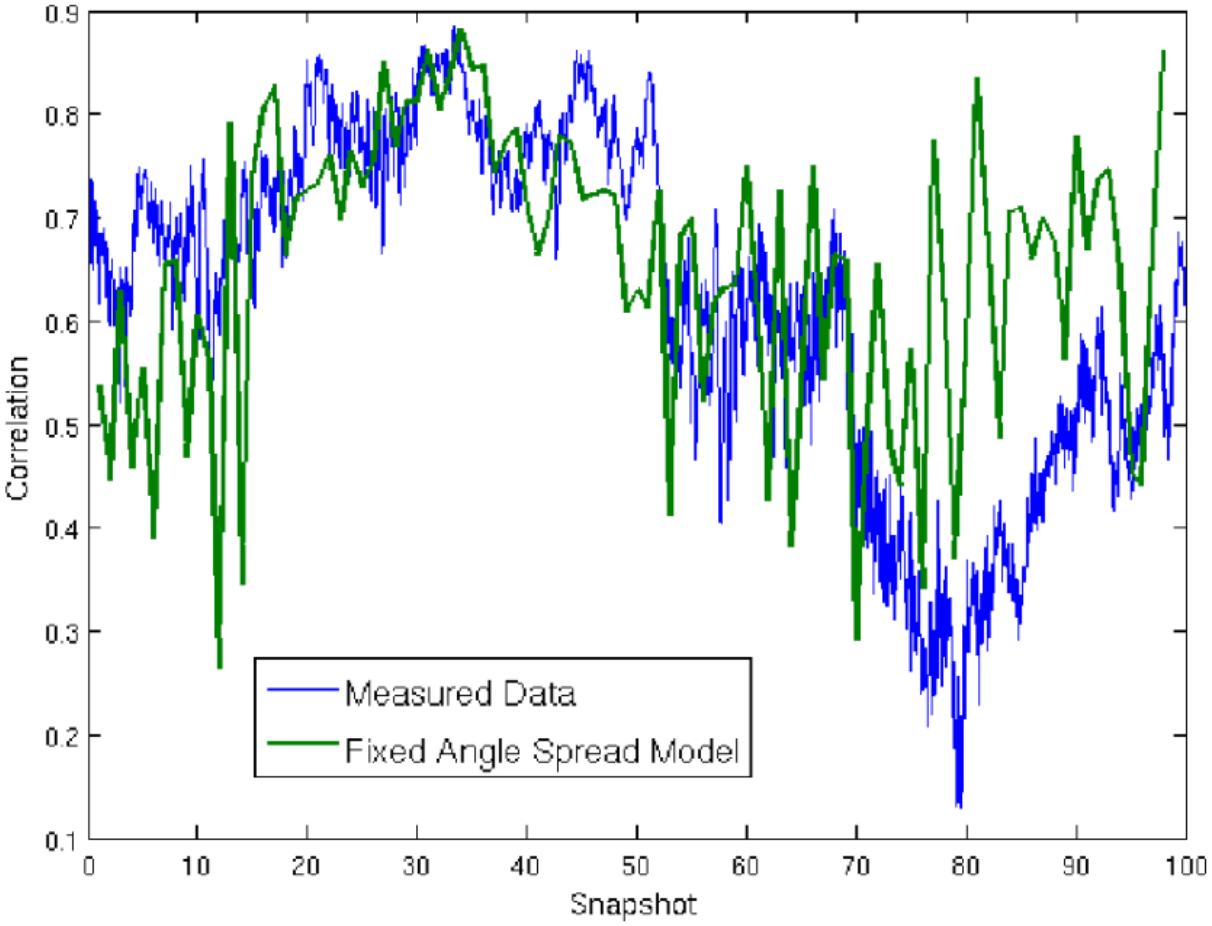

Figure 2.21: Antenna correlation along segment 34 of the measured route.

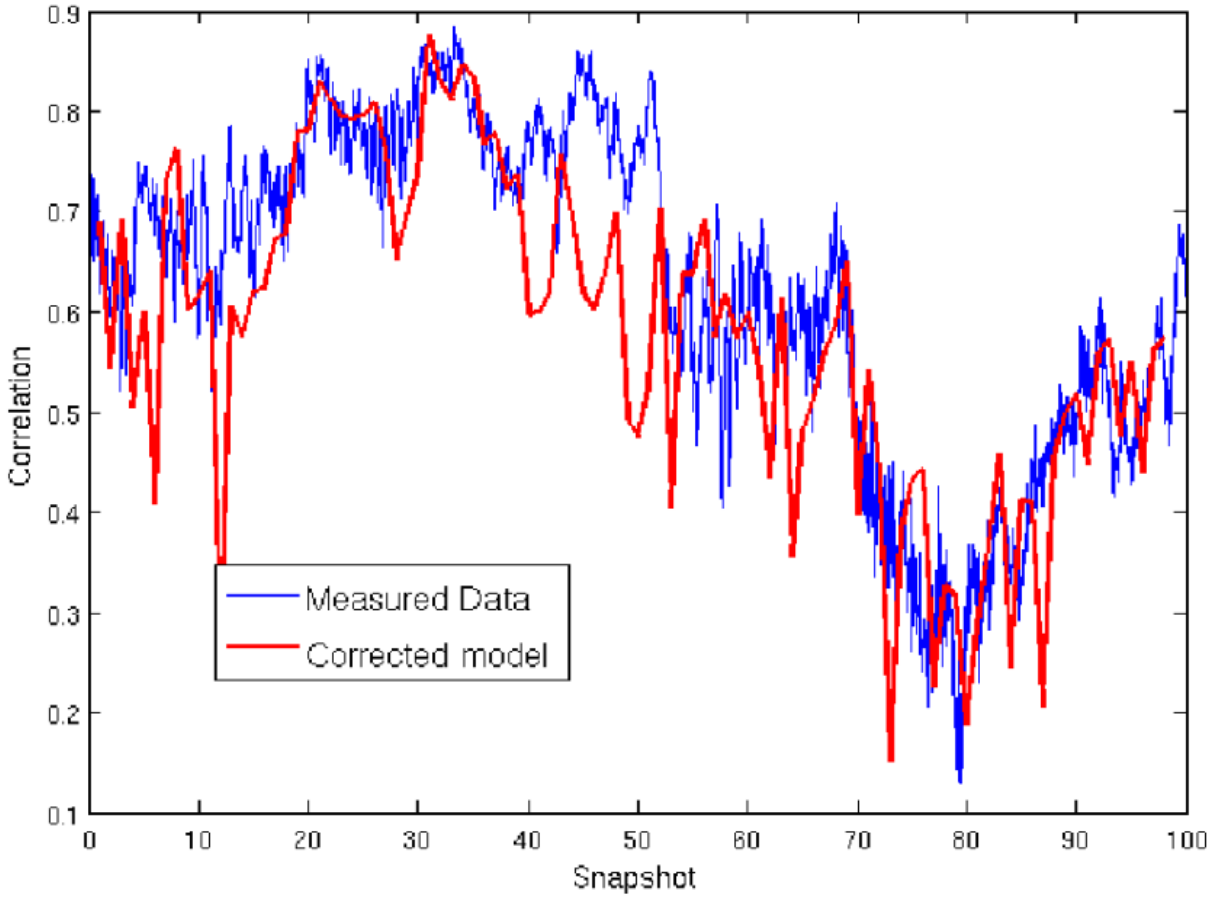

Figure 2.22: Antenna correlation along segment 34 of the measured route, obtained with the optimized model.

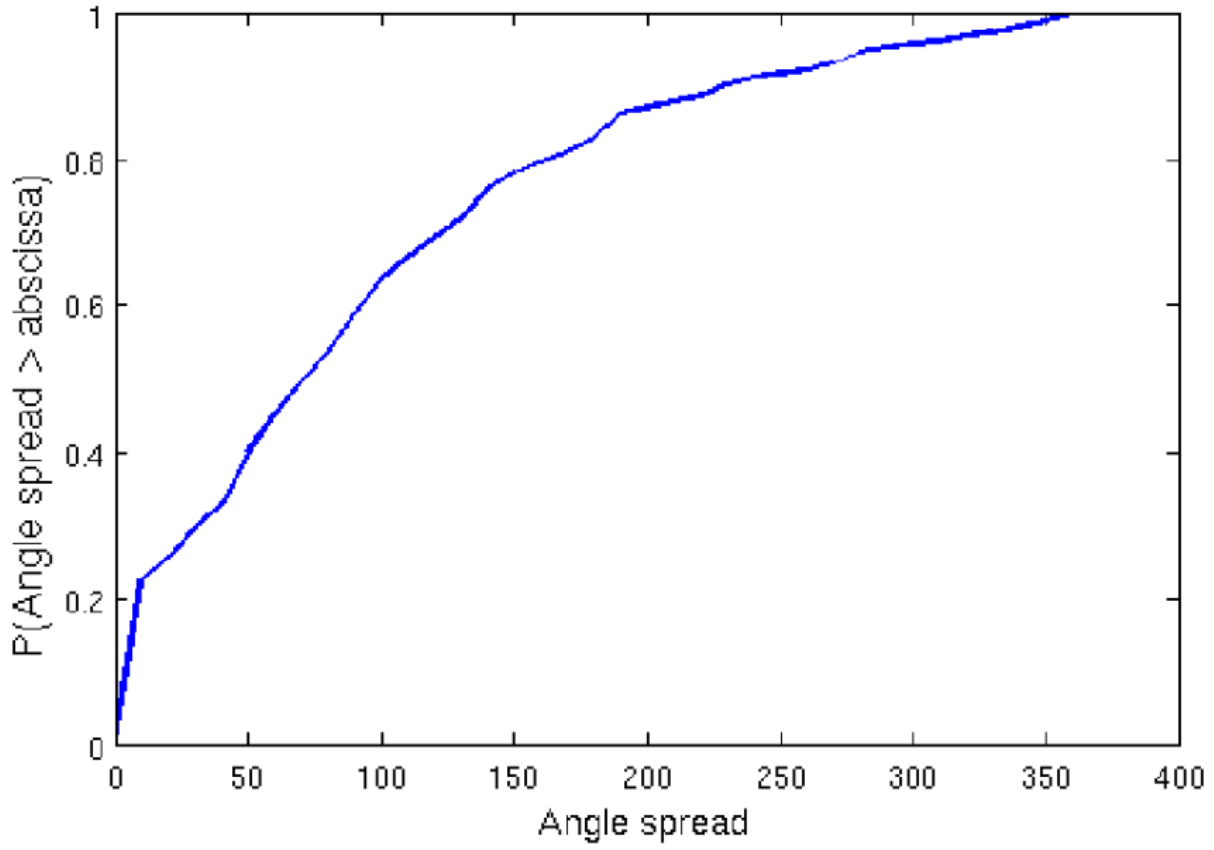

Figure 2.23: Cumulative distribution function of the cluster angle spread for all route.

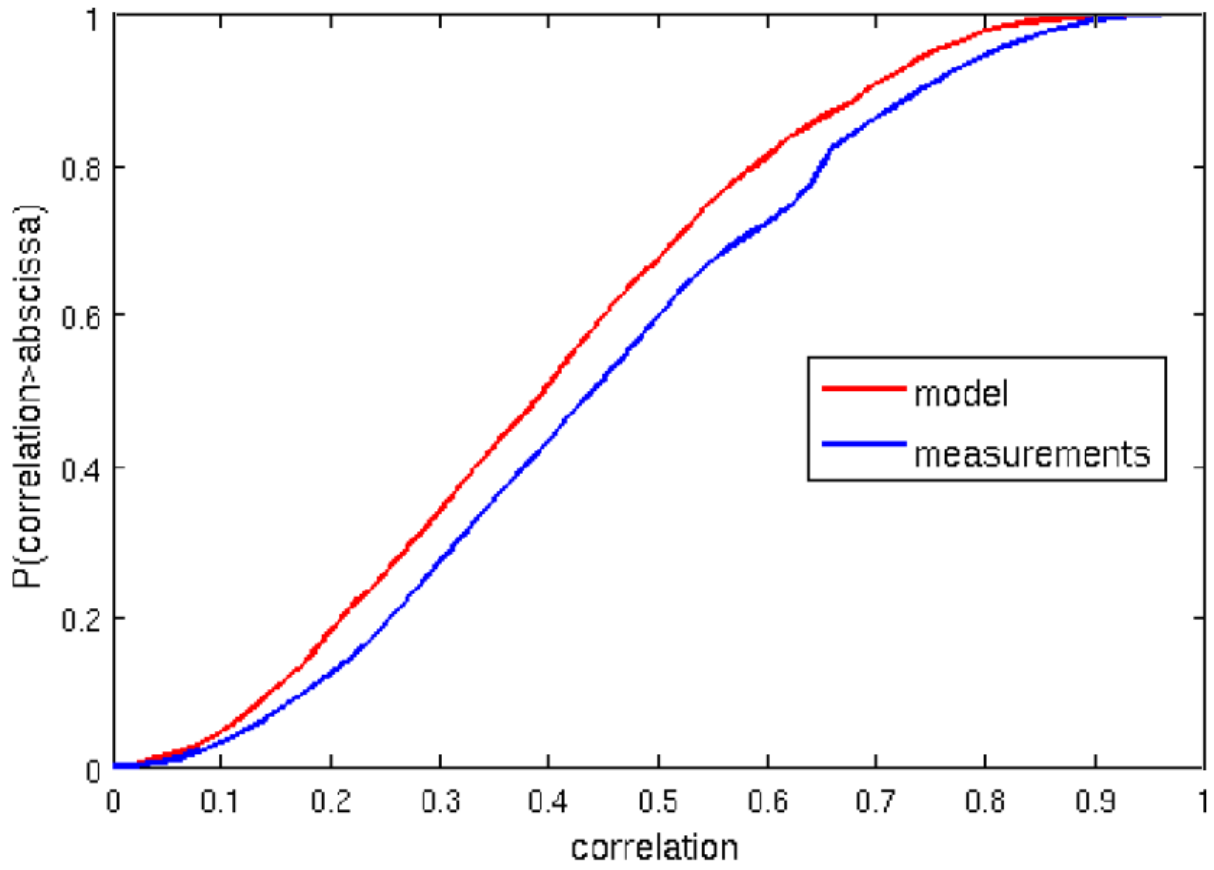

Figure 2.24: Cumulative distribution function of the receive antennas correlation for all route.

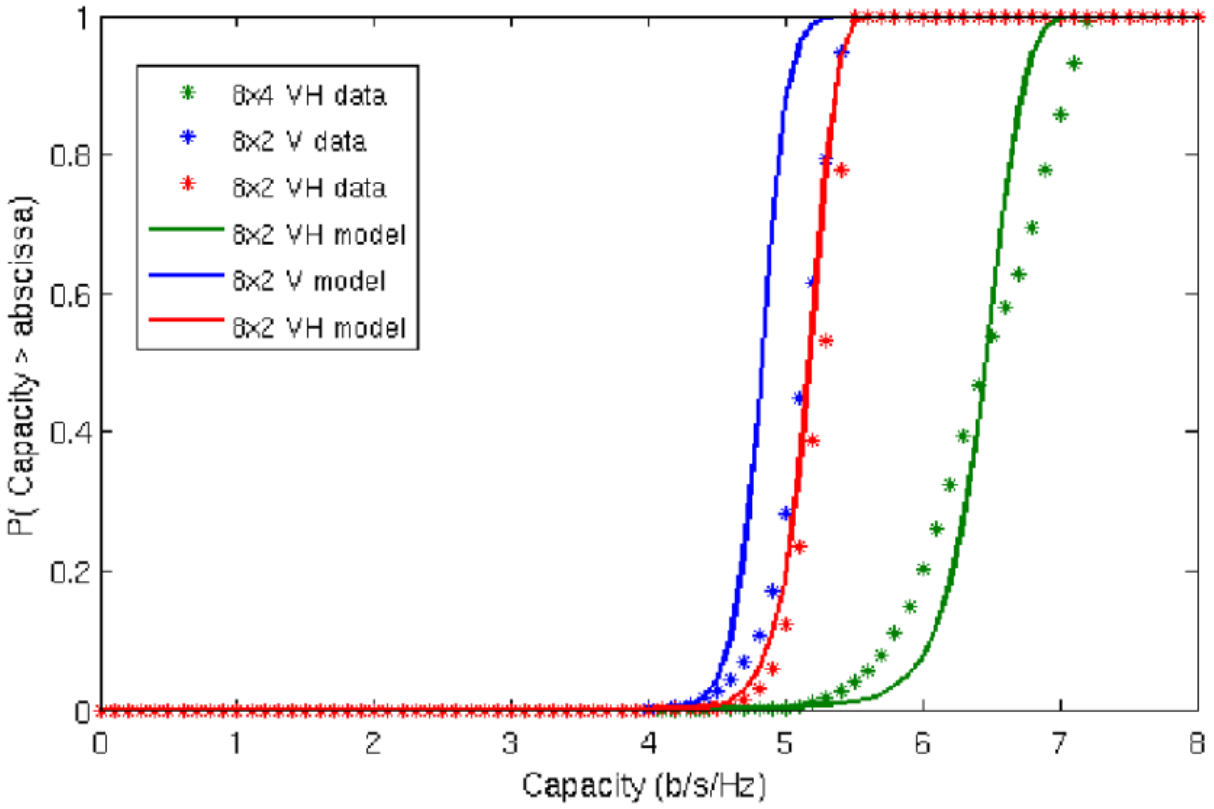

Figure 2.25: Cumulative distribution function of the ergodic capacity for all route.

Chapter 3

MIMO Array Capacity Optimization Using a Genetic Algorithm

3.1 Introduction

In the last chapter, an analysis of MIMO measurements was presented with some insights on the channel and antenna array characteristics that increase MIMO ergodic capacity. This chapter will present a tool to search the characteristics of the antenna array that maximizes the channel capacity for a given propagation scenario. MIMO systems have been an important research topic due to their capability of providing a significant increase in channel capacity proportional to the number of transmit and/or receive antennas. This is generally achieved by exploiting spatial diversity at the transmit and receive branches [1], [2]. When considering realistic antenna models, the channel capacity will depend on three main variables: the transmit antenna array configuration, the receive antenna array configuration and the environment configuration, namely, the distribution of the channel scatterers [51].

Multiplexing and diversity gains in MIMO systems can be obtained, for instance, by resorting to not only spatial divesity but also to polarization diversity. While spatial diversity can be achieved by ensuring enough antenna separation, polarization diversity can be achieved by exploiting different antenna orientations in the array configuration [13]. In cellular systems, a reasonable degree of spatial diversity can be obtained at the base-station. However, at the mobile terminal, this situation is completely different, since a good separation of the antennas ensuring spatial diversity is not always possible. Moreover, electromagnetic coupling between terminal antennas is a practical problem that affects system performance. Therefore, under these constraints, optimizing the antenna placement at the mobile terminal to yield a satisfactory performance is a challenging problem [16], [17].

The work in [11] shows some important aspects about implementation of MIMO transceivers in small terminals. In [12], planar inverted-F antenna (PIFA) compact arrays are compared to dipole arrays with the same antenna separation. That work states that PIFA antennas are an ideal candidate for compact array designs due to the low interference between antennas caused by the proximity to the ground plane. Although finding the globally optimal antenna set was not in the scope of [12], the work allows one to conclude about the importance of empirical inference from the designer. The dipoles were ULA while the PIFAs had a 180^o difference in orientation between the two elements. The PIFA arrays outperformed the dipoles. The paper attributes this result to the nearly omnidirectional pattern of the PIFA,

but it does not justify the position and orientation of the used PIFA antennas and does not investigate the influence of the orientation.

In [10], the relationship between MIMO capacity and array configuration is investigated for different outdoor propagation scenarios. The work concludes that for a small angular spread of 8^o, the best separation of antenna array elements would be 4 wavelengths in order to approximate the uncorrelated channel performance. While for 68^o, the optimum distance is the typical $1/2$ wavelength. It is also noted in that work, that with higher angle spreads the system was less sensitive to array orientation changes. In general, these works corroborate the relevance of the propagation environment characteristics in the design of the MIMO array.

Another important MIMO diversity technique is true polarization diversity (TPD). In TPD, instead of typical alternated 0^o and 90^o polarization, we can use any angle to change polarization. This is specially useful for small mobile terminals that have small space for exploring spatial diversity. The study in [13] shows that TPD can significantly improve MIMO capacity. But now the designer has to deal not only with antenna positioning in the array, but also with antenna orientation, bringing more complexity to the transceiver design. Not just orientation of individual array elements is important, but the orientation of the whole array has an important impact in MIMO capacity, specially for small angle spreads, typically in outdoor environments, according to [52]. In [53], a model for antenna correlation using arbitrary antenna orientation is used, and the work also shows that using different orientations for the antennas, the MIMO capacity increases. In [54], the challenges of antenna configurations in small mobile terminals are discussed. The work uses a measurement system to evaluate antenna configurations. The conclusions of the work are that small changes in antenna configuration can cause drastic changes in capacity and that the directive properties of the antennas and propagation channel cause important fluctuations on performance.

In [14], the question is whether UCAs are better for MIMO capacity than ULAs. It turns out that ULAs are better for some directions of arrival (DOA) configurations while UCAs have a more stable behavior. A similar analysis is made in [15]. But the question in a MIMO transceiver design is much wider. Which arbitrary array arrangement is better for a given propagation scenario, or for a given set of scenarios? Which array configuration, from a MIMO capacity viewpoint, is more stable?

Reviewing these works we can see that the possibilities for the MIMO system designer are endless, and just studying reference cases might not be enough to find a solid solution. Using optimization tools that can take all these possibilities into account may yield more robust MIMO designs.

Suppose that the designer knows the antenna model and the number of antenna elements to be used in a mobile terminal. Given an available space at the terminal for placing the antennas, a pertinent question is now in order. What are the best antenna configurations to be used in a given propagation environment? For answering this question, a possible road to take is to make use of experimental results or intuition to find a probable good antenna configuration for a certain propagation scenario, and then use simulation or prototype measurements to see if the design fulfills the project requisites. The second approach is to use an optimization method for finding an optimal (or suboptimal) solution to the antenna array configuration problem and then check if this solution is satisfactory. In this case, we jump from a computer-aided design paradigm to a computer design one. This approach has become more and more common as seen in [19].

Genetic algorithm (GA) based optimization has been used with success in various engineering problems and in antenna array optimization in particular. In [20], a genetic

algorithm is used to optimize antenna arrays used for channel characterization, i.e. determination of multipaths DOA. The system starts with large regular bi-dimensional or three-dimensional array of antennas (more than 20 antennas), and then the algorithm changes individual antennas position and orientation trying to find the array that minimizes the parameter estimation error. Although the obtained antenna positioning patterns may seem random and, sometimes, not intelligible for the designer, they offer a better precision in terms of channel characterization than regular (or uniformly spaced) patterns.

In [21], the authors resort to GA-based optimization to perform channel estimation and find parameters such as multipath attenuations and delays. In [22], GA is used for blind channel estimation. The study reports that the GA method can offer a better channel estimation accuracy than traditional methods. A similar approach was also proposed in [23]. Recently, GA has been used to find good antenna element positions in sparse MIMO radar arrays [24] by minimizing the side-lobes of the radar pattern. Another recent work [25] uses GA to find the optimal distribution of a 3×3 MIMO system for an indoor propagation channel. An interesting aspect of that work is the inclusion of electromagnetic coupling in the model. However, the work does not show either which distributions were found or how the distributions change according to different multipath channel parameters.

The work of [26] defends the idea of using nature inspired methods for MIMO antenna design, but the works mentioned there in deal with the problem of antenna geometry definition and not antenna array topology for different propagation environments. In [27] a method of moments is proposed to optimize MIMO antenna position and orientation. The optimization is done by minimizing the antenna cross correlation, by considering an i.i.d propagation scenario. Although antenna cross correlation degrades capacity, we cannot say that the configuration that minimizes antenna correlation is the same that maximizes MIMO capacity in non i.i.d. propagation scenarios. A similar approach is used in [29]. The work in [30] solves the problem of MIMO PIFA placement for an i.i.d. channel also minimizing antenna cross correlation, but using infinitesimal dipoles method and invasive weeds optimization, another nature inspired method.

This chapter address the antenna array capacity optimization problem in small mobile terminals by resorting to a genetic algorithm. The goal is to find an optimal or suboptimal configuration for antenna position and orientation that maximizes the ergodic channel capacity. Assuming an array of dipoles and a channel model that interfaces the propagation environment with the antenna array response pattern, the genetic algorithm manages to find, for each antenna, the best position and orientation subject to a spatial constraint. The results show that the proposed antenna array optimization method can be a valuable tool for small MIMO terminal design, and it can also give insights about different strategies to achieve MIMO diversity.

Due to the nature of genetic algorithms, the proposed method is very general. It can incorporate different types of antenna models, and it can also be used with different propagation and channel models. The simulations take into account different sets of antennas and constraints in terms of available space, and also consider electromagnetic coupling effects. It also compares the capacity provided by the optimized MIMO array with that of standard linear and circular arrays. The results corroborate the importance of jointly exploiting polarization and antenna pattern diversities, as shown recently in [55] and [56].

In Section 3.2, an introduction to genetic algorithms is given. In Section 3.3, the channel model that is exploited by the proposed algorithm is presented. Section 3.4 presents the genetic algorithm used for the optimizations and also details how the population is

```
generate initial population
while error<max_error and generation<max_generations
        compute fitness function
        select parents of next generation
        generate offspring by crossover or cloning
        apply mutation
return best individual
```

Figure 3.1: basic genetic algorithm.

represented, how reproduction occurs, and how we used the ergodic channel capacity as the fitness function of the genetic algorithm. Section 3.5 presents the simulation results and results discussion. Finally, in Section 3.6 the conclusions are drawn.

3.2 Genetic Algorithms

Genetic algorithm is a heuristic search method inspired in nature. In nature we can observe a robust method for the evolution of organisms. Organisms that are not well adapted for an environment have a greater chance of dying before reproduction, but well adapted organisms have a greater chance of producing offspring. This offspring carriers on the characteristics of the previous generation. If the environment changes slowly, the species gradually evolve with it, but if a sudden change happens in the environment, more drastic changes can happen to the species or it can be extincted. The mechanism that promotes change in the population is mutation. Most of the mutations will cause a quick death, but eventually a mutation can improve the individual leading to a more successful species [57].

This characteristic of nature was discovered by Charles Darwin with his work Origin of Species [58], where he introduced the idea of natural selection, but his work remained unknown for 30 years. The augustinian monk Gregor Mendel [59] discovered the genetics, the mechanism responsible for inheritance. Later, Hugo de Vries developed the concept of genetic mutations. These latter discoveries helped to consolidate Darwin's theory [60].

A genetic algorithm is an artificial system that emulates this behavior. One important difference between typical GA and natural selection is the fitness function. While in GA we have a specific, well defined, *a priori* fitness function, in nature the fitness function is always *a posteriori* and is always changing as the environment changes along with the species [60]. The artificial selection, used by man for plant and animal breeding, seems to be a much more adequate analogy, since a fitness function is defined *a priori*, such as better production of milk or crop, as noted in [60].

As an illustration of how a genetic algorithm works, consider figure 3.1. It starts with a set of individuals and applies the selection, mutation and reproduction operators to evolve a successful individual, i.e. a solution, as measured by a fitness function. The genetic algorithm is a form of reinforcement learning since it learns the agent function based on rewards (the offspring of an individual selected by the fitness function). The GA searches directly in the space of possible solutions trying to find one that maximizes the fitness function. In nature, all individuals are born, live and die in parallel. In GA, each individual is a separated search, making it a parallel search. This characteristic favors the implementation of GA in clusters of parallel computers. The search is also "hill climbing" because small changes are made to the individuals and the best resulting offspring is selected. The selection is a key point for the

search performance; focusing in the best elements of the offspring is necessary, but ignoring too many low ranked individuals might make the search stop in a local maximum. To model a problem using GA it is necessary to answer the following questions [57]:

- What is the fitness function?
- How is an individual represented?
- How are individuals selected?
- How do individuals reproduce?

3.2.1 Genetic Code

The genetic code, which is the structure that represents the encoded individual is the genotype and the observed characteristics of the individual is the phenotype [60]. Each individual is represented by its genetic code, a string over a finite alphabet, each element of the string is a gene. In nature, the alphabet is AGTC (adenine, guanine, thymine, cytosine). Genetic algorithms can choose any alphabet to represent its data, but the most common is the binary alphabet (01), since it is how digital computers represent information and then no extra overhead is needed to translate information from the alphabet to the format the computer uses to manipulate numbers [57]. Recently, it has become common the use of direct manipulation of real-value chromosomes using float point representations. In some problems, using float point representations improves the computation performance and many practical problems have been solved using this aproach [61].

3.2.2 Fitness Function

The fitness function is modeled according to the problem. It is the most problem-specific component of the GA. But in all cases, the interface is the same: the function receives an individual as the input and returns a real number as output [57]. The fitness function works by intrinsically transporting information from the model representing the environment to the model representing the species. It is also the most resource consuming part of the method. Some authors, like [57], consider the fitness function as being the process of evaluating the individual and giving an output for the selection process. Other authors, like [61], separate the objective function from the fitness function; with the objective function being the evaluation method related to the system modeled and the fitness function being the mapping from the scale of the objective function to a scale practical for the selection mechanism. In this case, there are 4 main models for the fitness function mapping [61]:

Linear Scaling: The fitness function f_i crates a linear relationship with the objective function o_i. Parameter a and b are chosen in such a way to provide a good quality of the resulting scale. In order to implement this method it is necessary to have a good knowledge of the range of the values in the objective function:

$$f_i = ao_i + b \tag{3.1}$$

Sigma Truncation: In sigma truncation negative values are truncated to zero:

$$f_i = o_i - (o_m - c\sigma) \tag{3.2}$$

where c is a small integer, o_m is the mean of the objective function and σ is the standard deviation in the population. In this case, even more knowledge is necessary about the objective function and the population.

Power Law Scaling: The fitness value is calculated as a specific power of o_i:

$$f_i = {o_i}^k \tag{3.3}$$

.

Ranking: In this approach, the individuals are sorted according to their objective function. It does not require extra knowledge about o_i and is generally implied when there is no information about the mapping used.

The use of a particular fitness function mapping will depend on the behavior of the objective function. If the objective function has negative values, for example, a sigma truncation mapping could be used in order to set a zero probability for the negative results. Another option would be use a linear scaling mapping in order to translate all values the to a positive range. The fitness mapping functions also map the range of the objective function to a range suitable for probability processing such as $[0..1]$.

3.2.3 Selection Process

In the selection process a certain percentage of individuals is chosen based on their fitness function result [57]. There are several methods to solve this problem, and according to [62], the methods can be classified in 3 main approaches:

Stocastic Sampling: this is the method of most earlier works in GA. In this method the result of the fitness function will determine number of offsprings of the individual. A sampling procedure using random number generators will convert the fitness function into the number of offsprings. The best known method of this class is Holland's roulette wheel selection where the selection probability of an individual is determined by the fitness function. For individual k, with fitness function f_k and population size p, the selection probability p_k is calculated by [62]:

$$p_i = frac f_k, \sum_{j=1}^{p} f_j \tag{3.4}$$

A wheel (circular list) is create for the calculated probabilities. The selection procedures spins the wheel p times, each time selecting an individual. Some versions of this procedure prohibit duplicated selections. This is done in order to prevent super chromosomes to dominate the population, which could lead to a local minimum [62].

Deterministic Sampling: in this approach, the best p individuals are selected from the previous generation. Truncation selection and block selection methods belong to this approach. In truncation selection, a threshold T is defined in order to select $T\%$ best individuals as parents. Each parent will then generate $100/T$ offspring. Block selection is similar to truncation selection, for a population of p, s offspring is given to the p/s best elements. Both implementations are equivalent when $s = p/T$. When a selection method ensures that the best individual is selected it is also called an elitist selection [62].

Mixed Sampling: it tries to combine both previous approaches. An example is tournament selection. It randomly chooses a set of individuals and then chooses the best individual

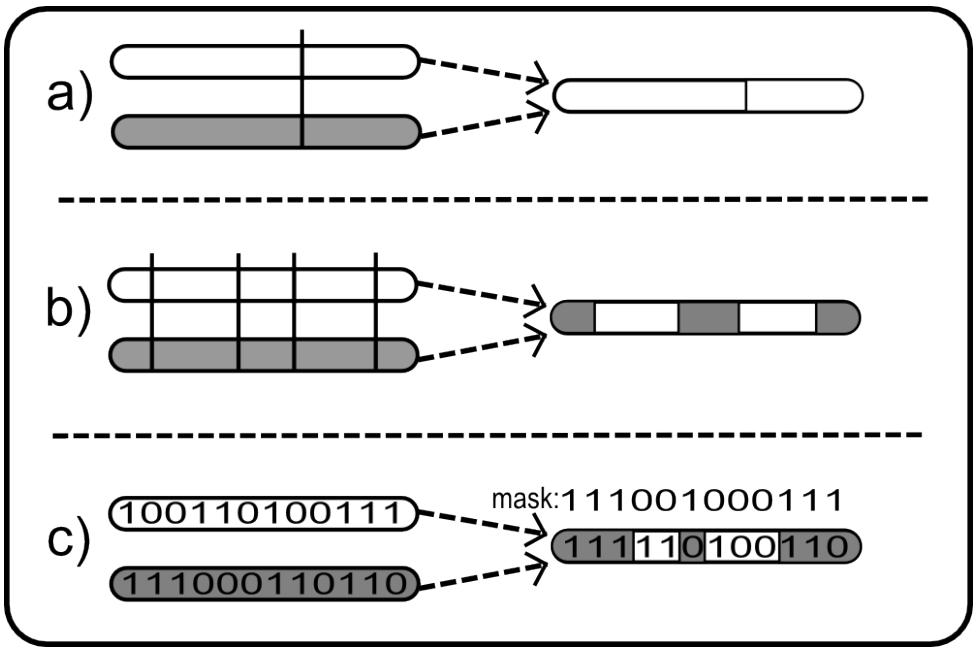

Figure 3.2: a) Singlepoint crossover. b) Multipoint crossover. c) Uniform crossover.

in the set. It repeats the procedure until the set of parents is complete. When the set is randomly selected, it resembles the stochastic selection, and when the best individual within the set is selected, it resembles the deterministic sampling.

3.2.4 Reproduction

Figure 3.2 shows the reproduction process. Reproduction is done using the processes of crossover and mutation. Crossover or recombination produces individual that are combination of more than one parent genotypes. It emulates the natural process of sexual reproduction in nature, where a male and a female specimen combines their genotypes in new offspring. The main methods for crossover are: single point crossover, multipoint crossover and uniform crossover [63]. In singlepoint crossover, one point is randomly selected along the genetic string, the genes from the left side of the new individual will come from the first parent and genes from the right will come from the second parent. In multipoint selection, more than one crossover points are select along the genetic string. In uniform crossover as binary mask indicates which genes will come from the first parent and which will come from the second parent [63], [64].

In the mutation procedure, some genes are randomly chosen and their values are changed; the aim of the procedure is to bring diversity to the population [57]. In nature numerous factors can cause mutation, some are biochemical and inherent to the process of DNA replication; other factors are external, such as radiation. These processes are virtually impossible to model, due to their chaotic nature, being considered a white noise in most simulated systems. In non binary representations, such as in real valued-coded GA, the mutation is achieved by perturbations in the genotype values [63].

3.3 Channel Model

This section describes the channel model used in the GA simulations. The chosen model is general enough to easily describe different propagation scenarios, unlike pure ray tracing models; but has the geometric information necessary to interface to the antenna model, unlike pure stochastic models. In Figure 3.3 the channel geometric model used to generate the plane

waves and to interface it to the antenna arrays is illustrated. It is assumed that the distance between antenna arrays and the scattering clusters is much higher than the distance between the array elements. This case assumes that the DOA and direction of departure (DOD) of a given plane wave are the same for all the antenna elements of the array. Each cluster is modeled by a finite set of plane waves, and has a main direction of arrival/departure, both in azimuth and elevation. Angle spread and polarization spread within a cluster follow a gaussian distribution.

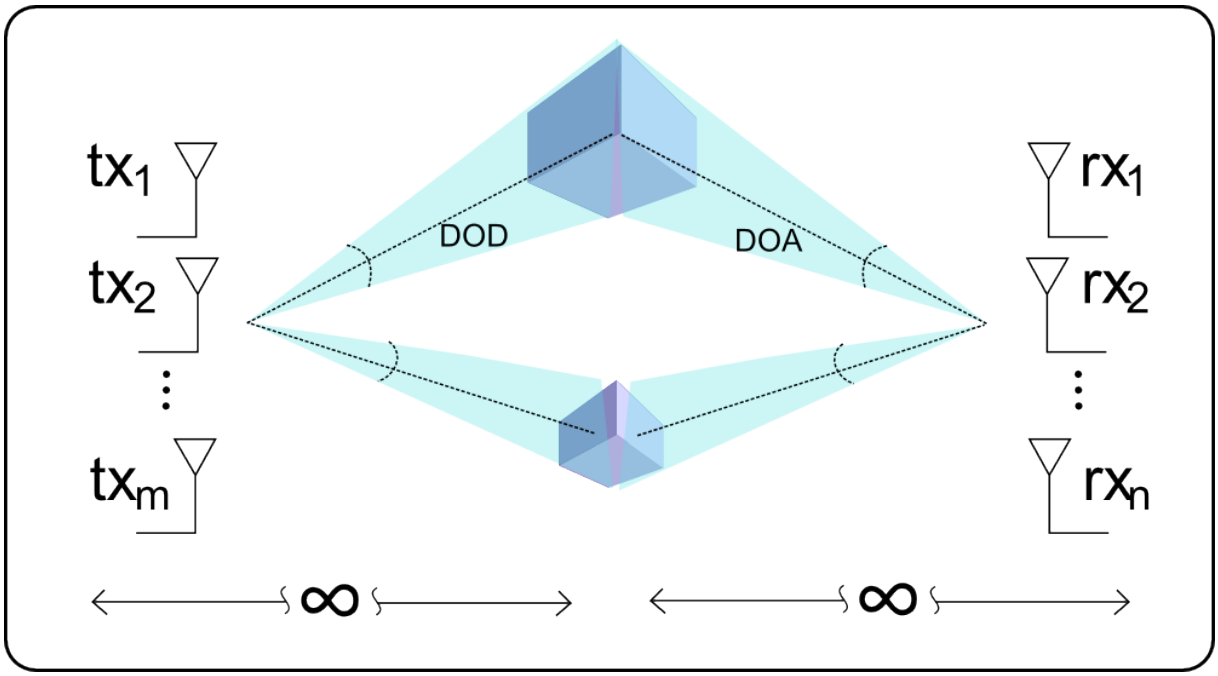

Figure 3.3: Geometric Channel model used in simulations.

The channel double-directional impulse response, associated with the DOA pair (ϕ_{Rx}, θ_{Rx}) and DOD pair (ϕ_{Tx}, θ_{Tx}) is given by the contribution of a finite number of dominant multipaths components [65]:

$$\mathbf{A}(\phi_{Rx}, \theta_{Rx}, \phi_{Tx}, \theta_{Tx}) = \sum_{l=1}^{L} \mathbf{A}_l(\phi_{Rx,l}, \theta_{Rx,l}, \phi_{Tx,l}, \theta_{Tx,l}), \tag{3.5}$$

where L is the number of arriving paths, and ϕ and θ denote, respectively, azimuth and elevation angles. The contribution of each path A_l can be expanded as follows:

$$\begin{aligned} \mathbf{A}_l(\phi_{Rx}, \theta_{Rx}, \phi_{Tx}, \theta_{Tx}) &= \mathbf{W}_l e^{j\phi_l} \\ &\times \delta(\phi_{Rx} - \phi_{Rx,l})\delta(\theta_{Rx} - \theta_{Rx,l}) \\ &\times \delta(\phi_{Tx} - \phi_{Tx,l})\delta(\theta_{Tx} - \theta_{Tx,l}), \end{aligned} \tag{3.6}$$

where $\phi_l = j2\pi f_c$, and $\mathbf{W}_l$ is the polarimetric transmission matrix defined as:

$$\mathbf{W}_l = \begin{bmatrix} \gamma_{HH} & \gamma_{VH} \\ \gamma_{HV} & \gamma_{VV} \end{bmatrix} \tag{3.7}$$

where γ_{HH} is the factor for the horizontally polarized wave vector component that results from the horizontal component of the wave vector transmitted by the antenna, after it passes through the channel. The γ_{VH} is the factor for the horizontally polarized wave vector

component that results from the vertical component of the wave vector transmitted by the antenna, after it passes through the channel. This happens because a horizontally polarized wave may rotate its polarization after reflections and refractions throughout the channel. The same idea applies to elements γ_{HH} and γ_{HV}.

The $(m,n)^{th}$ entry $h_{m,n}$ of the MIMO channel matrix $\mathbf{H}$ ($M \times N$) can be expressed in terms of the directional channel impulse response according to the following expression [65]:

$$\begin{aligned} h_{mn} = \sum_{l=1}^{L} & \mathbf{g}^T{}_{Tx}(\phi_{Tx,n,l}, \theta_{Tx,n,l}, \mathbf{r}_{Tx,n}) \\ & \times \mathbf{A}_l(\phi_{Rx,l}, \theta_{Rx,l}, \phi_{Tx,l}, \theta_{Tx,l}) \\ & \times \mathbf{g}_{Rx}(\phi_{Rx,m,l}, \theta_{Rx,m,l}, \mathbf{r}_{Rx,m}) \\ & \times exp(j[\mathbf{k}(\phi_{Rx,l}, \theta_{Rx,l}) \cdot \mathbf{x}_{Rx,m}]) \\ & \times exp(j[\mathbf{k}(\phi_{Tx,l}, \theta_{Tx,l}) \cdot \mathbf{x}_{Tx,n}]), \end{aligned} \tag{3.8}$$

where $\mathbf{g}_{Rx}$ is the antenna pattern response to the direction $(\phi_{Rx,m,l}, \theta_{Rx,m,l})$ while $\mathbf{g}_{Tx}$ is the antenna pattern response to the direction $(\phi_{Tx,m,l}, \theta_{Tx,m,l})$ at the transmitter. The response of the antenna considers de impact of mutual electromagnetic coupling of nearby antennas. This effect is calculated integrating a numerical electromagnetics code in the simulation. The (2×1) vector $\mathbf{g}_{Rx}$ is the product of the complex scalar gain g_{Rx} (phase and amplitude) of the receiver antenna, and the unitary (2×1) polarization vector $\mathbf{p}_{Rx}$ composed by the vertical and horizontal responses:

$$\mathbf{g}_{Rx}(\phi_{Rx,n,l}, \theta_{Rx,n,l}, \mathbf{r}_{Rx,n}) = g_{Rx}(\phi_{Rx,n,l}, \theta_{Rx,n,l}, \mathbf{r}_{Rx,n})\mathbf{p}_{Rx} \tag{3.9}$$

Similarly, for the transmitter antenna pattern response $\mathbf{g}_{Tx}$:

$$\mathbf{g}_{Tx}(\phi_{Tx,n,l}, \theta_{Tx,n,l}, \mathbf{r}_{Tx,n}) = g_{Tx}(\phi_{Tx,n,l}, \theta_{Tx,n,l}, \mathbf{r}_{Tx,n})\mathbf{p}_{Tx} \tag{3.10}$$

The vector $\mathbf{r}_{Rx,m}$ defines the antenna orientation, $\mathbf{k}$ is the wave vector, $\mathbf{x_{Rx}}$ is the relative position of the m^{th} receiver antenna and $\mathbf{x}_{Tx}$ is the relative position of the n^{th} transmitting antenna. The inner product of the vector wave $\mathbf{k}$ (arriving or departuring wave) with an antenna position (transmitter or receiver), is defined by:

$$\mathbf{k}(\phi, \theta) \cdot \mathbf{x} = \frac{2\pi}{\lambda}(xcos\theta cos\phi + ycos\theta sin\phi + zsin\theta sin\phi) \tag{3.11}$$

Figure 3.4 illustrates the interface between the antenna and the propagation environment, used to build the effective MIMO channel response. It shows a dipole with its farfield pattern, where the color indicates the gain for the direction; θ and ψ are the angles for the direction of arrival of the incoming wave from the propagation model. Note that (3.8) is an entry of the *effective* MIMO radio channel, which includes the effect of antenna responses in the channel impulse response. As we will see later, the position and orientation of each receive antenna, defined, respectively, by vectors $\mathbf{x}_{Rx}$ and $\mathbf{r}_{Rx}$, are variables to be optimized by the proposed optimization algorithm. Vector $\mathbf{r}_{Rx}$ is composed by elements α, β and γ, which represent, respectively, the rotations around x, y and z axis [1]

[1] In this work, we limit ourselves to optimization of the receive array parameters. The joint optimization of the receive and transmit array parameters $\mathbf{x}_{Tx}$ and $\mathbf{r}_{Tx}$ is left to a future work.

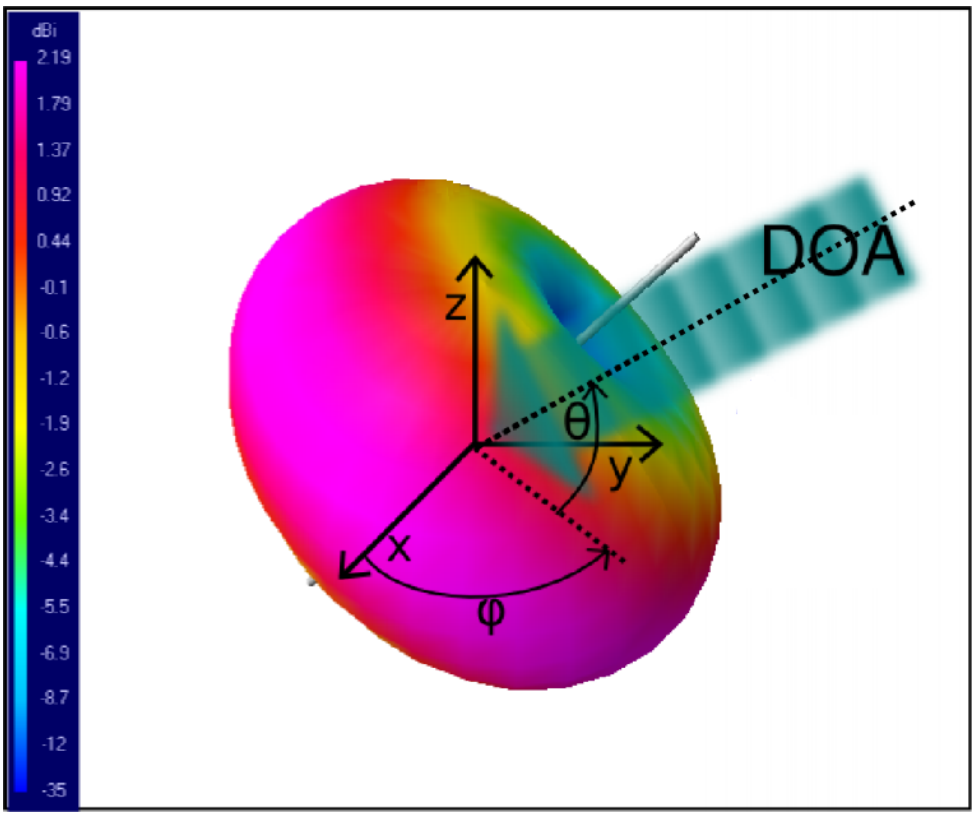

Figure 3.4: Antenna-Propagation environment interface.

3.3.1 Electromagnetic Coupling

The electromagnetic coupling has a strong effect when the antennas are separated by small distances (typically less than $\lambda/2$). With hand-held telecommunication devices this is often, if not always, the case. In order to incorporate coupling effects, instead of implementing an electromagnetic code from ground up, we chose in this work to use an available and well established code, integrated to our channel model. We use the NEC [66], which is a public domain software. The version we chose to work with is NEC2C, a C language implementation of the NEC2 Fortran original code. The NEC code uses the method of moments (MOM) to solve the electromagnetic field problem. One of its main qualities is the low computational cost of the solutions, since MOM codes are much faster than e.g. finite element method based codes.

The mutual coupling of the antennas affects the farfield response of the antennas in two ways. First, it changes the magnitude of the response modifying the directivity of the antenna. Second, it also perturbs the phase response of the antenna. Figure 3.5 shows both effects in a dipole antenna under the influence of mutual coupling with a nearby dipole antenna. It is worth noting that the effect of mutual coupling will not always degrade MIMO capacity. Depending on the considered channel model and on the antenna configuration, it may well increase capacity, by decorrelating the signal (true MIMO gain), or by increasing the directive gain towards a cluster direction. The work of [52] explains how electromagnetic coupling can decrease the antenna correlation, by means of pattern diversity. Since in small terminals it is not possible to use spatial separation of antennas to achieve diversity, it is important to consider mutual coupling as a possible source of pattern diversity, and not just a downside in MIMO antenna design.

Figure 3.6 shows the capacity of a 2×2 MIMO system as function of antenna separation, for a channel with one cluster. When the antennas are very close there is a strong gain

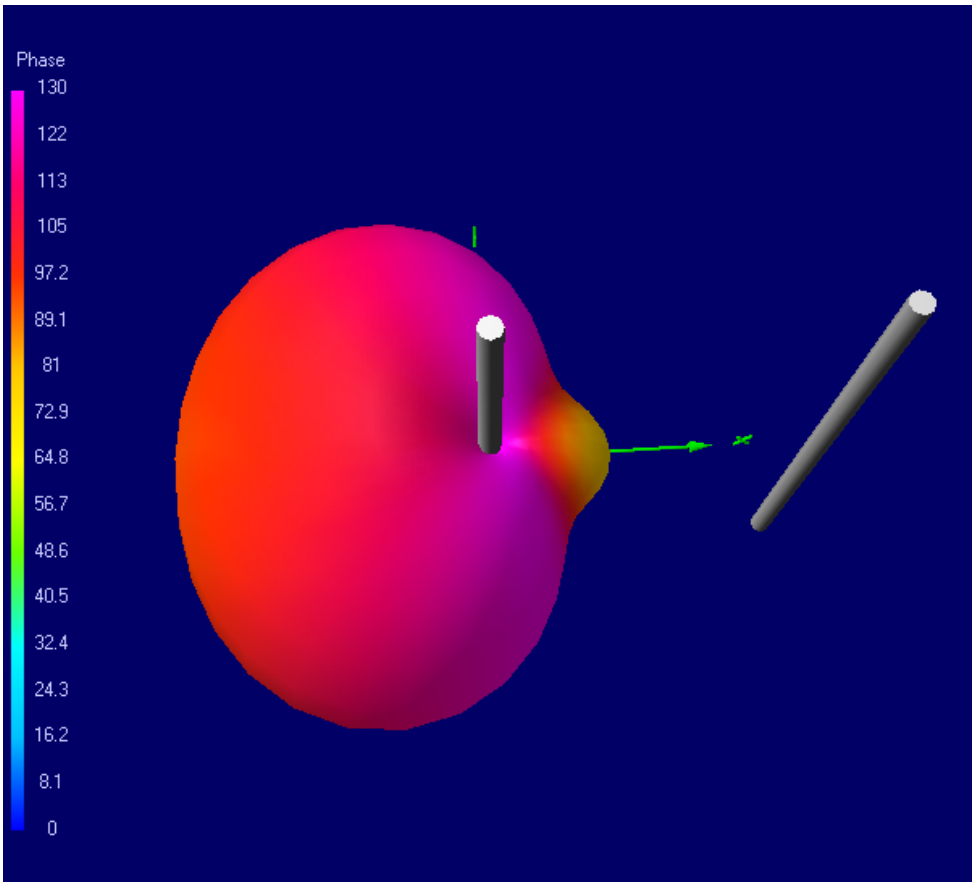

Figure 3.5: Effect of mutual coupling in the farfield of a dipole antenna.

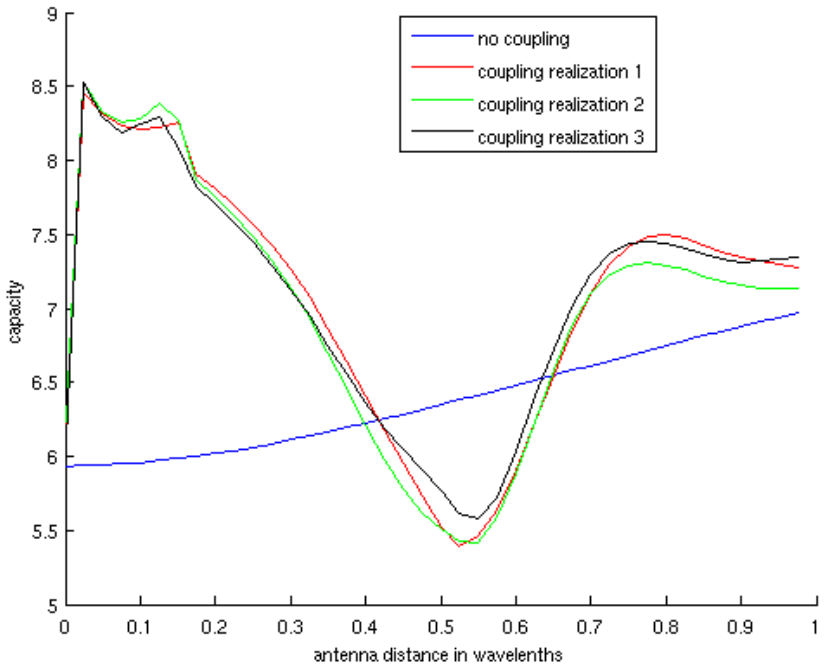

Figure 3.6: Effect of the mutual coupling on MIMO capacity.

in capacity for the system with antenna mutual coupling. This is caused for the signal decorrelation effect, but also by a directive gain towards the cluster. The drop in capacity for a distance of $\lambda/2$ and its raise at 0.8λ are caused by correlation and decorrelation effects of the mutual coupling. Our results, using dipole antennas simulated in NEC and the channel model previously presented, with on cluster with 15^o angle spread, corroborate the works [16] and [17], where the same pattern of raise of correlation (drop in capacity) at $\lambda/2$ and drop in correlation (raise in capacity) at 0.2λ and 0.8λ is found.

3.4 Genetic Algorithm Optimization

GA works by analogy to genetic inheritance and differentiation that occurs in biology that permits a species to fit itself to the environment in an adaptation process. We can think about the channel characteristics as the environment, and the antenna array as the biologic species that needs to fit in the environment (the channel). The fitness of the antennas to the environment can be measured by the ergodic capacity. As a bird can develop a beak more adapted to a specific kind of seed [58], by analogy an antenna array could develop characteristics better suited for a specific channel or kind of channel.

It is not possible produce antennas capable of self reproduction, but it is possible to simulate that in a computer using digital representations of antennas and channels. The genetic code is a digital code that represents the individual characteristics that can be inherited from previous generations and be passed by to the next generations. Our individual is the antenna array, our genetic code is the channel array model stored in the computer memory. A population, or generation, is a collection of antenna arrays. The genes that define an array are the antenna type, antenna position and antenna orientation. It starts with a random generation, where each antenna has a position and orientation assigned to it by a random variable with uniform distribution, within the limits of the desired volume space for the antennas. The number of individuals in the generation is increased by crossing and mutation. The crossing operation is the reproduction of new individuals that inherit part of the characteristics from one individual and other part from other individual, the parents. Which characteristic will come from each parent is decided by an aleatory factor and multipoint crossing. The mutation operation is an aleatory small change in the genes.

The next step is to select the individuals better suited to the environment using deterministic block selection using the fitness function for ranking, and then repeat the reproduction step with this selected group. The reproduction and selection steps are repeated until an optimization criteria is met, or a certain number of generations is met. Our fitness function is defined by the channel ergodic capacity as will be detailed later.

Figure 3.7 shows a general diagram of the genetic algorithm optimization method, applied to our problem. We can see the genetic algorithm as a method that explores a search space. The randomness of mutation makes the optimizer to explore different regions escaping from local maxima, while the fitness function gives direction to the search. One advantage of the proposed genetic algorithm is its low sensibility for initial conditions when compared to traditional numerical methods. A very useful aspect of genetic algorithms is that, as a searching algorithm, it is not limited to numerical field operations, and can use any operation that can be expressed in the algorithm. One example of this feature would be the search for the best model of antenna for a given scenario or even to use different models of antennas in the same solution. A limitation of this method is that it can stop in a local maximum, and in some cases it is not possible to know if the solution is local or global, or if the algorithm is capable or not of leaving the local maxima.

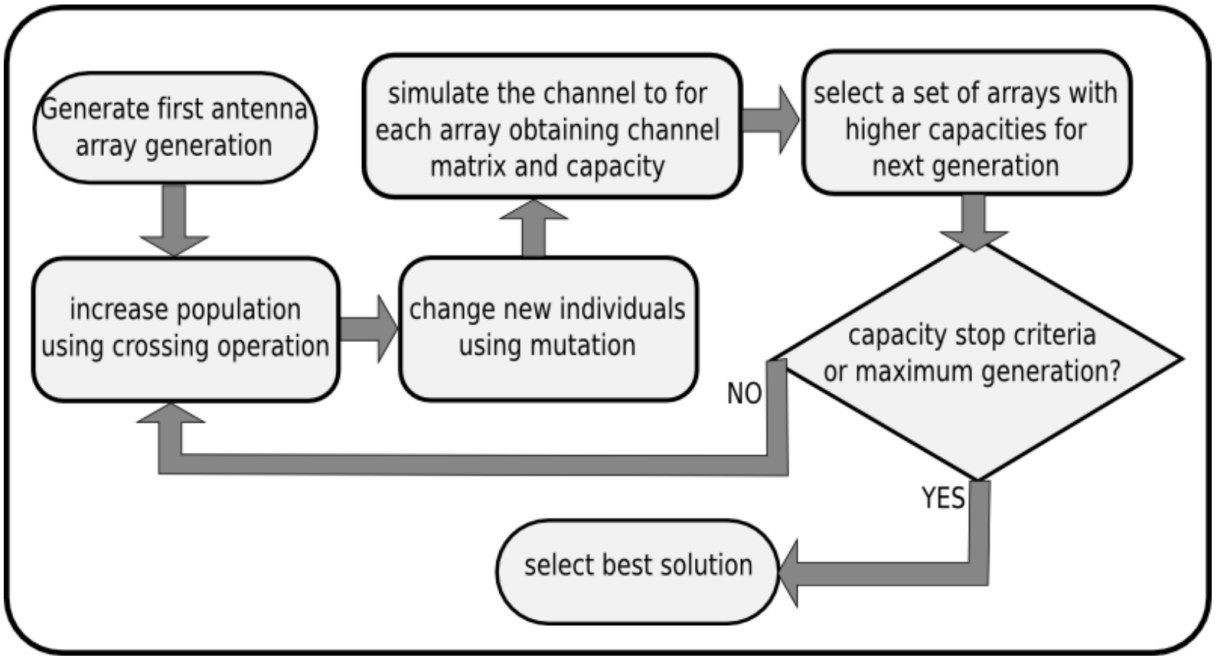

Figure 3.7: Fluxogram of the employed genetic algorithm.

3.4.1 Population and Reproduction

The antenna is represented in the system by the tuple $(kind, position, orientation)$. The kind is an integer token that identifies the antenna far-field pattern. In this work we consider ideal half-wave dipoles, although more realistic and more than one kind of antenna could be used. The position vector is denoted by $\mathbf{x} = [x, y, z]^T$ and the orientation vector denoted by $\mathbf{r} = [\alpha, \beta, \gamma]^T$. A collection of antennas $[a_1, a_2, ...a_M]$ defines an array. An array is one individual in the population. The genetic algorithm needs a finite set to search into, so position and orientation need to be both limited an quantized. The degrees of freedom of the position are limited by a limited volume defined prior to simulation. The available volume is generally a practical constraint of the antenna array design in small terminals. The quantization is naturally imposed by the computer quantization of the floating point numbers. Defining the antenna geometry by a collection of $3D$ points $\mathbf{S}$, its radiation pattern is rotated by the following transformation:

$$\mathbf{S}' = \begin{pmatrix} \mathbf{c}_1 & \mathbf{c}_2 & \mathbf{c}_3 \end{pmatrix} \mathbf{S} \tag{3.12}$$

, where

$$\mathbf{c_1} = \begin{pmatrix} cos\gamma cos\beta cos\alpha - sin\gamma sin\alpha \\ -sin\gamma cos\beta cos\alpha - cos\gamma sin\alpha \\ sin\beta cos\alpha \end{pmatrix} \tag{3.13}$$

$$\mathbf{c_2} = \begin{pmatrix} cos\gamma cos\beta sin\alpha + sin\gamma cos\alpha \\ -sin\gamma cos\beta sin\alpha + cos\gamma cos\alpha \\ sin\beta sin\alpha \end{pmatrix} \tag{3.14}$$

$$\mathbf{c_3} = \begin{pmatrix} -cos\gamma sin\beta \\ sin\gamma sin\beta \\ cos\beta \end{pmatrix} \tag{3.15}$$

The genotype (or DNA) of each individual in the collection is formed by the antennas' tuples. Figure 3.8 illustrates the reproduction and mutation operations, where $\alpha 1$ to $\alpha 6$ denote a random displacement. The reproduction is done by combining portions of DNA from two parents. A new array is derived by choosing antennas from two ancestor arrays. A pseudo-random function is used to choose from which parent each antenna will be copied for the new individual in the population. After the reproduction, a pseudo-random change is made in each antenna parameter. Such a change defines the mutation procedure. It is worth noting that the amount and extent of the mutation have a strong impact on the algorithm performance. Small probability of changes can make the algorithm converge faster but it is more prone to get stuck in a local maximum, while stronger changes make it leave local maximum for better maxima but makes the system less stable. Therefore, a tradeoff between convergence speed and stability exists, as usual in numerical optimization methods.

Another parameter to take into account is the size of the offspring in each generation. A small offspring provides faster computation and less memory usage, at the expense of more iterations necessary to solve the problem.

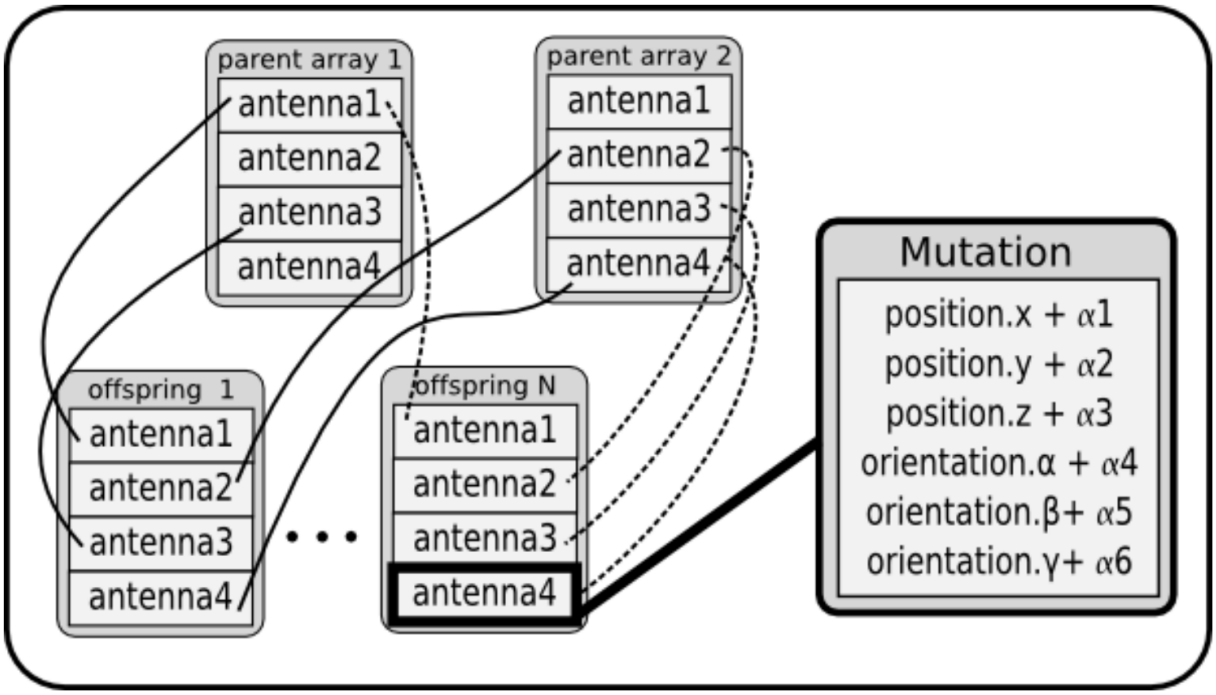

Figure 3.8: Crossing and Mutation procedure.

3.4.2 Fitness Function

In order to select the individuals for the next generation, it is necessary to use a fitness function, which is always problem-related. The interface between the fitness function and the genetic algorithm makes it possible to choose any kind of fitness function, as long as the function respects the intputs and outputs of the interface. The input for the fitness function has to be the current generation of individuals, in this case, the various array configurations obtained by the crossing and mutation operations. The output of the function has to be some value attached to each individual making it possible to classify it. In this work, that value corresponds to the ergodic channel capacity, in bits per channel use, which is given by [35]:

$$C = \frac{1}{N_q} \sum_{q=1}^{N_q} \log_2 \det \left[I_{Nr} + \frac{SNR}{Nt} \mathbf{H}_q \mathbf{H}_q^H \right]. \tag{3.16}$$

where N_q is the number of realizations to compute the expectation statistics and $\mathbf{H}_q$ represents the q^{th} channel realization. Note that, according to (3.8), each entry h_{mn} of $\mathbf{H}_q$ ($M \times N$) depends on relative antenna positions $\mathbf{x}_{Rx,1..M}$ and antenna far field patterns according to their orientations $\mathbf{r}_{Rx,1..M}$ at a given channel realization. Recall that only the receive antennas are the object of the present investigation. The antennas at the transmitter (i.e. the base station for the downlink) are supposed to have less placement constraints and are not optimized here. Therefore, the objective function of the genetic algorithm is to solve the following problem:

$$\underset{\mathbf{x}_{Rx,1..M},\mathbf{r}_{Rx,1..M}}{\arg\max} \quad C(\mathbf{x}_{Rx,1..M}, \mathbf{r}_{Rx,1..M}) \tag{3.17}$$

The diagram given in Figure 3.9 illustrates the fitness function. Index i refers to the i^{th} array configuration in the generation population, while index k refers to the k^{th} generation in the simulation. These two pieces of information generate a set of plane waves that are stored and remain constant during all the simulation. This is important because each generation is not a leap in time. The succession of generations is time-related in nature but has no relation to time variation of the radio channel. The collection of plane waves has two dimensions. We refer to w as the wave index, and q as the realization index. A number of wave realizations is first generated and stored and further used to compute the statistics of ergodic channel capacity. The same random realizations have to be applied for each individual of the generation, otherwise a noise would be added to the solution. It is interesting to note that this architecture makes possible to use any channel environment definition model that delivers a set of plane waves as the output. Even real site channel characterization measurements might be used.

The NEC code is integrated to our optimization software in the fitness function as depicted in Figure 3.9 . For each iteration, and for each array in the population of possible solutions, the input files that define the geometry and electric characteristics of the antennas are created. Then the NEC code is invoked and its solver calculates the farfileds of the antennas considering the mutual coupling effect. The NEC code writes then the farfileds to its output files. The software then reads the NEC output files e proceeds with the channel simulation for the fitness function.

One problem initially faced during the simulations was the fact that when two antennas had an intersection, the NEC code would see a short circuit between the antennas, generating incorrect farfiled results. The problem was solved applying a collision test during the phase of reproduction of antennas. Every antenna wire was protected by a capsule. The system measures the minimum distance between antennas' wires, if this distance is lower than the sum of the capsule radios $r1$ and $r2$, the antennas are considered to be in a collision, and the array is dropped from the population. This idea is illustrated in Figure 3.10.

3.5 Simulation Results

In this section, a set of computer simulation results are presented for some propagation scenarios and system configurations. It aims at investigating the link between the GA-optimized antennas' positions and orientations to the propagation environment in question. The theoretical channel capacity obtained by optimizing the antenna array configurations using the proposed GA algorithm is also evaluated.

For the simulations, the following GA parameters were used: a population size of 2000 individuals, the selection processes was deterministic with elitism, selection of 5% of the population and a mutation rate of 2%.

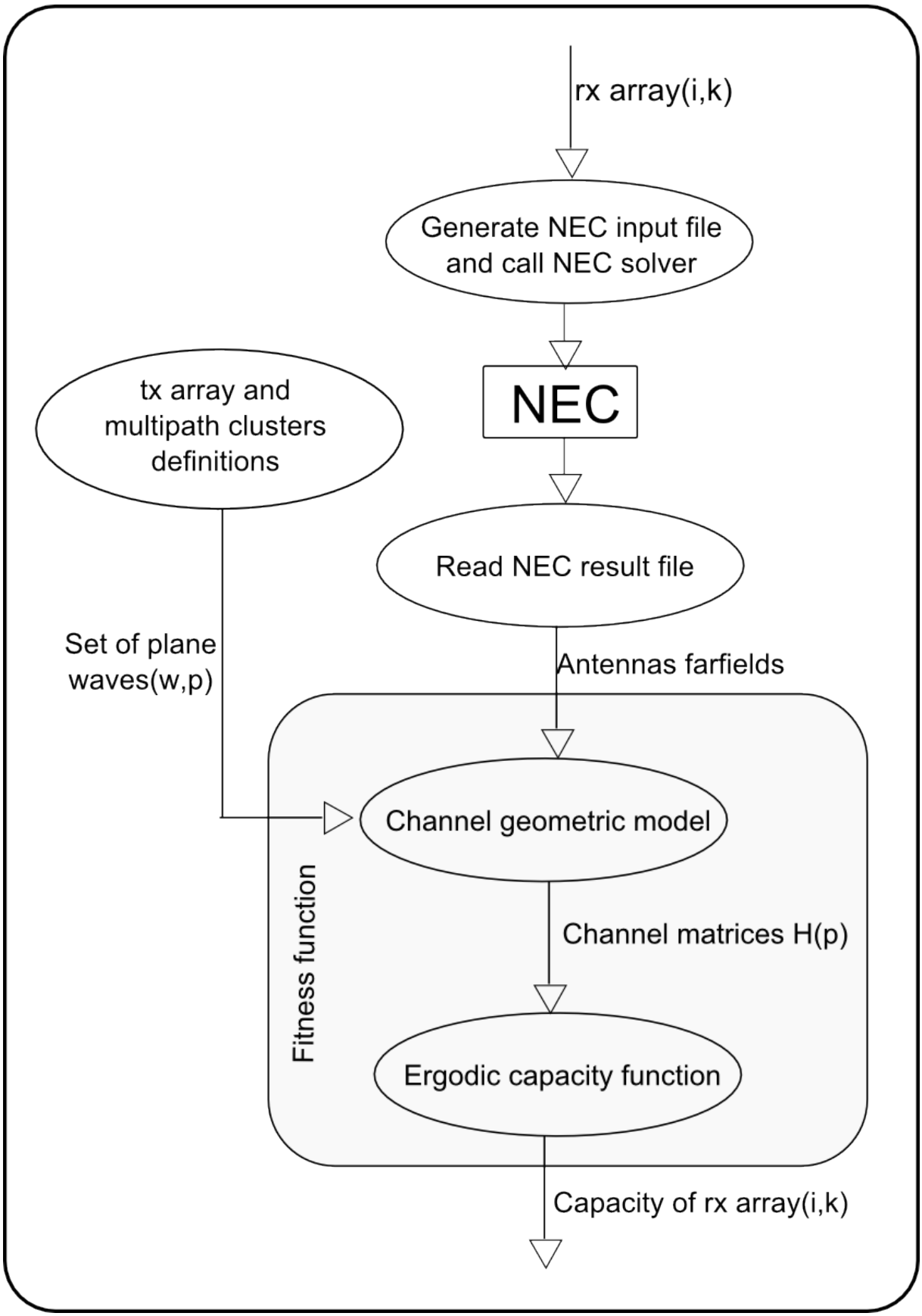

Figure 3.9: Fitness function used in the genetic algorithm.

3.5.1 One cluster, 3x3 MIMO

Figure 3.11, considers a 3×3 MIMO system using half wavelength dipoles. The transmitter antennas are spaced by 2 wavelengths. The propagation channel is characterized by a single

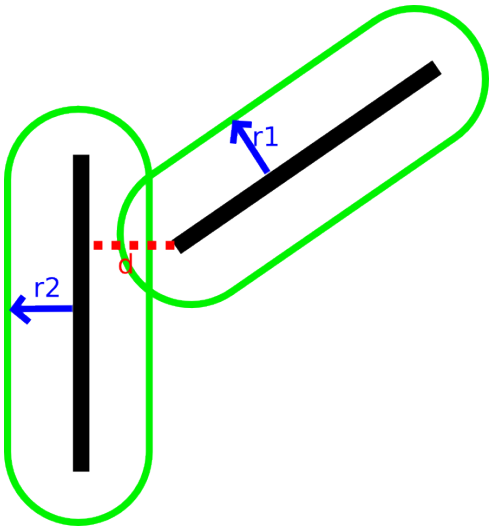

Figure 3.10: Capsule collision detection.

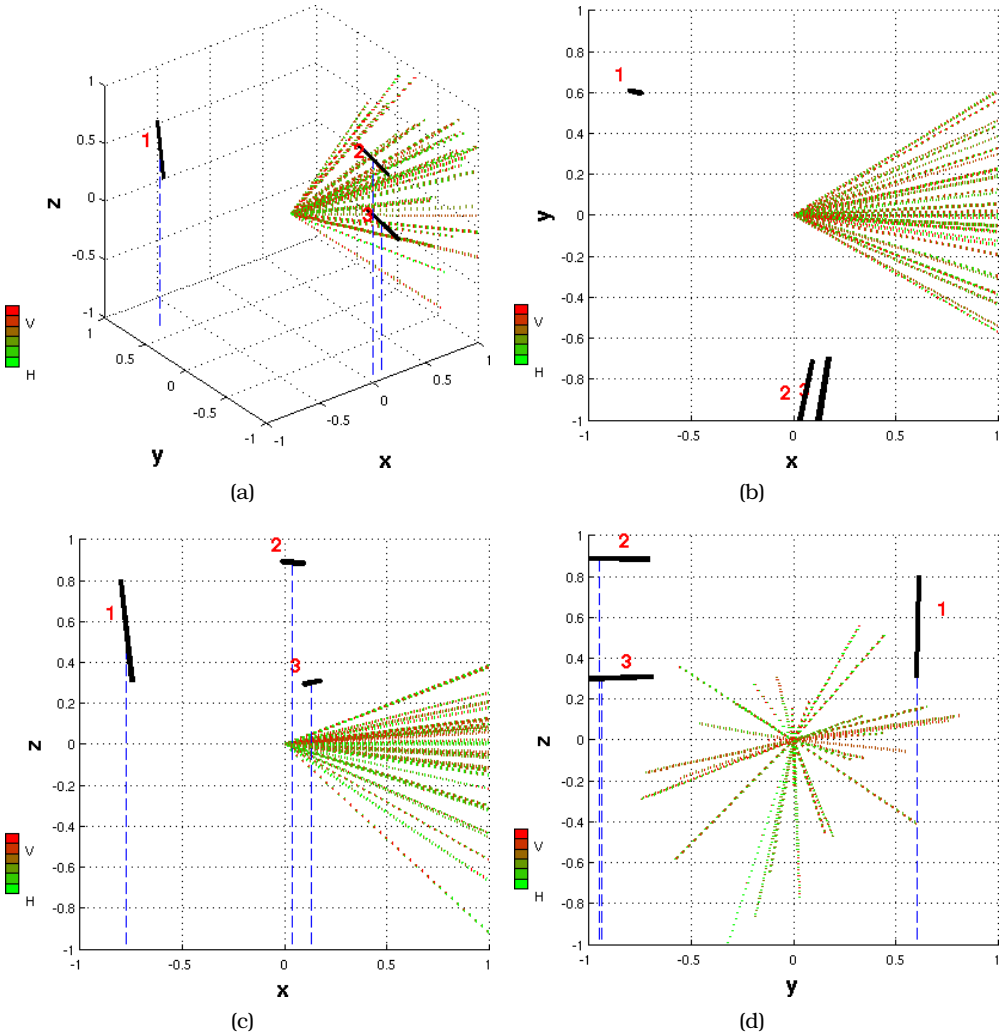

Figure 3.11: Evolved 3x3 MIMO configuration, One cluster. SNR=20dB. Volume=$(2\lambda)^3$.

scattering cluster with high angle spread and total polarization diversity. Since there is a large space for the system to exploit, any solution with antenna separation greater than $\lambda/2$ and polarization diversity will be a good solution. More than 20 simulations were made, and all results presented a pattern similar to that of Figure 3.11. The lines in the figure present a sampling of the directions of arrival, and line color represents its polarization ranging from fully horizontal to fully vertical. Figure 3.12 shows the histogram of ergodic capacity of the initial random antennas positions and orientation, and the ergodic capacities obtained after optimization. The initial ergodic capacity, with antennas randomly placed, had a mean of 9.48 bps/Hz, with standard deviation of 1.01 bps/Hz. The genetic algorithm improved it to a mean of 14.14 bps/Hz with standard deviation of 0.43 bps/Hz.

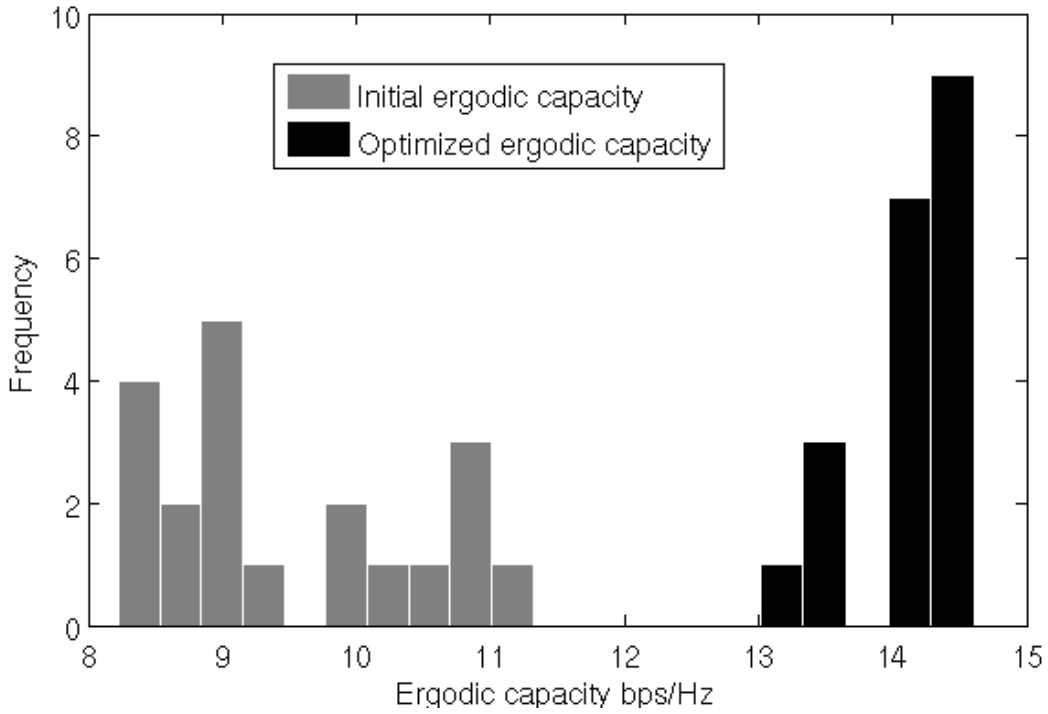

Figure 3.12: 3x3 MIMO array evolution.

3.5.2 One cluster, 3x3 MIMO, small volume

Figures 3.13 and 3.14 show two results that emerged for a 3×3 MIMO system, with one cluster with directions of arrival illustrated by the colored lines in the figure. The difference in this scenario is that the receiver antennas were limited to a search volume of $0.2^3\lambda$. 20 independent simulations were made, 16 of them showed a pattern equivalent to Figure 3.13, with mean of 11.15 bps/Hz and standard deviation of 0.1390 bps/Hz. But 4 of them presented a pattern similar to that of figure 3.14, with resulting ergodic capacity of mean 11.89 bps/Hz and standard deviation of 0.33 bps/Hz. The initial condition, with antennas randomly placed, had a mean of 6.76 bps/Hz and standard deviation of 0.92 bps/Hz. Figure 3.16 shows the histogram for all 20 simulations, the gray bars represent the initial state of the simulations and the black bars represent the final state of the same simulations. Figure 3.18 shows the evolution of the solutions for this last simulation scenario for the 20 independent simulations. We can see the ability of the system of escaping from local maximum.

Figure 3.15 shows the simulation results for a 3×3 MIMO system, with search volume limited to $0.2^3\lambda$. It also considers one cluster, but this time, the cluster main direction is not

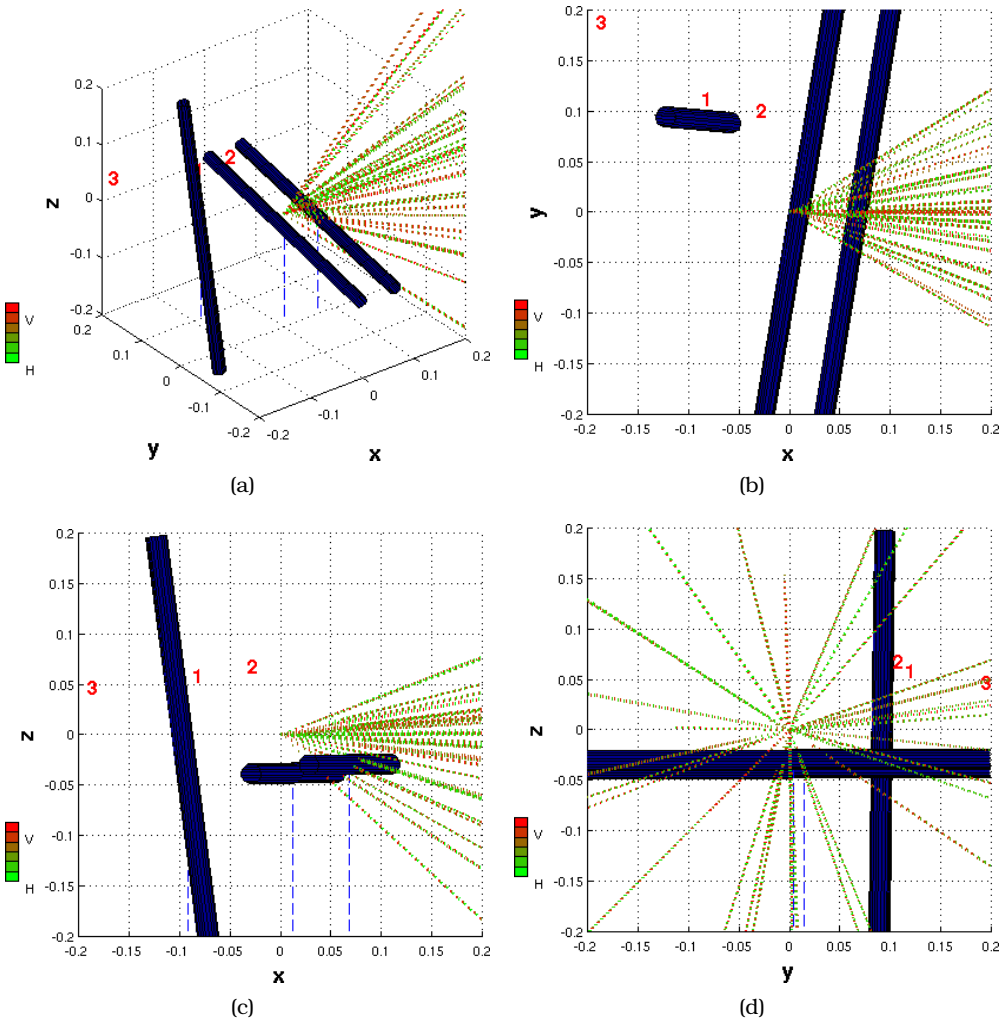

Figure 3.13: First evolved 3x3 MIMO configuration, One cluster. SNR=20dB. Volume=$(0.2\lambda)^3$.

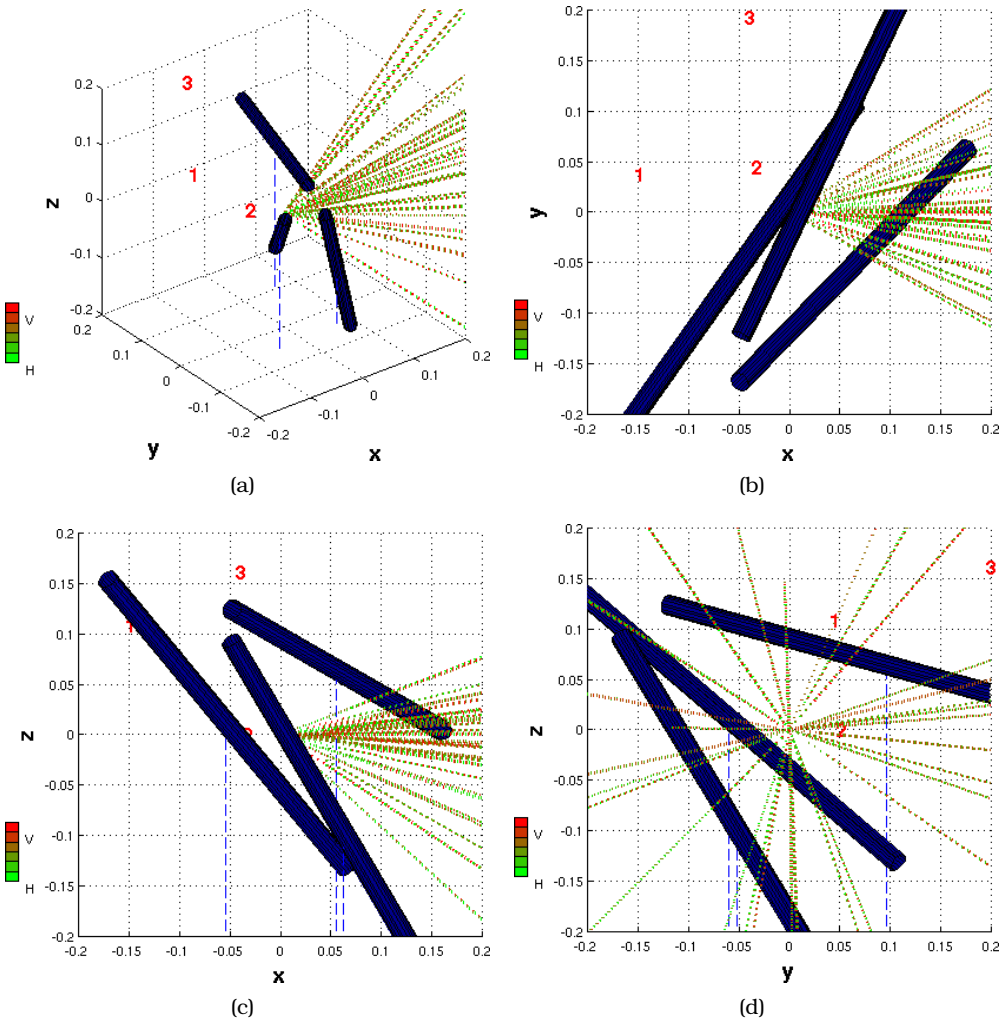

Figure 3.14: Second evolved 3x3 MIMO configuration, One cluster. SNR=20dB. Volume=$(0.2\lambda)^3$.

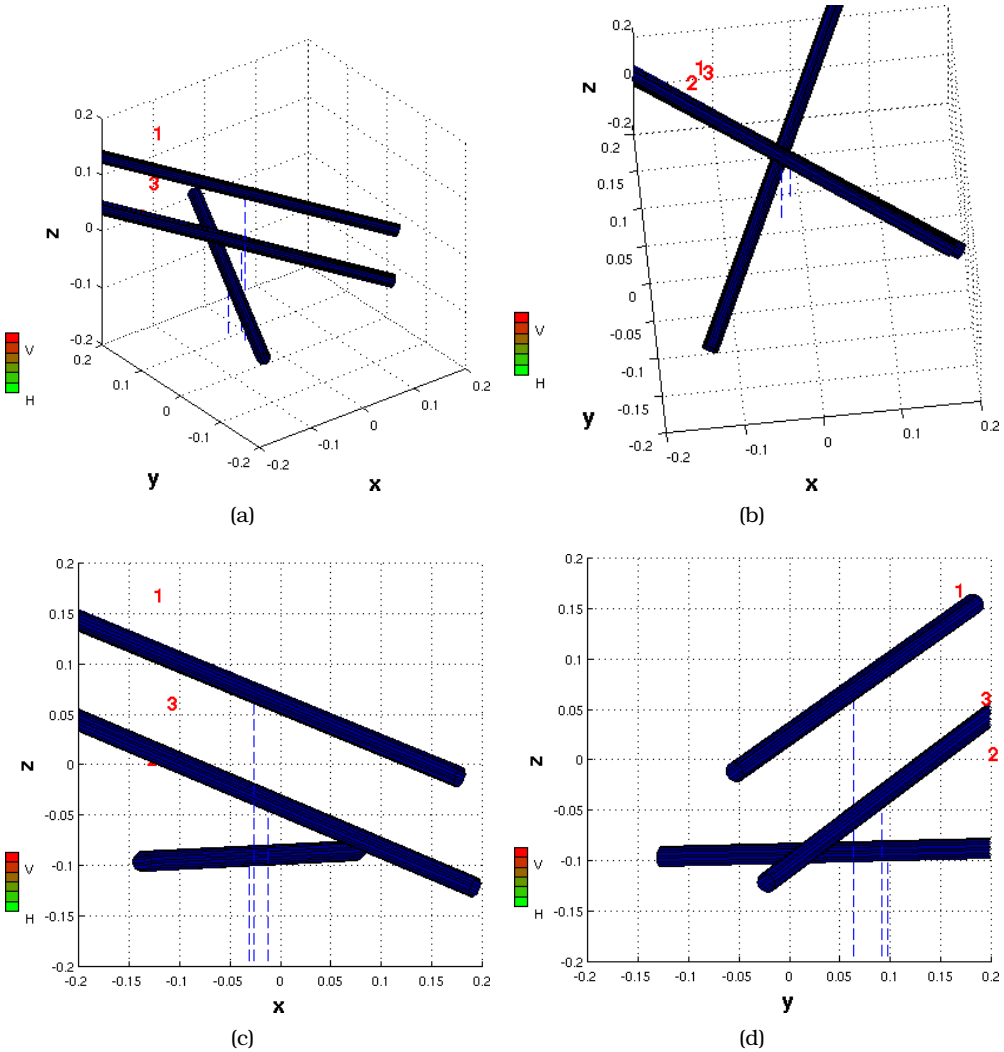

Figure 3.15: Evolved 3x3 MIMO configuration, One cluster. Uniform cluster main direction distribution. SNR=20dB. Volume=$(0.2\lambda)^3$.

fixed, but uniformly distributed around the space. The cluster has the same angle spread of other simulations, but is not plotted in the figure due to its random direction distribution. In this case, all the 20 simulations had shown results similar to that of Figure 3.13. Since the available space is too small to achieve signal diversity trough antenna spacing, the optimizer made use of two strategies: orthogonal polarizations and orthogonal patterns. According to Figure 3.13, antenna 3 is orthogonally polarized to antennas 1 and 2. Antennas 1 and 2 are placed in parallel. The electromagnetic coupling effect makes antennas 1 and 2 to get directional gains in opposite directions. Figure 3.19 shows how the optimizer made use of polarization and pattern diversity, exploiting the electromagnetic mutual coupling effect, in order to produce MIMO diversity.

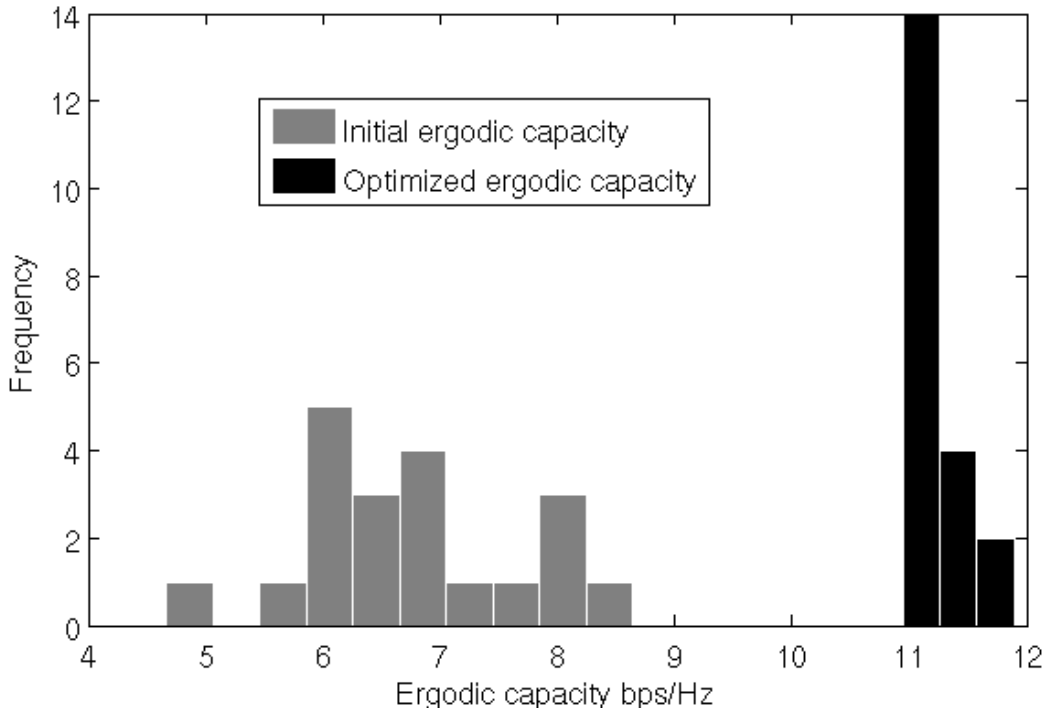

Figure 3.16: Histogram for evolved 3x3 MIMO configuration, One cluster. SNR=20dB. Volume=$(0.2\lambda)^3$.

3.5.3 Array topology comparison

In work [14], an ULA is compared to a UCA. The work in [46] shows the impact of DOA over correlation for ULA, and the correlation degrades MIMO capacity. The capacity is calculated for one cluster for different DOAs using 4×4 MIMO system. They have concluded that the ULA achieves very high capacities for some DOAs but also very low capacities for other DOAs. The UCA could not achieve the ULA top capacity but had a much more stable behavior.

This subsection will compare the ULA and UCA arrays to an array resulted from the genetic algorithm presented in this chapter. The simulations will use a channel with a cluster having 15^o of angle spread with normal multipath distribution. The schematic is shown in Figure 3.20. It also uses the proposed genetic algorithm to evolve a 2D topology solution for the problem. For this problem the fitness function was the average ergodic capacity, considering the cluster to be in a different DOA at each statistical realization. The constraint for the evolved array was that the distance between elements should not be greater than $\lambda/2$. The array resulting from the genetic algorithm is shown in Figure 3.21. As we can see in Figure 3.22, we found results for ULA e UCA similar to [14], with the UCA being more stable. The

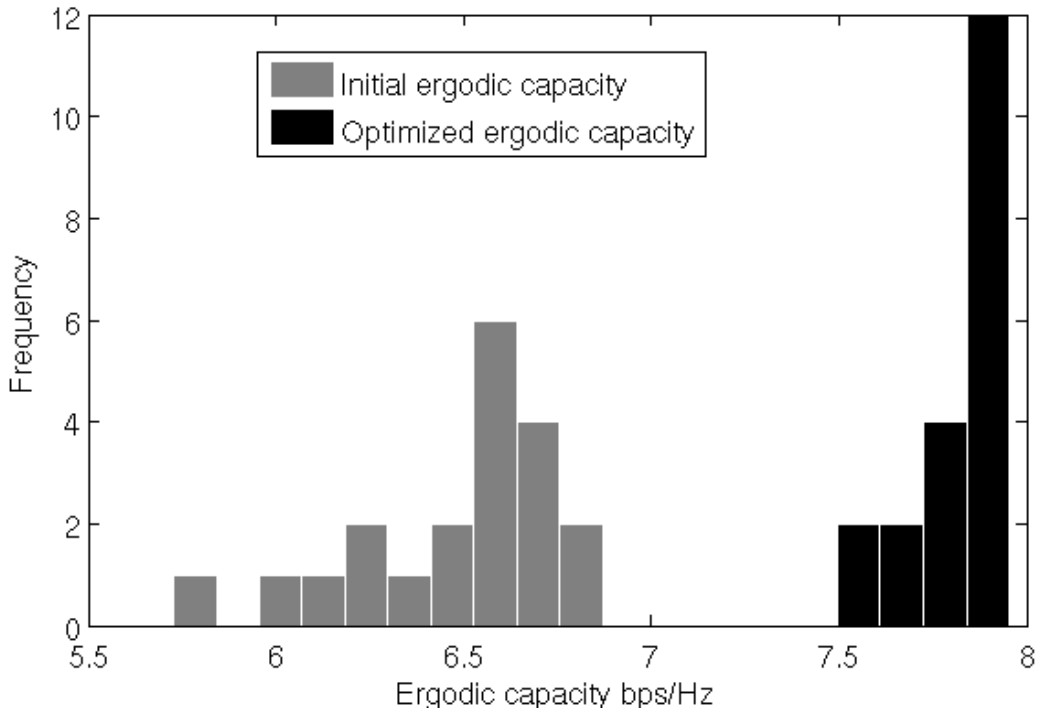

Figure 3.17: Histogram for evolved 3x3 MIMO configuration, One cluster. Uniform cluster main direction distribution. SNR=20dB. Volume=$(0.2\lambda)^3$.

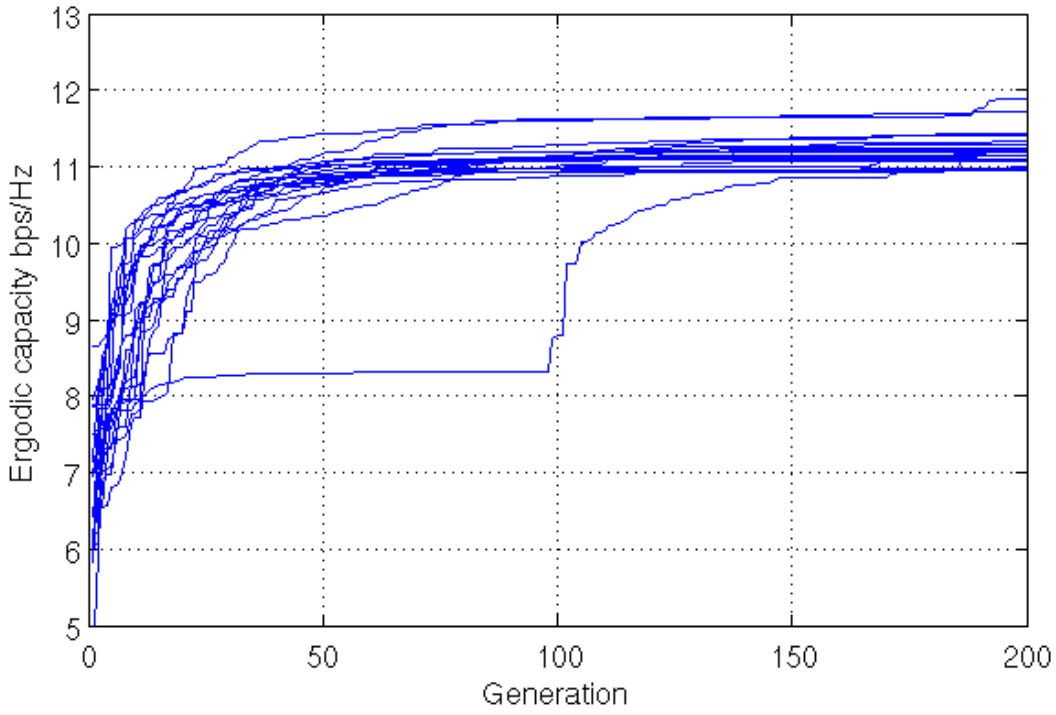

Figure 3.18: 3x3 MIMO array evolution in a small volume.

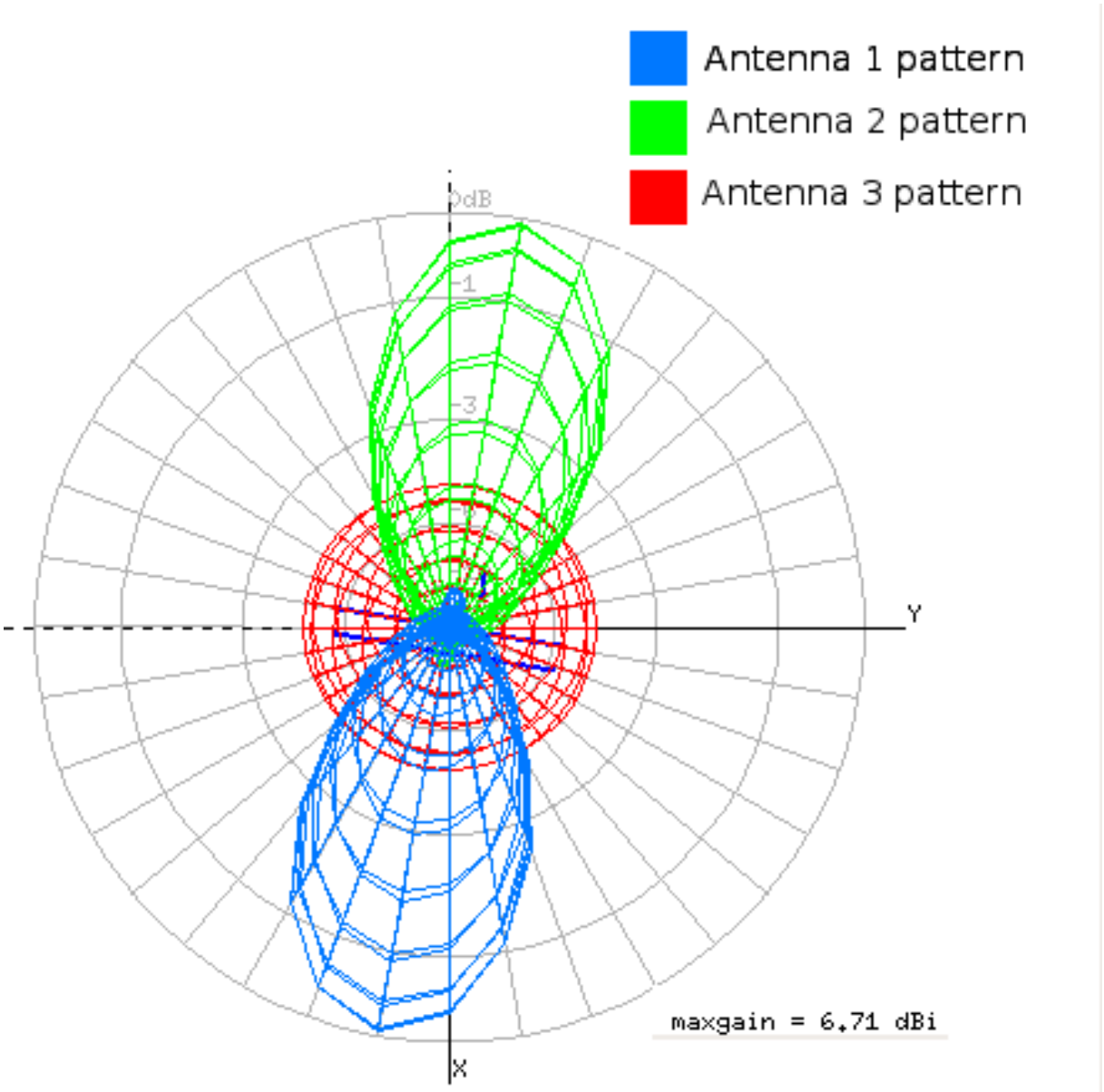

Figure 3.19: Resulting antenna pattern for evolved 3x3 MIMO configuration, One cluster. SNR=20dB. Volume=$(0.2\lambda)^3$.

ULA had higher peak and average capacity, but had very strong capacity losses for some DOAs, agreeing with [46]. The evolved GA solution was better than both. It had the highest average ergodic capacity while being much more stable than ULA and with all capacities above the UCA solution. Figure 3.20 shows the histogram for the solutions. Although, there were different resulting capacities, all solutions are geometrically similar.

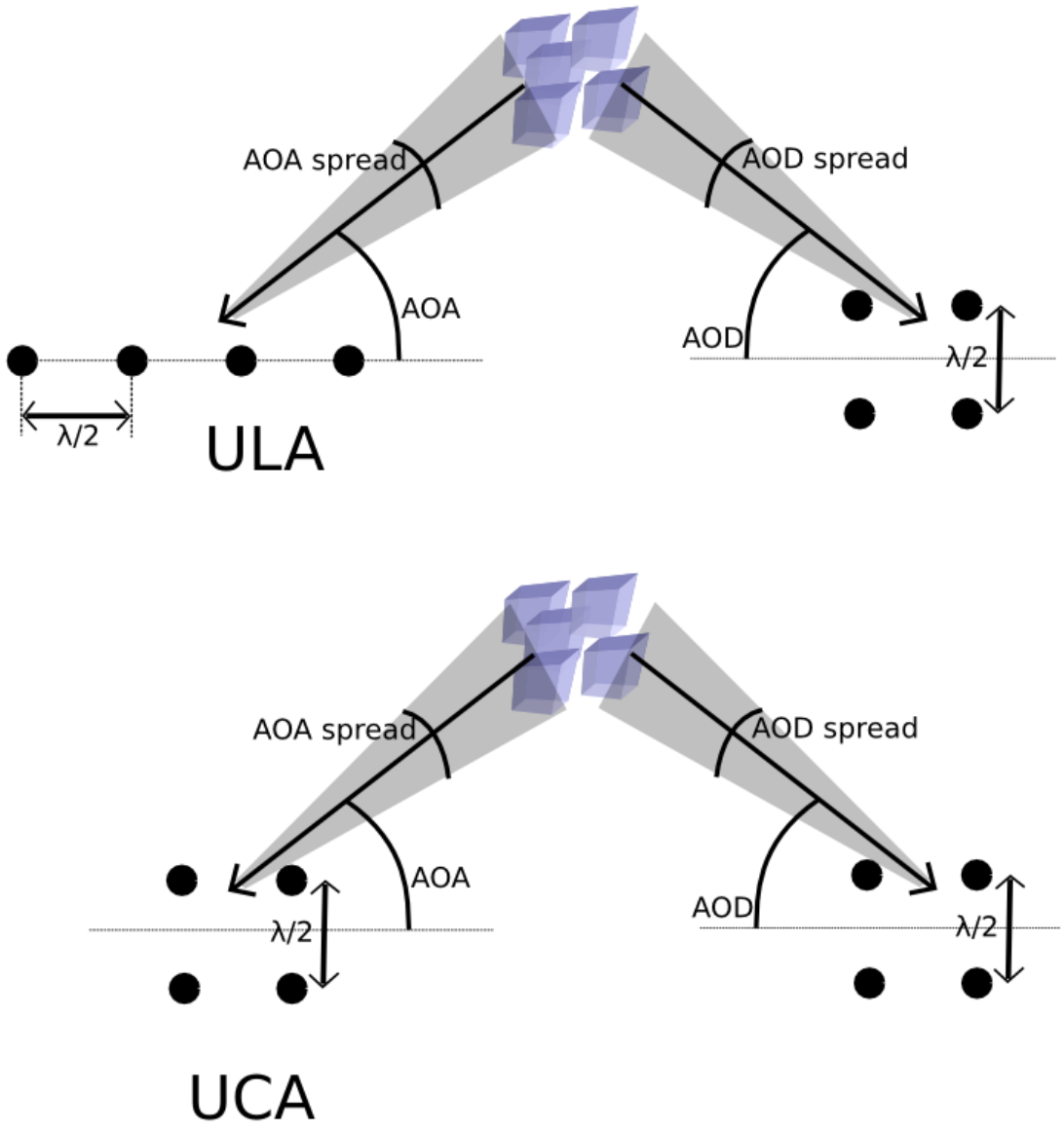

Figure 3.20: Schematic of ULA and UCA arrays.

3.6 Conclusion

The proposed GA based optimization algorithm for antenna array positioning has proved to be successful in finding good MIMO antenna schemes for a given propagation scenario. Some solutions found by the GA optimizer were very subtle, and a human designer would have difficulties trying to identify the best location and orientation for the antennas according to the specified propagation environment. The comparison of ULA, UCA and the array evolved by our method shows that it is a much more efficient engineering method than the intuitive and trial and error approach.

The results so far have shown that pattern and polarization diversities play an important

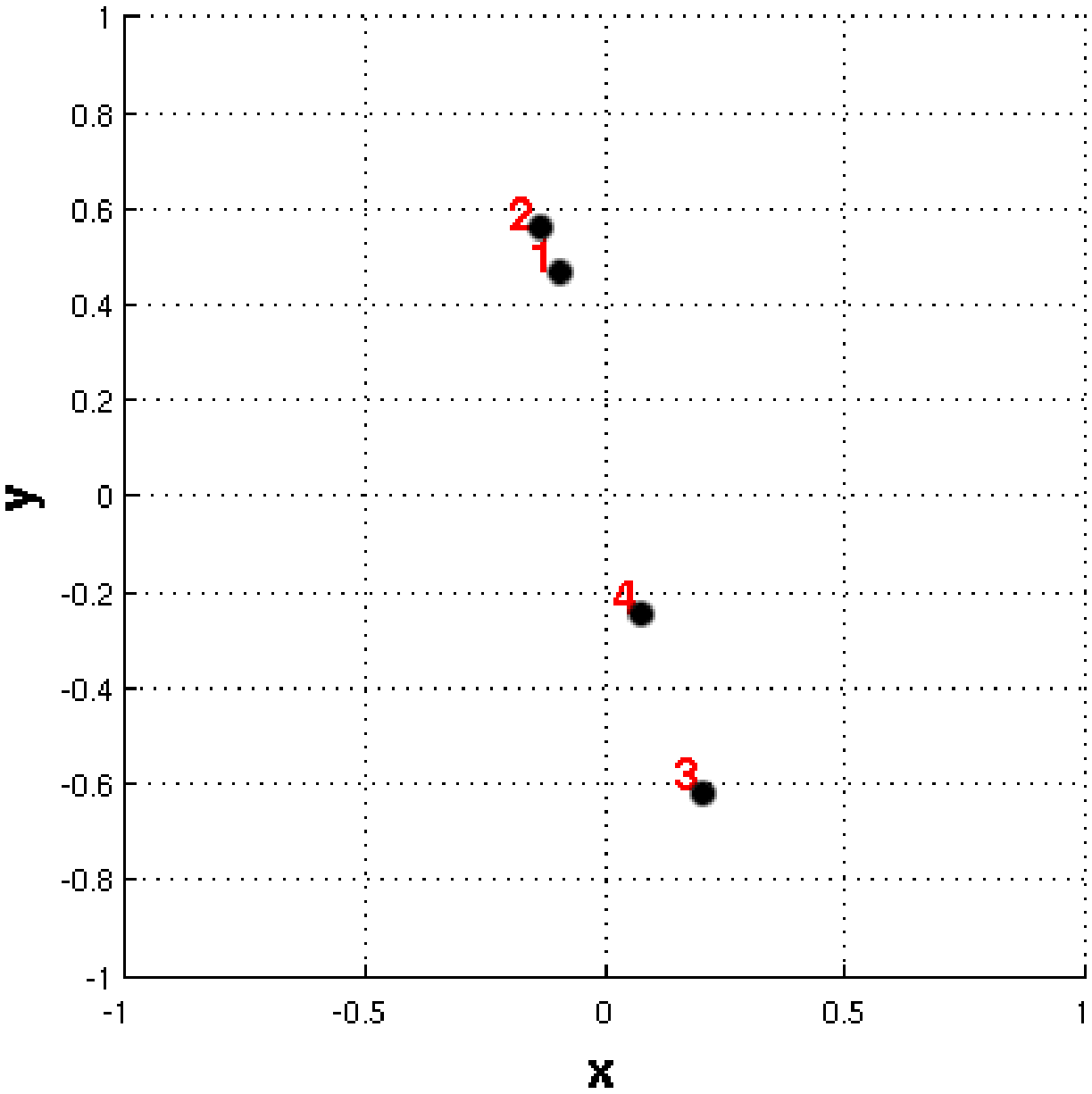

Figure 3.21: Array topology resulted from GA optimization.

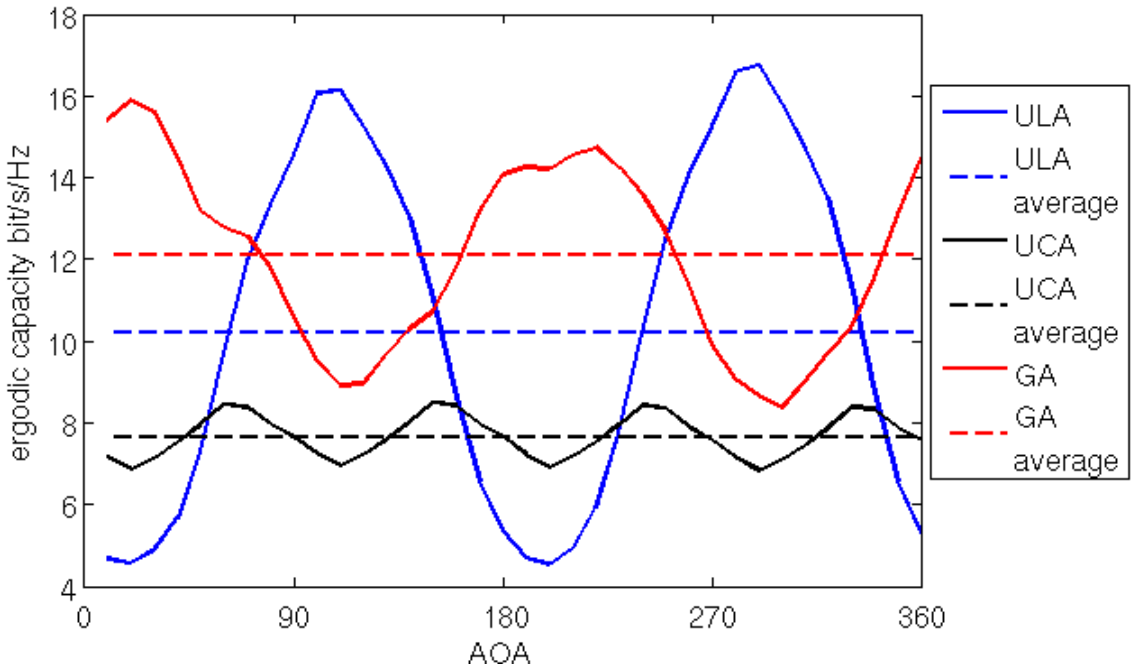

Figure 3.22: Performance comparison of ULA, UCA, and GA array topologies.

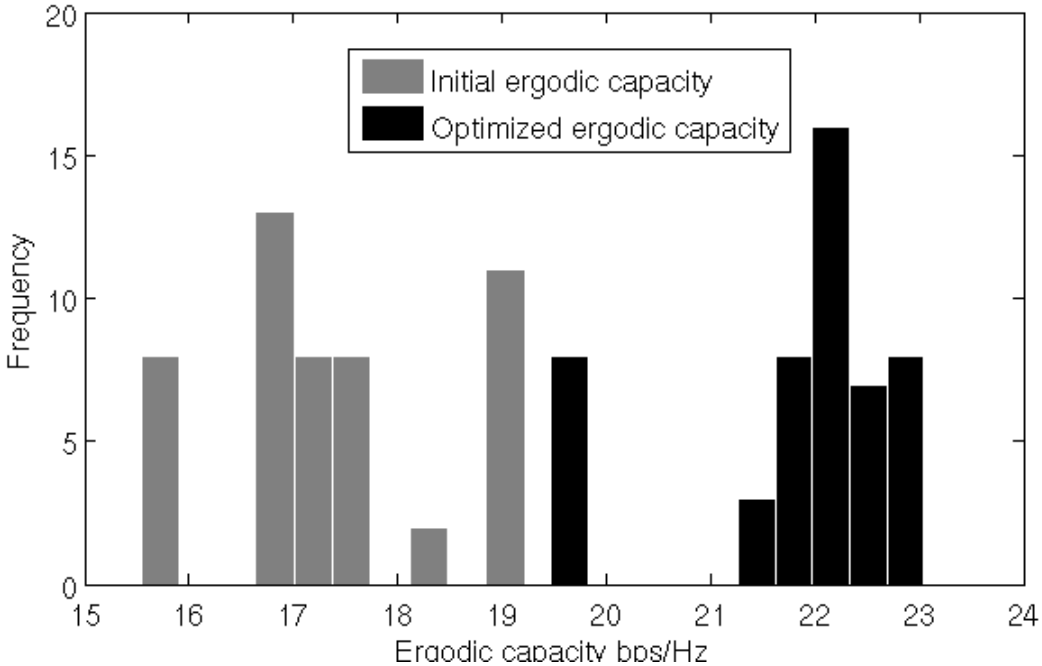

Figure 3.23: Histogram for evolved 4x4 MIMO configuration. Uniform cluster main direction distribution. SNR=20dB. Volume=$(0.2\lambda)^3$.

(if not the most important) role in MIMO capacity when there is little space available for positioning the antennas. One important aspect of the proposed method is its generality, as it can be adapted to be used with different antenna and propagation models.

Chapter 4

Extension of the Genetic Algorithm to Consider Antenna Selection

4.1 Introduction

The adoption of MIMO in commercial systems has been slow, and one of the main reasons is hardware requirements that considerably raise the implementation cost. It is not expensive to add additional antenna elements, since they are just small metal parts. But for each new antenna it is necessary to add a complete RF chain which includes such elements as low noise amplifiers, frequency down-converters and analog to digital converters. These extra RF chains are what raises the costs of MIMO terminals. [33]

Therefore one key problem to bring MIMO systems into practice is the increase of cost and complexity due to the need of a complete radio frequency (RF) chain for each antenna [67]. An approach to solve this problem is the use of antenna selection. The idea is to have more antennas than RF chains and then select the antenna subset that fulfills a given criterion at a given moment. This approach is called hybrid selection/MIMO (H-S/MIMO) in [68].

In [69], it is shown that the achieved capacity in a H-S/MIMO system can be close to the capacity of a full-complexity system provided that the number of selected antennas is at least as large as the number of antennas at the other link-end. Works such [68], [67], [70], [69] and [71] have studied the effect of antenna selection. Most works use ideal i.i.d. channels and do not consider the impact of antenna array configuration when using H-S/MIMO instead of standard MIMO systems.

The work [72] shows an experimental study for MIMO channels with antenna selection. According to this study, antenna selection can provide an increase of more than 100% in system capacity, when comparing a system that selects L_r antennas at the receiver to a standard MIMO system with M antennas at the receiver, given that $M = L_r$, considering lossless switching networks[1]. With realistic switching networks, the gain decreases to only 11%. The work [74] also presents an experimental study with antenna selection in MIMO systems and shows that antenna selection can increase the system capacity even in LOS scenarios, but it investigates a single propagation scenario and does not investigate the effect

[1] Lossless switching networks are idealized networks that do not consider the losses caused by the time necessary to witch off and witch on the antennas during the antenna selection process. These losses are investigated in [73].

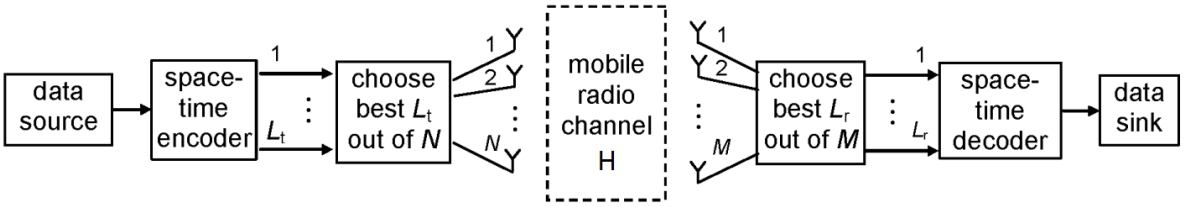

Figure 4.1: General MIMO antenna selection diagram.

of antenna array topology properties such as antennas position and mutual coupling effect.

In this chapter the method proposed in Chapter III is modified in order to obtain an array suited for antenna selection. As we will show, the MIMO array configuration that maximizes the ergodic capacity is not the same for systems that consider antenna selection and systems not considering it.

4.2 Antena Selection

Antenna subsection selection is used when the number of available antenna elements is larger than the number of RF chains in the system (noting that it is necessary at least two RF chains at each link end for enabling a MIMO system). The available antennas are dynamically connected to a subset of the available antenna elements according to a predefined criteria, taking the channel current state into consideration. Some systems use antenna selection just in the transmitter side, the so called transmit antenna selection (TAS). Other systems perform the selection at the receiver side, the so called receive antenna selection (RAS). There are also systems that perform antenna selection at transmitter and receiver side (T-RAS) [33].

Figure 4.1, from [75], shows the block diagram for T-RAS antenna selection. The transmit signal vector is first obtained by means of space-time coding or linear weighting, with size equals to the number of RF chains available at the transmitter (L_t). A set of antennas is selected from the N_t available antenna elements at the transmitter. The signal vector is then mapped to the selected antenna elements resulting in the transmit signal vector s with size N_t. The vector s will contain L_t non-zeros elements and $N_t - L_t$ zero elements. The signal vector passes through the MIMO propagation channel $\mathbf{H}$ resulting in the received signal vector $\mathbf{y}$:

$$\mathbf{y} = \mathbf{H}\mathbf{s} + \mathbf{n} \tag{4.1}$$

[33] where n is the noise vector. At the receiver, L_r from the Nr received elements are selected for processing by connecting the antenna elements to the L_r available RF chains.

The ergodic capacity for a MIMO system using antenna selection is given by:

$$C = \max_{S(\tilde{\mathbf{H}})} \left(\log_2 \det \left[I_{L_r} + \frac{SNR}{N_t} \tilde{\mathbf{H}} \tilde{\mathbf{H}}^H \right] \right) \tag{4.2}$$

[33], where $\tilde{\mathbf{H}}$ is the modified channel matrix of size $L_t L_r$ formed by the rows and columns of $\mathbf{H}$ corresponding to the selected antennas. $S(\tilde{\mathbf{H}})$ is the set of all possible sub-matrices $\tilde{\mathbf{H}}$. Here it is also considered perfect knowledge of the channel at the transmitter (CSIT) [33]. For simplicity, uniform power allocation was considered.

An important aspect noted by [33], is that the mean capacity increases linearly with $min(L_t, L_r)$, but the slope of the capacity distribution, which determines the fading margin for outage capacity for a given mean capacity is determined by N_t and N_r. That is the main advantage of having more antenna elements than RF chains.

4.2.1 The impact of channel characteristics on antenna selection

Most analysis of MIMO systems with antenna selection consider a channel model where matrix **H** elements are independent, identically distributed complex Gaussian entries, corresponding to a system with uncorrelated isotropic antennas with multipath components arriving from all directions. Practical scenarios cannot have these characteristics, realistic scenarios have different characteristics that impact MIMO performance and should be taken into account for good antenna selection strategies. The most important effects are summarized by [33]:

- Signal correlation: There are two reasons for signal correlation, the antennas might be too close and/or there might not exist enough diversity in multipath components, such as in scenarios with strong LOS. These effect degrades MIMO system capacity and can force the system to select the antennas with directive patterns towards the LOS.
- Mutual coupling among antenna elements: Mutual coupling, as seen in the last chapter, can have a negative or positive impact on MIMO performance. An important aspect that should be noted is that the antennas not selected by the system still contribute to electromagnetic coupling effect with shadowing and reflection of incoming waves. This way, not selected antennas can still have some negative or positive impact in the system and should also be part of the electromagnetic simulations.
- Unequal mean powers: Antennas with different far field patterns or different polarization can result in different mean power received depending on the characteristics of the propagation environment. Even antennas with the same form factor, may present different patterns due to electromagnetic coupling effects, as seen in the last chapter. Antennas with more mean power will have a higher likelihood of selection [33].
- Frequency Selective Channels: If the bandwidth of the transmitted signal is larger than the coherence bandwidth, the channel is said to be frequency selective. Most research have focused on flat fading channels, but space-time trellis codes (STTCs) design principles have been developed for frequency selective fading channels [75]. If a codeword of length lN is transmitted from N available antennas and transverses a L-path fading channel, it can be expressed by a matrix of size $LN(l+L-1)$. The channel matrix in this case will have size MLN When the system is modeled in this way, STTCs over frequency-selective channels can be considered as codes over frequency with NL virtual transmit antennas, turning possible to apply existing results for STTCs over flat fading channels. [75]

4.2.2 Selection Algorithms

An antenna selection algorithm can take different metrics as its objective function. The main metrics used are channel capacity and SNR [75].

4.2.2.1 Selection Based on Channel Capacity

For convenience, let us recall here the function of ergodic capacity for the MIMO channel [35]:

$$C = \frac{1}{N_q}\sum_{q=1}^{N_q}\log_2\det\left[I_{Nr} + \frac{SNR}{Nt}\mathbf{H}_q\mathbf{H}_q^H\right]. \tag{4.3}$$

When the receiver selects the best L_r antennas, it maximizes the resulting channel capacity that is upper bounded by [75]

$$C_{select} = \sum_{i=1}^{L_r} \log_2 \left(1 + \frac{SNR}{Nt}\gamma_i\right). \tag{4.4}$$

where γ_i is the squared norm of the ith row of the channel matrix $\mathbf{H}$ in ascendent order. It was shown that most of the complete MIMO system capacity is retained with antenna selection if the number of selected antennas on the receiver is at least equal to the number of antennas available at the transmitter.

If the system does a joint selection of antennas at the transmitter and at the receiver, the capacity is bounded by 4.6 and the system has to solve the maximization problem:

$$\tilde{\mathbf{H}}_{\mathbf{sel}} = \arg\max_{\tilde{\mathbf{H}}} C_s(\tilde{\mathbf{H}}) \tag{4.5}$$

where $\tilde{\mathbf{H}_{\mathbf{sel}}}$ is the channel sub-matrix that maximizes the channel capacity C_s resulting from the selected antennas set according to:

$$C_s = \log_2 \det \left[I_{L_r} + \frac{SNR}{L_t}\tilde{\mathbf{H}}\tilde{\mathbf{H}}^H\right] \tag{4.6}$$

The selection might also be made in order to prevent an outage event. An outage event happens when the information rate is greater than the instantaneous mutual information. The probability of occurrence of such an event is known as outage probability [75].

For the optimal antenna selection using exhaustive search, considering that $L_t = L_r = L$ the computational complexity is of order $O({N_t}^L {N_r}^L L^3)$, only practical for small values of N_t,N_r and L [76]. For this reason various sub-optimal algorithms have been proposed. One example is [76] that proposes the so called JTRAS, a greedy algorithm that jointly selects the receive and transmit antennas with results close to the optimal solution and with complexity $O(N_t N_r L^4)$.

Work [77] proposes a method for antennas selection to be used in systems with optimum transmit beamforming, also known as maximum ratio transmission (MRT). The algorithm proposed by them had a performance nearly as good as optimum selection. A fast antenna selection algorithm is proposed by [78], achieving similar outage capacity as the optimal selection with computation complexity of $O(max\ N_t, N_r\ N_t L_r)$. In [79] a fast and global-search receive antenna algorithm is proposed. The algorithm acquires the near-optimal channel matrix by directly searching the maximum-volume sub-matrix of the original channel matrix.

The optimal receive antenna subset selection problem for maximizing the mutual information is sub-modular. It means that a greedy step-wise optimization algorithm, where at each step the antenna that maximizes the incremental gain is added to the existing antenna subset, is guaranteed to be within a $(1 - 1/e)$-fraction of the global optimal value as recently demonstrated by [80].

4.2.2.2 Antenna selection based on receiver SNR

An easier solution for antenna selection algorithms is to use instantaneous receiver SNR as its criteria. It is an attractive solution because it is much more pragmatic than channel capacity, and much less computationally expensive. However, maximizing the SNR does not mean to maximize the channel capacity, the true objective of a communication channel [75]. This happens because of the impact of spatial multiplexing, as previously noted in this thesis.

The work [81] examined the performance of transmit antenna selection for STTCs over

```
1. generate initial population
2. while error>max_error and generation<max_generations
   {
3.       for each antenna array configuration:
         {
4.              for each instance of the propagation model:
                {
5.                     for each realization of the propagation model instance:
                       {
6.                            select best set of antennas
7.                            compute mutual information of the channel for the selected antennas
                       }
8.                     compute ergodic capacity for the propagation instance
                }
9.              compute mean ergodic capacity for the antenna array configuration
         }
10.      select parents of next generation
11.      generate offspring by crossover
12.      apply mutation
   }
13. return best individual
```

Figure 4.2: Genetic algorithm considering antenna selection.

quasi-static fading channels using computer simulations. The study used several elements at the transmitter and selects the two antenna elements that would maximize the received SNR. It was demonstrated that the order of diversity was maintained with antenna selection, showing that the SNR criteria, although not perfect, can work well for certain scenarios.

Another example is [82], which presents a method that allows reconfigurable multi-element antennas to select the antenna configuration at the receiver of MIMO communication system using spatial correlation and average Signal to Noise Ratio (SNR) information to select the antenna radiation pattern.

The effect of antenna directivity on MIMO antenna selection is studied by [73]. It is demonstrated that antenna directivity at the receive antenna array can take the benefit of channel sectorization in order to have an interference suppression. In order to find the optimum solution for the diversity gain, [73] maximizes the SNR gain, defined as the ratio of the combiner output SNR to the nominal receiver SNR. The study uses 2 isotropic antennas at the transmitter side and 4 orthogonal directive antennas at the receiver. The study compares this setup with 4 isotropic antennas and concludes that the directivity of the antennas has a positive impact in the MIMO channel capacity. According to [73], the increase in capacity happens because of the interference cancelation due to the directional nature of the interference.

4.3 Genetic Algorithm Optimization

For the antenna selection problem, the objective is not to use the genetic algorithm to find the best antenna subset. The objective is to use the genetic algorithm in order to find the MIMO array which provides the maximum capacity considering that at each point, the system will choose the best antennas for the given channel. Thus, intrinsically, the algorithm will try to find an arrangement that will allays provide a good subset of antennas to be chosen.

The general algorithm is presented in figure 4.2. First an initial population of antenna array configurations is generated. Each antenna array configuration is composed by all antennas in the MIMO system with their respective positions and orientations. For each antenna array configuration, the fitness function for the genetic algorithm has to be computed. The fitness function considers the mean ergodic capacity of all instances of the propagation model. Each instance can be a realization of the propagation model with different parameters, such as different number of clusters, different AOA, different angle spreads. This can be interpreted as different points in a route or different locations within a propagation environment. This is done in such a way to test the versatility of the antenna array, considering that it will have to perform antenna selection in different circumstances.

For each instance of the propagation model, the ergodic capacity is computed using various realizations of that instance. At each realization the antenna selection is performed. The algorithm is not interested in the method used for antenna selection, so it chooses the best antenna set by brute force, considering the instantaneous mutual information. The mean ergodic capacity is used to sort the antenna arrays and to select the best arrays for the next generation of the genetic algorithm.

In the simulations of this chapter, we used the data from the channel modeled according to the procedure described in Chapter II. Since we are trying to find the best MIMO configuration for all the route, the objective function (3.16) was modified to consider the mean capacity along the route:

$$C = \frac{1}{N_s}\sum_{s=1}^{N_s}\frac{1}{N_q}\sum_{q=1}^{N_q}\log_2\det\left[I_{Nr} + \frac{SNR}{Nt}\mathbf{H}^a{}_{qs}\mathbf{H}^{a\,H}_{qs}\right]. \tag{4.7}$$

where N_s is the number of snapshots in the route, N_q is the number of realizations to compute the expectation statistics and $\mathbf{H}^a{}_{qs}$ is a sub-matrix of the channel matrix $\mathbf{H}$ for the channel realization q of snapshot s of the route.

In order to consider the antenna selection problem, at each snapshot s of the route, we have to select the channel matrix that consists of the subset of the $\mathbf{H}$ cannel matrix that provides the highest channel capacity. Define $\mathbf{H}_s$ as the set of $\mathbf{H}$ channel matrix realizations at snapshot s, and $\mathbf{H}_{su}$ a valid subset columns according the number of antennas that can be selected.The subset $\mathbf{H}^a{}_s$ that provides the highest channel capacity for the given snapshot can be found by maximizing:

$$\mathbf{H}^a{}_s = \underset{\mathbf{H}_{s\,u,u=1..U}}{\arg\max}\ C_s(\mathbf{H}_{s\,u,u=1..U}) \tag{4.8}$$

where:

$$C_s = \frac{1}{N_q}\sum_{q=1}^{N_q}\log_2\det\left[I_{Nr} + \frac{SNR}{Nt}\mathbf{H}_{qsu}\mathbf{H}^H_{qsu}\right] \tag{4.9}$$

where $\mathbf{H}_{qsu}$ is the valid subset u of columns for a selection of antennas in the realization q of snapshot s of the route. Since the number of possible subsets is typically very small, it is possible to solve (4.8) by simply trying all possibilities. This work is not interested in the selection algorithm used and assumes that at least a near-optimal solution is adopted.

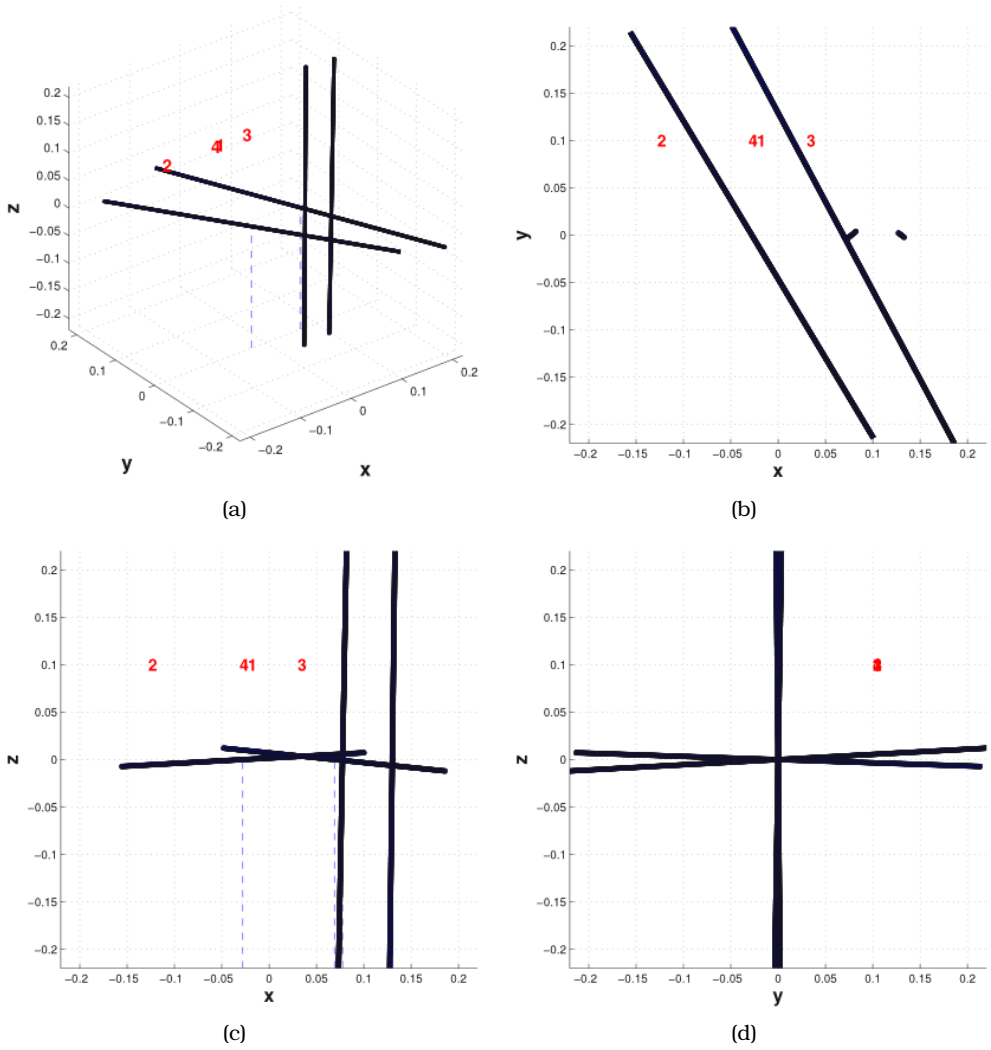

Figure 4.3: Evolved 4x4 MIMO configuration, SNR=20dB. No antenna selection considered. Total volume is $(0.2\lambda)^3$.

4.4 Simulation Results

The simulations considered the channel defined in Section II. At least 20 independent realizations of the simulation were made in order to verify the convergence stability of the GA solution. Since the electromagnetic code used (NEC) only works for wire antennas, half wavelength dipoles were used. Those are not practical mobile antennas but can be used in order to validate the method. Indeed, the NEC simulator can be reaplaced by other simulators without any impact on the rest of the proposed method.

For the simulations, the following GA parameters were used: a population size of 2000 individuals, the selection processes was deterministic with elitism, selection of 5% of the population and a mutation rate of 2%.

Figure 4.3 shows the tridimensional position and orientation of the simulated antenna array evolved for a 4×4 MIMO system not considering antenna selection, i.e. all four antennas are used by the system. The size constraint, i.e. the total volume allowed for the positioning of the antennas, was fixed at $(0.2\lambda)^3$. Figure 4.4 shows the evolution of the system for 100 generations. Since the space was too small, the GA implicitly explored other features in order to gain signal uncorrelation. The system used orthogonal polarization, and in case of antennas in parallel, pattern diversity. The antenna pattern is due to the fact that parallel

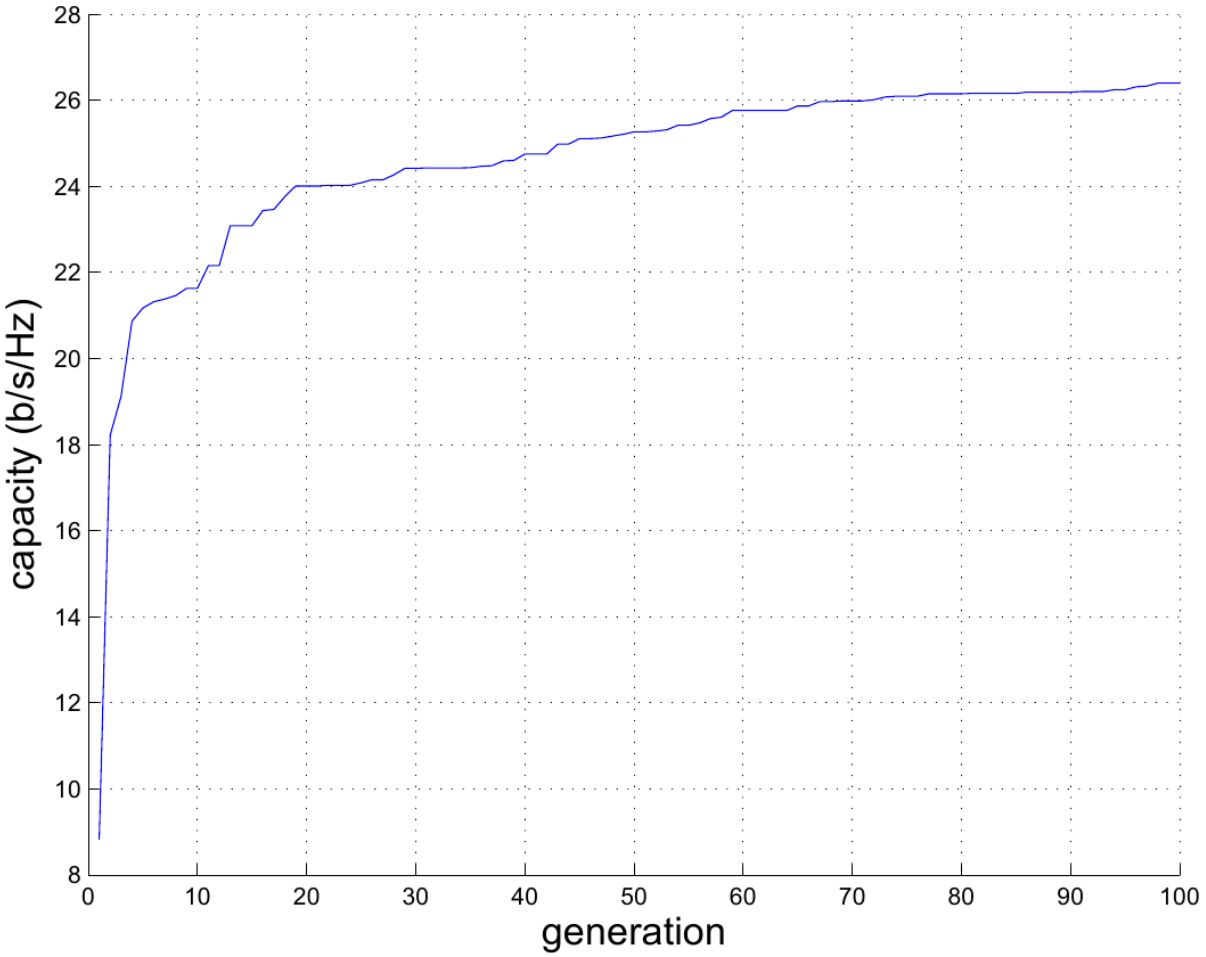

Figure 4.4: Evolution of 4x4 MIMO configuration without antenna selection. Total volume is $(0.2\lambda)^3$.

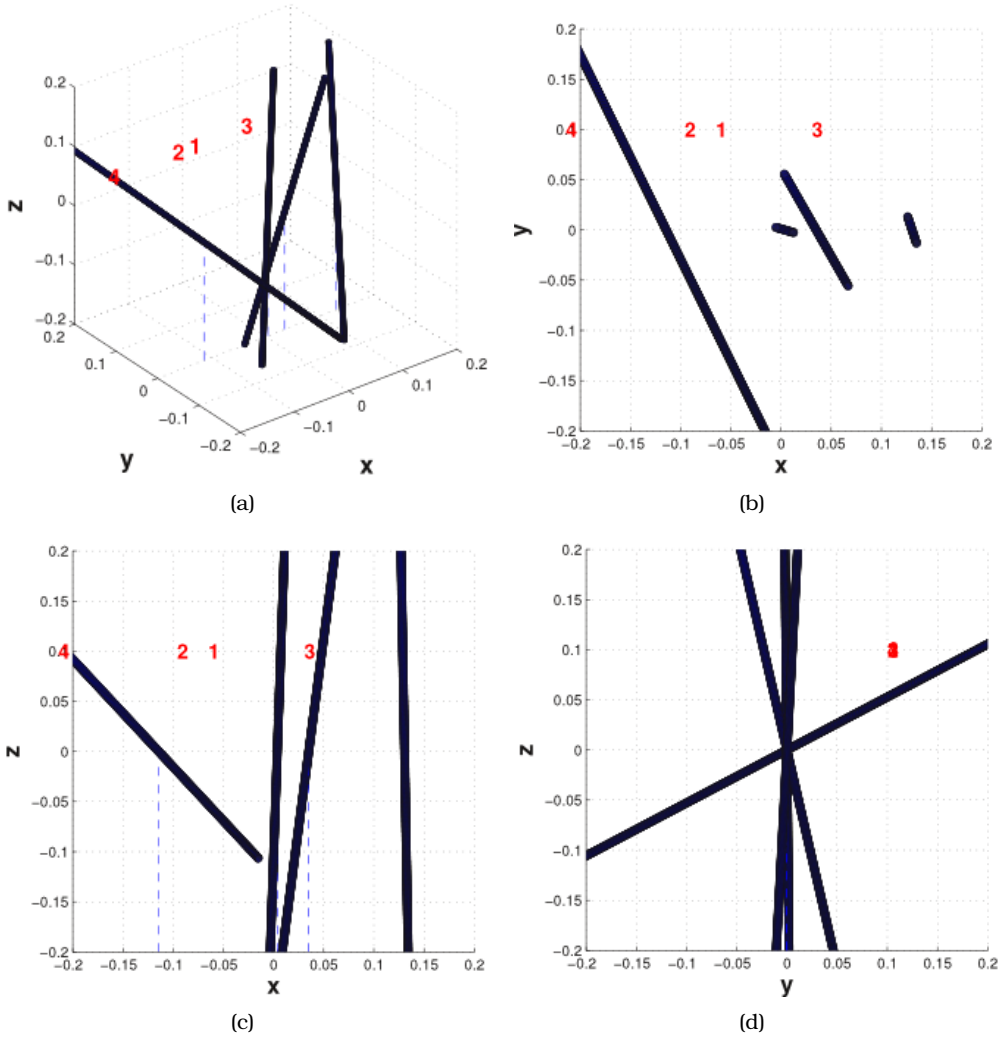

Figure 4.5: Evolved 4x4 MIMO configuration, SNR=20dB. Antenna selection, with 2 antennas selected out of 4 antennas. Total volume is $(0.2\lambda)^3$.

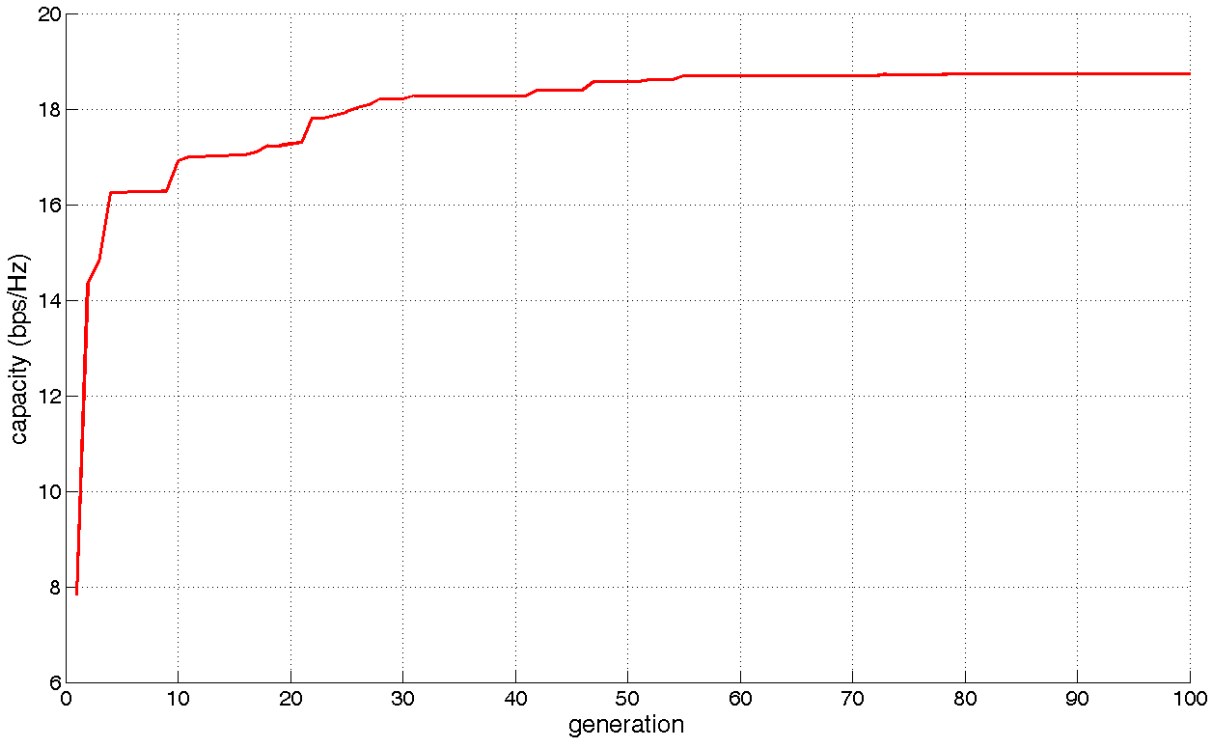

Figure 4.6: Evolution of 4x4 MIMO configuration. Antenna selection, with 2 antennas selected out of 4 antennas. Total volume is $(0.2\lambda)^3$.

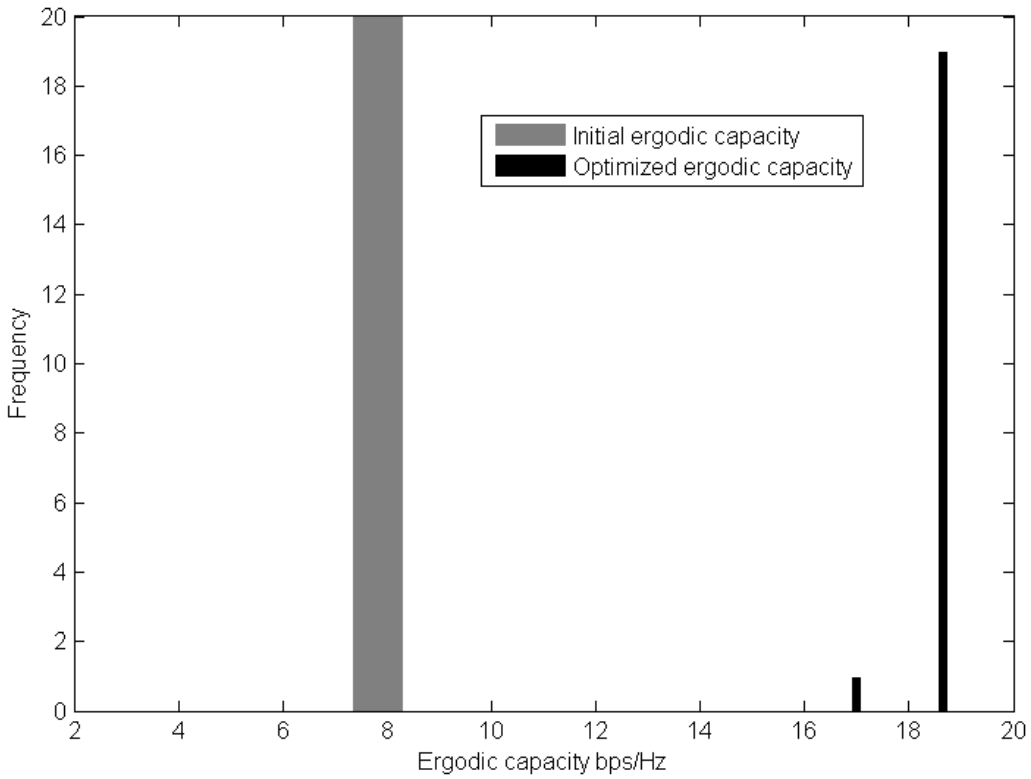

Figure 4.7: Histogram of 4x4 MIMO configuration considering 20 solutions of the GA Antenna selection, with 2 antennas selected out of 4 antennas. Total volume is $(0.2\lambda)^3$.

dipoles points outwards in opposite directions. It is interesting to note that in this case the optimization tool stressed the orthogonality of the system not opting for a TPD scheme. This result corroborates those of [18].

Figure 4.5 shows the simulation of a 4×4 MIMO system with antenna selection of 2 out of 4 antennas, resulting in a 4×2 MIMO system. Here we can see a different disposition of the antennas. Since only 2 antennas are selected at a time, there is no important gain for the system having all 4 antennas orthogonal to each other. In this case, the system opted for a solution more similar to that of TPD systems, using different angles for the antennas. It is possible to say that using different angles, the system enables the option of always having a pair of antennas, which are at the same time, orthogonal to each other and also in a direction that favors the main DOAs for a given point of the route.

Figure 4.6 shows the evolution of the system in 100 generations for one of the algorithm realizations. We can see that the GA method has good convergence, doubling the system capacity in the first 10 generations and reaching convergence after 50 generations. Figure 4.7 shows a histogram for 20 realizations of the GA The histogram shows very little dispersion of the results, confirming that the method is very stable and robust against local maxima.

4.5 Conclusion

The GA proposed by in Chapter IV was successfully integrated with the channel model based on propagation measurements. The results corroborate those of [18] showing that electromagnetic coupling can be exploited in order to provide signal diversity in MIMO systems within devices of limited physical space. The results also show the importance of orthogonality among antennas, which can be compromised on TPD schemes.

The proposed GA optimizer also cosidered antenna selection. In this case, a scheme similar to TPD emerged from the optimizer. On the one hand, this scheme provided enough orthogonality between the selected antennas. Since only 2 antennas must be select at each time, there is a good chance of finding 2 orthogonal antennas. On the other hand, it also provided antennas in more different angles, making the system adaptable for different DOA configurations.

Chapter 5

Conclusions and Perspectives

5.1 Conclusion

This works started with an analysis of measurement data of a outdoor urban channel. The main motivation of these analysis is the fact the, in small terminals, there is no sufficient space for adequate antenna separation, in order do achieve multiplexing gain. With this analysis we came to interesting conclusions, that polarization diversity can play an important hole wen spatial diversity is absent. The study also provided a basis for a realist channel model to be used in subsequent developments.

The next step of this work was to create an optimization tool to define the best position and orientation of antennas in the array for a given channel. The importance of this tool is two-folded. First, the method has the practical capability of been applied in the industry for the design of mobile terminals. Without an optimization tool like this, the engineer has rely on intuition and trial and error approach. Second, this tool can provide interesting insights in what characteristics can be exploited in order to achieve signal diversity for a better MIMO system performance. In this regard, a very important result is the importance of orthogonality among antennas when there is restricted space to place them. This orthogonality can be achieved, first using polarization orthogonality, as expected. But a even more interesting result is the importance of antenna pattern diversity, This pattern diversity one side result of electromagnetic coupling among nearby antennas. This effect, at first usually seen a problem for antenna design can be manipulate in order to improve MIMO capacity in small terminals.

Interfacing the channel model created for the GA with the measurements MIMO channel from Stochastic, it was possible to apply the GA in a more realistic scenario. The GA was also extended to consider the use of antenna selection. It is very important because the cost of RF chains are much higher than antennas. Applying the GA for this particular case brought a very interesting result: array configurations well suited for a 44 MIMO system were vastly different than those evolved for a 44 system with 22 antenna selection. Namely, TPD-like schemes, that proved to be a poor choice for regular MIMO systems, proved to be the best choice for antenna selection systems.

The contributions could be summarized in the following points:

i. An analysis a the measurement data of a MIMO channel.

ii. A optimization tool based on GA for the design of MIMO antenna arrays that can be interfaced with different propagation channels and electromagnetic antenna simulators.

iii. The analysis of the optimization of antenna arrays considering antenna selection.

iv. Valuable insights on the source of signal diversity for MIMO arrays in restricted space. conditions and important characteristics for MIMO arrays when antenna selection is to be employed.

For the electromagnetic simulations, these work used NEC, a electromagnetic code for wire antennas. Its use was valuable for proof of concept of the method, but realistic mobile terminals use more complex antenna such as PIFA and usually integrated in the terminal body structure. For future work, it would be very interesting to use other codes capable of simulating realistic mobile terminals.

Other interesting perspective for the work would be the addition of other communication layers in the simulation, such a codification. This would allow the optimizer to seek other variables e.g. bit error rate (BER).

Bibliography

[1] G. J. Foschini and M. J. Gans, "On limits of wireless communications in a fading environment when using multiple antennas," *Wireless Personal Communications*, vol. 6, pp. 311–335, 1998.

[2] I. E. Telatar, "Capacity of multiantenna gaussian channels," *European Transactions on Telecommunications*, vol. 10, pp. 585–595, 1999.

[3] C. Oestges and B. Clerckx, *MIMO Wireless Communications: From Real-World Propagation to Space-Time Code Design*, ser. MIMO Wireless Communications: From Real-World Propagation to Space-Time Code Design. Academic Press, 2007.

[4] J. W. Wallace, M. A. Jensen, A. Gummalla, and H. B. Lee, "Experimental characterization of the outdoor MIMO wireless channel temporal variation," *IEEE Transactions on Vehicular Technology*, vol. 56, no. 3, pp. 1041–1049, May 2007.

[5] V. Eiceg, H. Sampath, and S. Catreux-Erceg, "Dual-polarization versus single-polarization MIMO channel measurement results and modeling," *IEEE Transactions on Wireless Communications*, vol. 5, no. 1, pp. 28–33, Jan. 2006.

[6] L. Jiang, L. Thiele, and V. Jungnickel, "Polarization rotation evaluation for macrocell MIMO channel," *Wireless Communication Systems, 2009. ISWCS 2009. 6th International Symposium on*, pp. 21–25, Sept. 2009.

[7] K. Sulonen, P. Suvikunnas, J. Kivinen, L. Vuokko, and P. Vainikainen, "Study of different mechanisms providing gain in MIMO systems," *Vehicular Technology Conference, 2003. VTC 2003-Fall. 2003 IEEE 58th*, vol. 1, pp. 352–356 Vol.1, Oct. 2003.

[8] A. Molisch, "Effect of far scatterer clusters in MIMO outdoor channel models," *Vehicular Technology Conference, 2003. VTC 2003-Spring. The 57th IEEE Semiannual*, vol. 1, pp. 534–538 vol.1, April 2003.

[9] T. Kan, R. Funada, J. Wang, H. Harada, and J.-I. Takada, "MIMO channel capacity of a measured radio channel for outdoor macro cellular systems at 3ghz-band," *Vehicular Technology Conference Fall (VTC 2009-Fall), 2009 IEEE 70th*, pp. 1–5, Sept. 2009.

[10] P. Lusina and F. Kohandani, "Analysis of MIMO channel capacity dependence on antenna geometry and environmental parameters," *Vehicular Technology Conference, 2008. VTC 2008-Fall. IEEE 68th*, pp. 1 –5, 21-24 2008.

[11] D. Manteuffel, "MIMO antenna design challenges," *Antennas Propagation Conference, 2009. LAPC 2009. Loughborough*, pp. 50 –56, 16-17 2009.

[12] D. Browne, M. Manteghi, M. Fitz, and Y. Rahmat-Samii, "Experiments with compact antenna arrays for MIMO radio communications," *IEEE Transactions on Antennas and Propagation*, vol. 54, no. 11, pp. 3239 –3250, nov. 2006.

[13] J. Valenzuela-Valdes and D. Sanchez-Hernandez, "Increasing handset performance using true polarization diversity," *Vehicular Technology Conference, 2009. VTC Spring 2009. IEEE 69th*, pp. 1 –4, 26-29 2009.

[14] X. Liu and M. Bialkowski, "Effective degree of freedom and channel capacity of a MIMO system employing circular and linear array antennas," *Wireless Communications, Networking and Mobile Computing, 2009. WiCom '09. 5th International Conference on*, pp. 1 –4, 24-26 2009.

[15] L. Jian-gang, L. Ying-hua, H. Peng-fei, and L. Peng, "Evaluation of capacity of indoor MIMO channel with different antennas array," *Microwave, Antenna, Propagation and EMC Technologies for Wireless Communications, 2005. MAPE 2005. IEEE International Symposium on*, vol. 1, pp. 204 – 207 Vol. 1, 8-12 2005.

[16] B. Lindmark, "Capacity of a 2 times;2 MIMO antenna system with mutual coupling losses," in *Antennas and Propagation Society International Symposium, 2004. IEEE*, vol. 2, 2004, pp. 1720 – 1723 Vol.2.

[17] X. Liu and M. E. Bialkowski, "Effect of antenna mutual coupling on MIMO channel estimation and capacity," *IEEE Transactions on Antennas and Propagation*, vol. 2010, no. 8, pp. 1452–1463, 2010.

[18] M. Binelo, A. de Almeida, and F. Cavalcanti, "MIMO array capacity optimization using a genetic algorithm," *IEEE Transactions on Vehicular Technology*, vol. 60, no. 6, pp. 2471 –2481, july 2011.

[19] X. Chen, K. Huang, and X.-B. Xu, "Automated design of a three-dimensional fishbone antenna using parallel genetic algorithm and nec," *IEEE Antennas and Wireless Propagation Letters*, vol. 4, pp. 425 – 428, 2005.

[20] P. Karamalis, A. Kanatas, and P. Constantinou, "A genetic algorithm applied for optimization of antenna arrays used in mobile radio channel characterization devices," *IEEE Transactions on Instrumentation and Measurement*, vol. 58, no. 8, pp. 2475 –2487, aug. 2009.

[21] A. Ebrahimi and A. Rahimian, "Estimation of channel parameters in a multipath environment via optimizing highly oscillatory error functions using a genetic algorithm," *Software, Telecommunications and Computer Networks, 2007. SoftCOM 2007. 15th International Conference on*, pp. 1 –5, 27-29 2007.

[22] L. Hua, Z. Wei, Z. Qing-hua, W. Hua-kui, and Z. Zhao-xia, "Blind estimation of MIMO channels using genetic algorithm," *Natural Computation, 2009. ICNC '09. Fifth International Conference on*, vol. 4, pp. 163 –167, 14-16 2009.

[23] S. Chen and Y. Wu, "Genetic algorithm optimisation for maximum likelihood joint channel and data estimation," *Acoustics, Speech and Signal Processing, 1998. Proceedings of the 1998 IEEE International Conference on*, vol. 2, pp. 1157 –1160 vol.2, 12-15 1998.

[24] Z. Zhang, Y. Zhao, and J. Huang, "Array optimization for MIMO radar by genetic algorithms," *Image and Signal Processing, 2009. CISP '09. 2nd International Congress on*, pp. 1 –4, 17-19 2009.

[25] A. Farkasvolgyi, R. Dady, and L. Nagy, "Channel capacity maximization in MIMO antenna system by genetic algorithm," *Antennas and Propagation, 2009. EuCAP 2009. 3rd European Conference on*, pp. 1119 –1122, 23-27 2009.

[26] Y. Rahmat-Samii, "Modern antenna designs using nature inspired optimization techniques: Let darwin and the bees help designing your multi band MIMO antennas," *Radio and Wireless Symposium, 2007 IEEE*, pp. 463 –466, jan. 2007.

[27] M. Mohajer and S. Safavi-Naeini, "MIMO antenna optimization using method of moments analysis," *Antenna Technology, 2009. iWAT 2009. IEEE International Workshop on*, pp. 1 –4, mar. 2009.

[28] L. P. X. L. Hao Wang, Peng Wang, "On the impact of antenna correlation in multi-user MIMO systems with rate constraints," *IEEE Communications Letters*, vol. 8, no. 12, pp. 935 –937, 2009.

[29] M. Mohajer, G. Rafi, and S. Safavi-Naeini, "MIMO antenna design and optimization for mobile applications," *Antennas and Propagation Society International Symposium, 2009. APSURSI '09. IEEE*, pp. 1 –4, jun. 2009.

[30] S. Karimkashi, A. Kishk, and D. Kajfez, "MIMO antenna system optimization for mobile applications using equivalent infinitesimal dipoles," *Antennas and Propagation Society International Symposium (APSURSI), 2010 IEEE*, pp. 1 –4, jul. 2010.

[31] I. Berenguer, X. Wang, and V. Krishnamurthy, "Adaptive MIMO antenna selection," in *Signals, Systems and Computers, 2003. Conference Record of the Thirty-Seventh Asilomar Conference on*, vol. 1, nov. 2003, pp. 21 – 26 Vol.1.

[32] I. Bahcccci, T. Duman, and Y. Altunbasak, "Performance of MIMO antenna selection for space-time coded ofdm systems," in *Wireless Communications and Networking Conference, 2004. WCNC. 2004 IEEE*, vol. 2, march 2004, pp. 987 – 992 Vol.2.

[33] A. Molisch, N. Mehta, H. Zhang, P. Almers, and J. Zhang, "Implementation aspects of antenna selection for MIMO systems," in *Communications and Networking in China, 2006. ChinaCom '06. First International Conference on*, oct. 2006, pp. 1 –7.

[34] S. Sanayei and A. Nosratinia, "Capacity of MIMO channels with antenna selection," *IEEE Transactions on Information Theory*, vol. 53, no. 11, pp. 4356 –4362, nov. 2007.

[35] A. Goldsmith, *Wireless Communications*. New York: Cambridge, 2005.

[36] T. Taniguchi, S. Sha, and Y. Karasawa, "An approximation of eigenvalue distribution in i.i.d MIMO channels under rayleigh fading," in *IEEE/SP 13th Workshop on Statistical Signal Processing*, 2005, pp. 1072–1077.

[37] D. Tse and P. Viswanath, *Fundamentals of Wireless Communication*. Cambridge, UK: Cambridge University Press, 2005.

[38] T. Murakami, N. Honma, K. Nishimori, R. Kudo, Y. Takatori, and M. Mizoguchi, "Multi site MIMO channel analysis at 4.85ghz in outdoor environment," in *IEEE 20th International Symposium on Personal, Indoor and Mobile Radio Communications*, 2009, pp. 3005–3009.

[39] P. Almers, E. Bonek, A. Burr, N. Czink, M. Debbah, V. Degli-esposti, H. Hofstetter, P. Kysti, D. Laurenson, G. Matz, A. F. Molisch, C. Oestges, and H. celik, "Survey of channel and radio propagation models for wireless MIMO systems," *EURASIP Journal on Wireless Communications and Networking*.

[40] C. nee Chuah, J. M. Kahn, and D. Tse, "Capacity of multi-antenna array systems in indoor wireless environment," in *IEEE Globecom*, 1998, pp. 1894–1899.

[41] W. Weichselberger, M. Herdin, H. Ozcelik, and E. Bonek, "A stochastic MIMO channel model with joint correlation of both link ends," *IEEE Transactions on Wireless Communications*, vol. 5, no. 1, pp. 90–100, 2006.

[42] J. Medbo, "Spatio-temporal channel characteristics at 5ghz ia a typical office environment," *Vehicular Technology Conference, 2001. VTC 2001 Fall. IEEE VTS 54th*, pp. 1256–1260, 2001.

[43] Y. Yang, G. Xu, and H. Ling, "An experimental investigation of wideband MIMO channel characteristics based on outdoor non-los measurements at 1.8 ghz," *IEEE Transactions on Antennas and Propagation*, vol. 54, no. 11, pp. 3274–3284, Nov. 2006.

[44] Y. Selen and H. Asplund, "3g lte simulations using measured MIMO channels," *Global Telecommunications Conference, 2008. IEEE GLOBECOM 2008. IEEE*, pp. 1–5, 30 2008-Dec. 4 2008.

[45] A. L. F. d. Almeida, "Capacity in space-polarization domain based on measured wireless channel," *Ericsson Research Technical Report*, 2002.

[46] J.-A. Tsai, R. Buehrer, and B. Woerner, "The impact of aoa energy distribution on the spatial fading correlation of linear antenna array," *Vehicular Technology Conference, 2002. VTC Spring 2002. IEEE 55th*, vol. 2, pp. 933 – 937 vol.2, 2002.

[47] W. Press, B. Flannery, S. Teukolsky, and W. Vetterling, *Numerical Recipes in C: The Art of Scientific Computing*. New York: Cambridge University Press, 1992.

[48] P. . F. B. Pedersen, K.I. ; Mogensen, "Power azimuth spectrum in outdoor environments," *Electronics Letters*, vol. 33, no. 18, pp. 1583–1584, august 1997.

[49] X. Y. B. F. Nicolai Czink, Ernst Bonek, "Cluster angular spreads in a MIMO indoor propagation environment," in *Personal, Indoor and Mobile Radio Communications, 2005. PIMRC 2005. IEEE 16th International Symposium on*, vol. 1, september 2005, pp. 664–668.

[50] G. Zhao and S. Loyka, "Performance study of MIMO systems in a clustered multipath channel," in *Electrical and Computer Engineering, 2004. Canadian Conference on*, vol. 1, may 2004, pp. 453–456.

[51] A. Glazunov, M. Gustafsson, A. Molisch, F. Tufvesson, and G. Kristensson, "Spherical vector wave expansion of gaussian electromagnetic fields for antenna-channel interaction

analysis," *IEEE Transactions on Antennas and Propagation*, vol. 57, no. 7, pp. 2055 –2067, 2009.

[52] L. Xin and N. Zai-ping, "Effect of array orientation on capacity of MIMO wireless channels," *Signal Processing, 2004. Proceedings. ICSP '04. 2004 7th International Conference on*, vol. 3, pp. 1870 – 1872 vol.3, 31 2004.

[53] L. Wang and H. G. Wang, "An analytical three dimensional correlation model for array with antennas having abitrarily oriented directions," *Microwave Conference, 2008. APMC 2008. Asia-Pacific*, pp. 1 –4, 16-20 2008.

[54] P. Vainikainen, M. Mustonen, M. Kyro, T. Laitinen, C. Icheln, J. Villanen, and P. Suvikunnas, "Recent development of MIMO antennas and their evaluation for small mobile terminals," *Microwaves, Radar and Wireless Communications, 2008. MIKON 2008. 17th International Conference on*, pp. 1 –10, may. 2008.

[55] M. Binelo, A. de Almeida, J. Medbo, H. Asplund, and F. Cavalcanti, "MIMO channel characterization and capacity evaluation in an outdoor environment," in *Vehicular Technology Conference Fall (VTC 2010-Fall), 2010 IEEE 72nd*, 2010, pp. 1 –5.

[56] L. Ximenes and A. de Almeida, "Capacity evaluation of MIMO antenna systems using spherical harmonics expansion," in *Vehicular Technology Conference Fall (VTC 2010-Fall), 2010 IEEE 72nd*, 2010, pp. 1 –5.

[57] S. Russell and P. Norvig, *Artificial Intelligence: A Modern Approach*, ser. Prentice Hall series in artificial intelligence. Prentice Hall, 1995.

[58] C. Darwin, *On the origin of species by means of natural selection; or, The preservation of favoured races in the struggle for life*. D. Appleton and Company, 1861.

[59] G. W. B. Mendel and W. Bateson, *Mendel's Principles of Heredity: A Defence, with a Translation of Mendel's Original Papers on Hybridisation*. Cambridge, UK: Cambridge University Press, 2009.

[60] C. Reeves and J. Rowe, *Genetic Algorithms - Principles and Perspectives: A Guide to GA Theory*, ser. Operations Research/Computer Science Interfaces Series. Springer, 2002.

[61] K. Man, K. Tang, and S. Kwong, *Genetic Algorithms: Concepts and Designs*, ser. Advanced Textbooks in Control and Signal Processing. Springer, 1999.

[62] M. Gen and R. Cheng, *Genetic Algorithms and Engineering Design*, ser. Wiley Series in Engineering Design and Automation. John Wiley & Sons, 1997.

[63] A. Zalzala and P. Fleming, *Genetic Algorithms in Engineering Systems*, ser. Iee Control Engineering Series. Institution of Electrical Engineers, 1997.

[64] A. Korol and S. Preigel, *Recombination Variability and Evolution: Algorithms of estimation and population-genetic models*. Springer, 1994.

[65] N. Costa and S. Haykin, *Multiple-Input Multiple-Output Channel Models, Theory and Practice*. New York: Wiley, 2010.

[66] D. Nitch and A. Fourie, "A redesign of NEC2 using the object-oriented paradigm," in *Antennas and Propagation Society International Symposium, 1994. AP-S. Digest*, vol. 2, Jun. 1994, pp. 1150 –1153 vol.2.

[67] A. Molisch, "MIMO systems with antenna selection - an overview," in *Radio and Wireless Conference, 2003. RAWCON '03. Proceedings*, aug. 2003, pp. 167 – 170.

[68] A. Molisch, M. Win, and J. Winters, "Capacity of MIMO systems with antenna selection," in *Communications, 2001. ICC 2001. IEEE International Conference on*, vol. 2, 2001, pp. 570 –574 vol.2.

[69] A. Molisch, M. Win, Y.-S. Choi, and J. Winters, "Capacity of MIMO systems with antenna selection," *IEEE Transactions on Wireless Communications*, vol. 4, no. 4, pp. 1759 – 1772, july 2005.

[70] P. Voltz, "Characterization of the optimum transmitter correlation matrix for MIMO with antenna subset selection," *IEEE Transactions on Communications*, vol. 51, no. 11, pp. 1779 – 1782, nov. 2003.

[71] G. Zhaozhi and L. Sheng, "Effect of antenna selection on channel capacity of MIMO system," in *Computer, Mechatronics, Control and Electronic Engineering (CMCE), 2010 International Conference on*, vol. 1, aug. 2010, pp. 471 –473.

[72] S. Ranvier, C. Icheln, and P. Vainikainen, "Measurement-based mutual information analysis of MIMO antenna selection in the 60-ghz band," *IEEE Antennas and Wireless Propagation Letters*, vol. 8, pp. 686 –689, 2009.

[73] J. Ahmadi-Shokouh, S. Jamali, S. Safavi-Naeini, and G. Rafi, "Switch loss and antenna directivity effects on MIMO antenna selection," in *Electrical and Computer Engineering, 2008. CCECE 2008. Canadian Conference on*, may 2008, pp. 000 641 –000 646.

[74] P. Almers, T. Santos, F. Tufvesson, A. Molisch, J. Karedal, and A. Johansson, "Measured diversity gains from MIMO antenna selection," in *Vehicular Technology Conference, 2006. VTC-2006 Fall. 2006 IEEE 64th*, sept. 2006, pp. 1 –6.

[75] A. Ghrayeb, "A survey on antenna selection for MIMO communication," *Information and Communication Technologies*, vol. 2, pp. 2104–2109, 2006.

[76] R. S. Blum1, ZheminXu, and S. Sfar, "A near-optimal joint transmit and receive antenna selection algorithm for MIMO systems," in *Radio and Wireless Symposium, 2009. RWS '09. IEEE*, 2009, pp. 554–557.

[77] C. Murthy and B. D. Rao, "On antenna selection with maximum ratio," in *Conference Record of the Thirty-Seventh Asilomar Conference on Signals, Systems and Computers, 2003*, 2003, pp. 228–232.

[78] M. Gharavi-Alkhansari and A. B. Gershman, "Fast antenna subset selection in MIMO systems," *IEEE Transactions on Signal Processing*, vol. 52, no. 2, pp. 339–347, 2004.

[79] B. H. Wang, H. T. Hui, and M. S. Leong, "Global and fast receiver antenna selection for MIMO systems," *IEEE Transactions on Communications*, vol. 52, no. 9, pp. 2505–2510, 2010.

[80] R. Vaze and H. Ganapathy, "Sub-modularity and antenna selection in MIMO systems," *IEEE Communications Letters*, vol. 16, no. 9, pp. 1446–1449, 2012.

[81] Z. Chen, B. Vucetic, and J. Yuan, "Space-time trellis codes with transmit antenna selection," *IEEE Electronics Letters*, vol. 39, pp. 854–855, 2003.

[82] D. Piazza, J. Kountouriotis, M. D'Amico, and K. Dandekar, "A technique for antenna configuration selection for reconfigurable circular patch arrays," *IEEE Transactions on Wireless Communications*, vol. 8, no. 3, pp. 1456–1467, 2009.